VENEZUELA-MEM/USA-DOE FOSSIL ENERGY REPORT IV-5

DOE/BC—89/1/SP
(DE89000702)

November
1988

SUPPORTING TECHNOLOGY FOR ENHANCED OIL RECOVERY

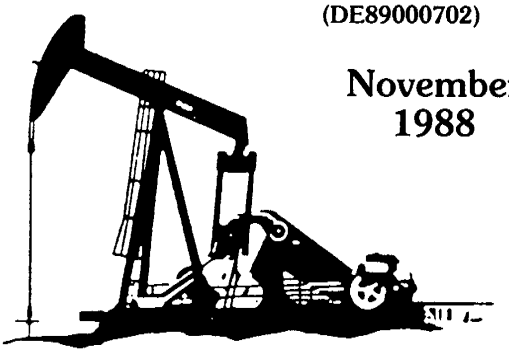

EOR THERMAL PROCESSES

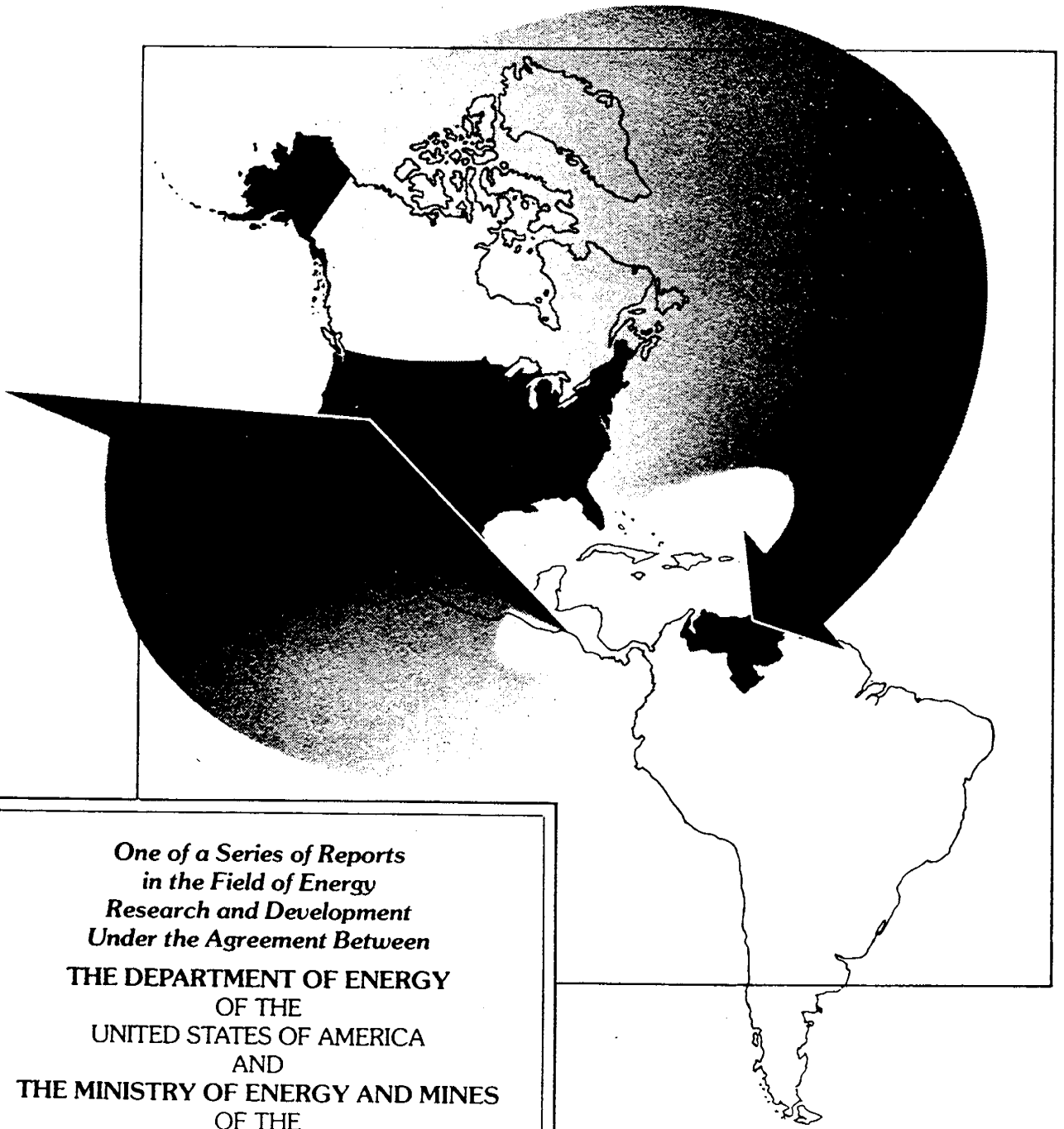

One of a Series of Reports in the Field of Energy Research and Development Under the Agreement Between

THE DEPARTMENT OF ENERGY
OF THE
UNITED STATES OF AMERICA
AND
THE MINISTRY OF ENERGY AND MINES
OF THE
REPUBLIC OF VENEZUELA

DISCLAIMER

This report was prepared as an account of work sponsored by an agency of the United States Government. Neither the United States Government nor any agency thereof, nor any of their employees, makes any warranty, express or implied, or assumes any legal liability or responsibility for the accuracy, completeness, or usefulness of any information, apparatus, product, or process disclosed, or represents that its use would not infringe privately owned rights. Reference herein to any specific commercial product, process, or service by trade name, trademark, manufacturer, or otherwise, does not necessarily constitute or imply its endorsement, recommendation, or favoring by the United States Government or any agency thereof. The views and opinions of authors expressed herein do not necessarily state or reflect those of the United States Government or any agency thereof.

Printed in the United States of America. Available from:
National Technical Information Service
U.S. Department of Commerce
5285 Port Royal Road
Springfield, VA 22161

NTIS price codes
Paper copy: **A08**
Microfiche copy: **A01**

DOE/BC—89/1/SP
(DE89000702)
Distribution Category UC-122

FOURTH AMENDMENT AND EXTENSION TO ANNEX IV ENHANCED OIL RECOVERY THERMAL PROCESSES

Implementing Agreement Between

THE DEPARTMENT OF ENERGY OF THE UNITED STATES OF AMERICA

And

THE MINISTRY OF ENERGY AND MINES OF THE REPUBLIC OF VENEZUELA

Submitted by:

Thomas B. Reid, Project Manager
Thermal Recovery
Bartlesville Project Office
U.S. Department of Energy

Orlando Rivas, Manager
Heavy Oil
INTEVEP, S.A.
Filial de Petroleos de Venezuela, S.A.

Approved by:

Thomas C. Wesson, Director
Bartlesville Project Office
P.O. Box 1398
Bartlesville, OK 74005

Enrique Vasquez, Technology Coordinator
Petroleos de Venezeula, S.A.
Apartado Postal 169
Caracas 1010A, Venezuela

United States Department of Energy

PREFACE

An Agreement between the Department of Energy of the United States of America and the Ministry of Energy and Mines of the Republic of Venezuela to cooperate in Energy Research and Development was signed March 6, 1980. The object of cooperation under this DOE/MEMV Agreement was to promote a balanced exchange of energy technologies and to conduct joint projects in the areas of Petroleum, Solar Energy, Geothermal Energy, Hydroelectric Energy and Coal.

This Agreement supported the Agreement for Scientific and Technological Cooperation between the two countries which was signed by the Secretary of State of the U.S.A. and the Minister of Foreign Relations of Venezuela on January 11, 1980.

The original DOE/MEMV Agreement was supplemented by six annexes to describe specifically the work to be done. Over the past eight years additional annexes have been signed, resulting in a total of thirteen annexes as of April 1, 1988. The Agreement has been extended to March 6, 1993. The annexes are:

I. Characterization of Heavy Crude Oils.

II. Supporting Research in the Area of Enhanced Oil Recovery.

III. Evaluation of Past and Ongoing Enhanced Oil Recovery Projects in the U.S. and Venezuela.

IV. Enhanced Oil Recovery Thermal Processes.

V. Drilling, Coring and Telemetry.

VI. Residual Oil Saturation.

VII. Petroleum Products, Use and Evaluation.

VIII. Coal Preparation, Combustion and Related Technology.

IX. Subsidence Due to Fluid Withdrawal.

X. On-Site Training of Petroleum Engineers.

XI. Energy Conservation.

XII. Geochemistry (Oil Generation, Migration and Accumulation).

XIII. Microbial EOR.

Each of these annexes has a document describing the work to be done as part of the cooperation. Amendments and Extensions to the Annexes are provided for in the Agreement.

Currently, nine annexes are active (Annexes I, II, III, IV, VIII, X, XI, XII, and XIII) and four annexes have been completed (Annexes V, VI, VII and IX).

CONTENTS

	Page
Preface	ii
Abstract	iv
TASK 32 DOE-Lawrence Livermore National Laboratory Thermal Front Tracking Tests	32-1
TASK 33 INTEVEP Electromagnetic and Seismic Studies	33-1
TASK 34 INTEVEP Steam-Foam Laboratory Research	34-1
TASK 35 DOE-Stanford University Petroleum Research Institute Steam Additive and Modeling Research	35-1
TASK 36 INTEVEP Steam Additive Field Test	36-1
TASK 37 DOE-NIPER Light Oil Steamflooding Research	37-1

APPENDIX A. Full text of the "Fourth Amendment and Extension of Implementing Agreement IV Between the Department of Energy of the United States of America and the Ministry of Energy and Mines of the Republic of Venezuela in the Area of Enhanced Oil Recovery Thermal Processes."

ABSTRACT

This report contains the results of efforts under the six tasks of the Fourth Amendment and Extension of Annex IV, Enhanced Oil Recovery Thermal Processes of the Venezuela/USA Agreement. The report is presented in sections (for each of the 6 tasks) and each section contains one or more reports prepared by various individuals or groups describing the results of efforts under each of the tasks.

A statement of each task, taken from the agreement, is presented on the first page of each section. The tasks are numbered 32 through 37. The first, second, third, and fourth reports on Annex IV, [Venezuela MEM/USA-DOE Fossil Energy Report IV-1, IV-2, IV-3, and IV-4 (DOE/BETC/SP-83/15, DOE/BC-84/6/SP, DOE/BC-86/2/SP, and DOE/BC-87/2/SP)] contain the results from the first 31 tasks. Those reports are dated April 1983, August 1984, March 1986, and July 1987, respectively.

Task 32 - DOE shall provide INTEVEP with information from the project and field tests conducted by the Lawrence Livermore National Laboratory on the use of seismic and electromagnetic methods for cross borehole probing to determine the location of steam zones and fronts within a reservoir.

Thermal Front Tracking With Cross Borehole Electromagnetic Imaging

(Task 32 of Annex IV of the Implementing Agreement)

P.E. Harben
M. Pihlman

April, 1988

Abstract

Field experiments at the Texaco Kern River Field were conducted to identify optimum transmission frequencies and assess the electromagnetic interference problems present in the system. We concluded that the transmitter must be operated below 3 MHz for attenuation measurements to be in the conduction regime. Operation in the conduction regime is necessary if we are to correlate images to independent measurements such as the dual induction logs. We also concluded that electromagnetic interference problems become more severe as the frequency is lowered.

We are currently designing a downhole active transmitter that will operate at 2 MHz. This frequency is low enough to be in the conduction regime and to increase our transmission distance capability but high enough so that we can still drive a 1 or 2 meter antenna. By driving the antenna with a downhole oscillator we dramatically reduce the chance of electromagnetic interference pathways.

Future plans are to test the transmitter at the Texaco field site and demonstrate correlation to induction logs. This will be followed by a brine tracing experiment at the same site. We will then move our equipment to a new pilot test site for a substantial series of cooperative experiments with Texaco.

Introduction

High frequency electromagnetic cross-borehole imaging has been used at LLNL to map and monitor fracturing in coal seams (Lytle, et. al.,1974), coal gasification fire fronts (Davis, et. al.,1979), oil shale retorting (Daily, et. al.,1981) and nuclear waste repository integrity (Ramirez, et. al.,1983). In all these applications the frequency used to transmit cross-borehole was 20 MHz or higher. High frequency operation has the advantage of reducing cross-talk and other electromagnetic interference problems as well as making it relatively easy to drive the 1/2 or 1 meter antennas used in transmission. High frequency operation, however, puts severe limitations on the distance through-the-earth that a signal can be transmitted since the signal attenuation increases dramatically with increasing frequency. In the conductivity ranges typical of many enhanced oil recovery fields, cross-borehole transmission at frequencies of 20 MHz or higher means boreholes must be spaced closer than 25 ft. for signal detection by the receiver.

Operating at high frequency also means the attenuation depends on the conductivity and permittivity of the medium. Tomographic images, therefore, represent the distribution of both of these electrical properties which makes it impossible to examine the behavior of a single property like conductivity. This means geophysical logs, like the dual induction log, cannot be directly compared to the tomographic images and hence there is no way of independently verifying the results of the reconstructed images. By operating at a frequency of 3 MHz or lower only conductivity affects electromagnetic attenuation and hence reconstructed images can be correlated directly to induction logs.

In this paper we will first present a short review of cross-borehole electromagnetic tomography and then present some theoretical attenuation curves that demonstrate the desirability for lower frequency operation. This is followed by a discussion of our future plans in building a lower frequency cross-borehole electromagnetic tomography system and our joint experimental plans at the new Texaco pilot site.

Background

Cross-borehole electromagnetic tomography is similar in principle to the Computerized Axial Tomography (CAT) X-ray scanners used in medical diagnostics. An important difference in cross-borehole tomography is that the projection angles are limited because we are in vertical boreholes and consequently complete viewing of the object to be imaged, such as by CAT scanners, is impossible. Figure 1 shows the source and receiver positions with the assumed straight line transmission paths used to acquire the data for tomographic reconstruction of the indicated region. Typically, the transmitter is fixed in a position and the receiver measures the signal strength at every position in the borehole. The transmitter is then moved to the next position and the process is repeated. This continues until the transmitter has been located at every position in the borehole.

Tomographic reconstruction is accomplished by dividing the image region into a grid of cells through which the individual data rays pass. As shown on figure 2, each cell has a constant attenuation value (alpha), each ray has a measured bulk attenuation (Atten), and a length (D) through each cell. Each ray, therefore, forms an equation in the unknown alphas. The set of equations for all rays is solved by iterative methods to determine the alphas.

Before the tomographic reconstruction is accomplished the measured ray data is corrected for such factors as the assumed antenna radiation pattern and geometrical spreading. Corrections are not, at present, made for wavelength changes in the medium, variations in transmitter power, antenna gain and receiver gain.

Attenuation in Media

We have calculated electromagnetic attenuation curves at a number of different frequencies and media properties representative of our enhanced oil recovery test site at the Kern River field in Bakersfield. The curves were calculated using the theoretical equations from Lytle and Lager, 1972 and help define the limits of maximum borehole separation at different frequencies. The curves also quantify the conduction and displacement frequency regimes applicable to the test site.

At 17 MHz, the curves on figure 3 show the electromagnetic attenuation measured in decibels per meter (db/m) as a function of the permittivity of the media. Each curve represents the attenuation function at a different fixed media conductivity. The conductivity of the Bakersfield test site formations can be expected to, in general, vary between .05 and .4 S/meter. The permittivity can be expected to vary between 5 and 40. The curves clearly show that at the highest values of conductivity, attenuation can be 40 db/meter. Since the minimum measurable signal for the receiver is about 100 db below the maximum transmitter radiated power of our system, a very high conductivity zone can attenuate the signal below measureable levels in only 2.5 meters. Although this is a worst case, it demonstrates the impossibility of operating at this frequency between boreholes spaced 100 ft. apart.

Figure 4 shows the same type of attenuation curve plot as figure 3 except the transmission frequency is 2 MHz. There is a significant reduction in the attenuation at each conductivity value compared to the 17 MHz case. Attenuation also becomes relatively independent of permittivity. Clearly, at the highest conductivities, 2 MHz through-the-earth transmission would not be possible between boreholes spaced 100 ft. apart. At low conductivities, however, it would be.

Attenuation curves at a transmission frequency of 500 kHz are shown on figure 5. Attenuation is further reduced but is still large enough at the highest conductivities to make 100 ft. through-the-earth transmission difficult to achieve.

It would appear that by simply operating at a low enough frequency, through-the-earth transmission would be feasable at large borehole separations and at high formation conductivities. Practically, it becomes increasingly difficult to drive a small antenna (1-2 meters) as the frequency is reduced. Furthermore, electromagnetic shielding becomes less effective as frequency is reduced which leads to major electromagnetic interference problems, as shown on figure 6, and "sneak paths" to the receiver that are not through-the-earth transmission paths. We concluded that 2 MHz was a good compromise frequency that allows us to transmit between boreholes spaced further apart (up to 100 ft. at lower formation conductivities) but not be overwhelmed by antenna driving and interference problems.

Low frequency operation is also important if we are to correlate images to induction logs for independent data verification. As shown on figure 7, when the transmission frequency is 17 MHz displacement currents are significant and even dominate conduction currents at the low conductivities and high permittivities. This means that the attenuation at this frequency, in general, is dependent on both the conductivity and permittivity of the medium. This makes it impossible to isolate just one of these physical properties and correlate to measurements using other techniques. Figure 8 shows the same curves at a 2 MHz transmission frequency. Except for the lowest conductivity and highest permittivity, conduction currents clearly dominate displacement currents. Consequently, attenuation depends on the medium conductivity only; which allows us to correlate our results to induction logs.

Future Plans

We are currently redesigning our electromagnetic transmission and data acquisition system to operate at 2 MHz. In lowering the operation frequency, we find it necessary to make major changes in the transmitting hardware. Figure 9 shows a block diagram of the old system. A signal generator located in the central processing trailer sends a low power signal at the operating frequency to a 100 watt power amplifier. The amplifier -located on the surface next to the transmit borehole- amplifies the signal which is sent down the coaxial cable connected to the downhole transmitter.

The new system we are developing is shown in the block diagram on figure 10. There is no trailer mounted signal generator or uphole power amplifier. The transmitter is driven by a downhole co-located oscillator. Ideally, the oscillator would be powered by a downhole battery powerpack but, due to the high temperatures and harsh conditions in the steam zone, it will be easier to power the oscillator from the surface with a DC powerpack. By locally driving the transmitter at the transmission frequency, electromagnetic interference problems that arise from the uphole power amplifier and the coaxial cable carrying the amplified signal to the transmitter are eliminated. These would be major problems if we tried to use the old system at 2 MHz.

As we develop the new transmission system we will continue to interact with Texaco and plan experiments that fit the schedule of their new hot water surfactant pilot schedule. The schedule, which has slipped by several months, is shown on figure 11. This represents a major and well-controlled experimental undertaking by Texaco and an excellent opportunity for practical experimental development of electromagnetic thermal front imaging.

References

Daily,W.D., Lytle,R.J., Laine,E.F., Okada,J.T., Deadrick,F.J., 1981, *Geotomography in Oil Shale*, Lawrence Livermore National Laboratory UCRL-85748.

Davis,D.T., Lytle,R.J., Laine,E.F.,1979, *Use of High Frequency Electromagnetic Waves for Mapping an In-situ Coal Gasification Burn Front*, In Situ 3, 95-119.

Lytle,R.J., Lager,D.L., 1972, *Electromagnetic Propagation, Transmission, Reflection, and Refraction: Equations and Numerical Results*, Lawrence Livermore National Laboratory UCRL-51245.

Lytle,R.J., Laine,E.F., Lager,D.L., 1974, *Coal Fracture Measurements Using In-situ Electrical Methods: Preliminary Results*, Lawrence Livermore National Laboratory UCID-16639.

Ramirez,A.L., Lytle,R.J., Harben,P.E., 1983, *Crosshole Geophysical Methods Used to Investigate the Near Vicinity of High Level Waste Repositories*, Lawrence Livermore National Laboratory UCID-20060.

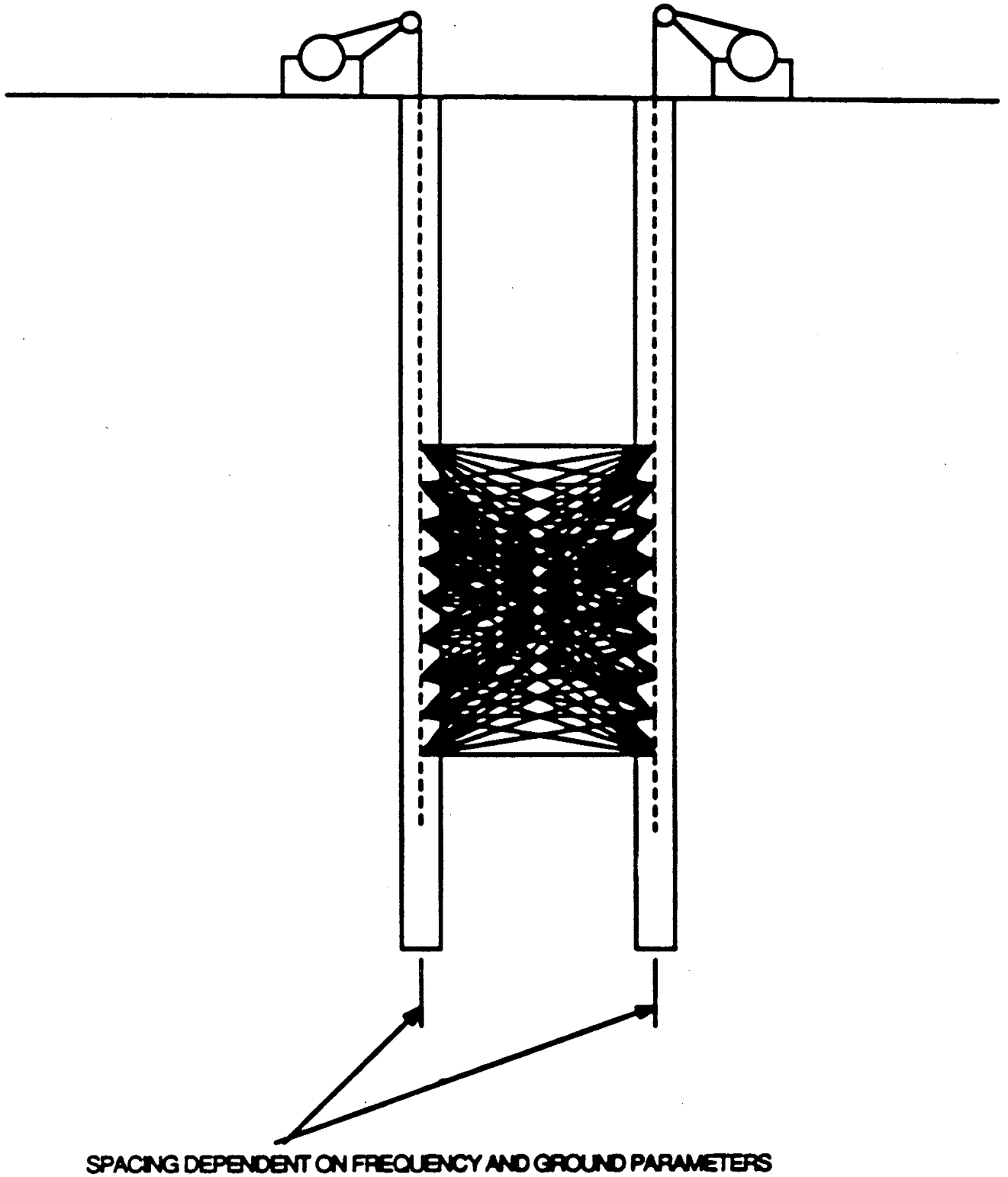

Figure 1) The transmitter and receiver positions used in acquiring the tomograph data. Each position set is connected with a straight line measurement ray.

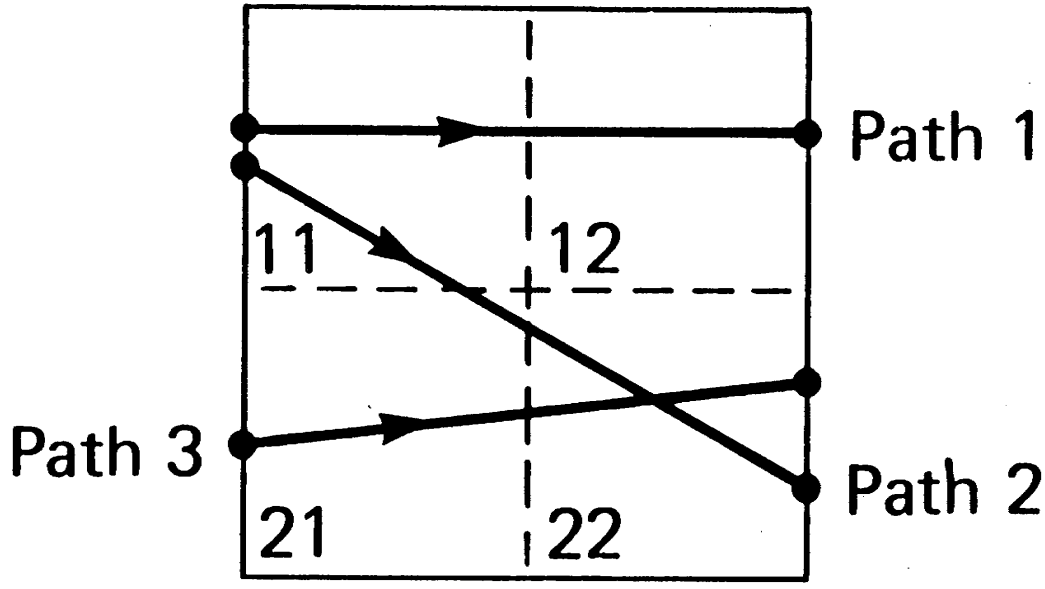

$$\mathrm{Atten}_1 = {}_1D_{11}\alpha_{11} + {}_1D_{12}\alpha_{12} + {}_1D_{21}\alpha_{21} + {}_1D_{22}\alpha_{22}$$

$$\mathrm{Atten}_2 = {}_2D_{11}\alpha_{11} + {}_2D_{12}\alpha_{12} + {}_2D_{21}\alpha_{21} + {}_2D_{22}\alpha_{22}$$

$$\mathrm{Atten}_3' = {}_3D_{11}\alpha_{11} + {}_3D_{12}\alpha_{12} + {}_3D_{21}\alpha_{21} + {}_3D_{22}\alpha_{22}$$

•

Figure 2) The reconstruction method is shown for a 4 cell tomograph. Each measured ray forms an equation in the unknown cell attenuations, alpha. Atten is the measured attenuation and the D's are the ray length in each cell.

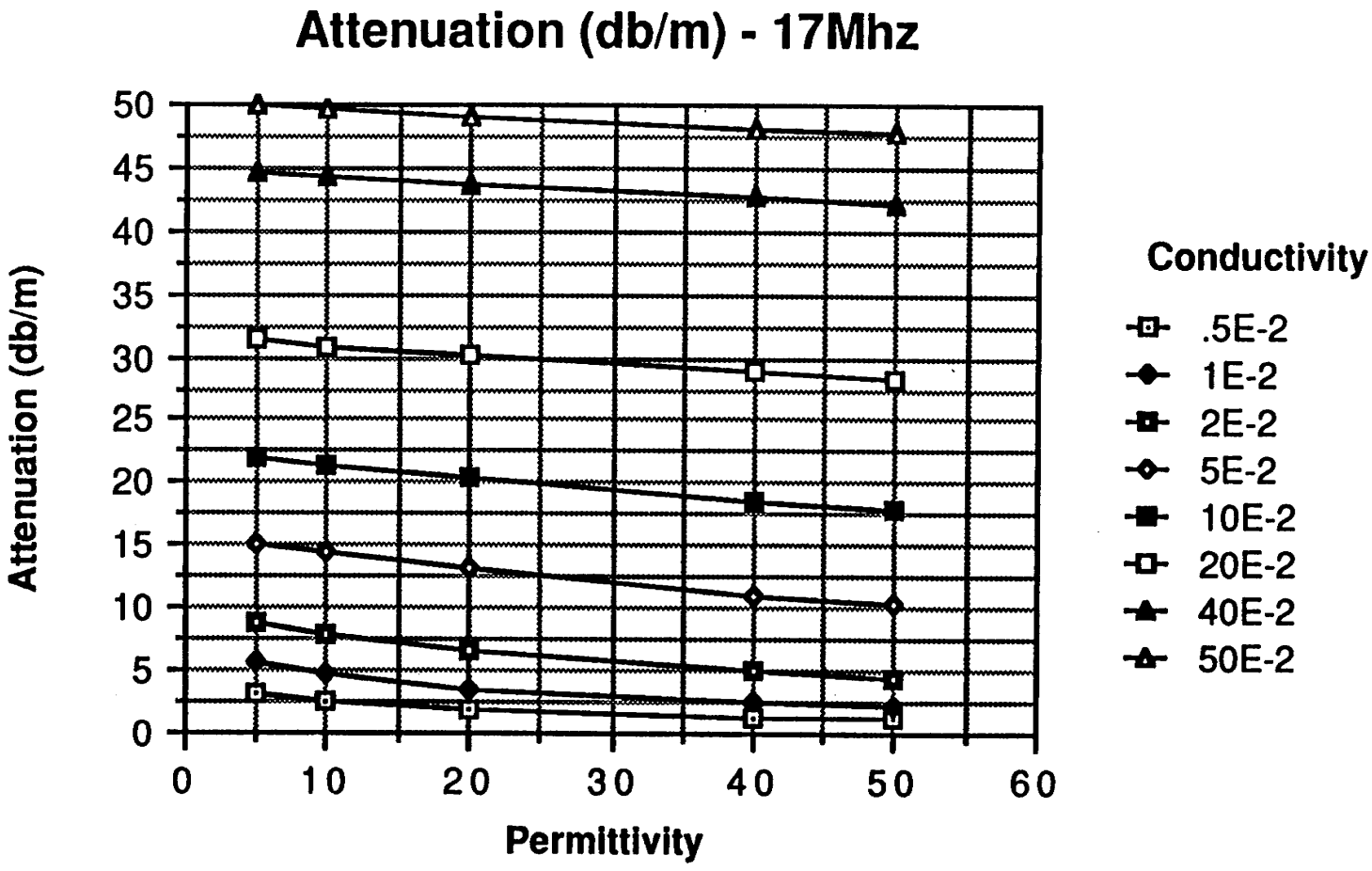

Figure 3) Attenuation curves at a fixed conductivity showing attenuation in db/meter as a function of permittivity at 17 MHz.

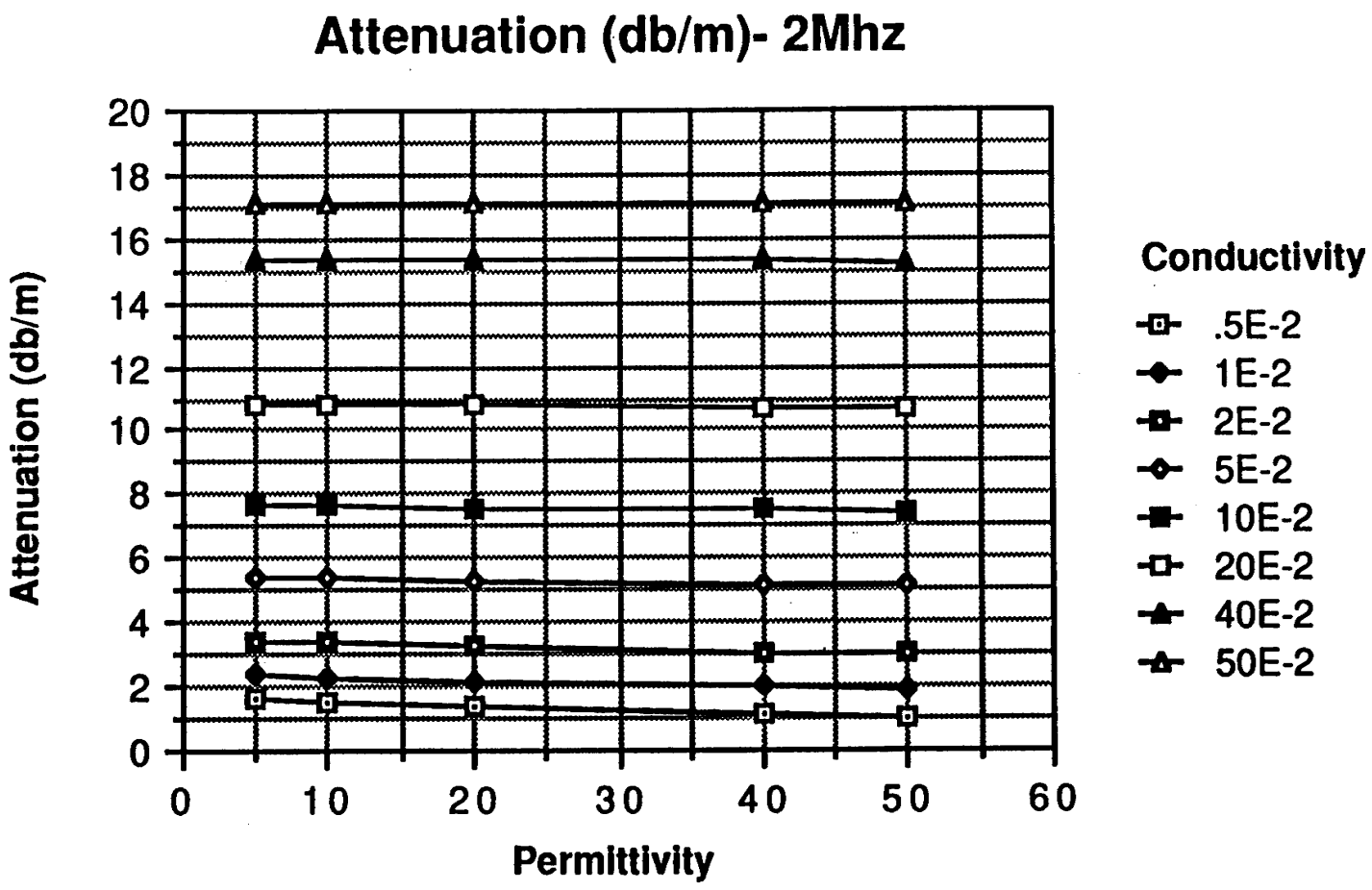

Figure 4) Attenuation curves at a fixed conductivity showing attenuation in db/meter as a function of permittivity at 2 MHz.

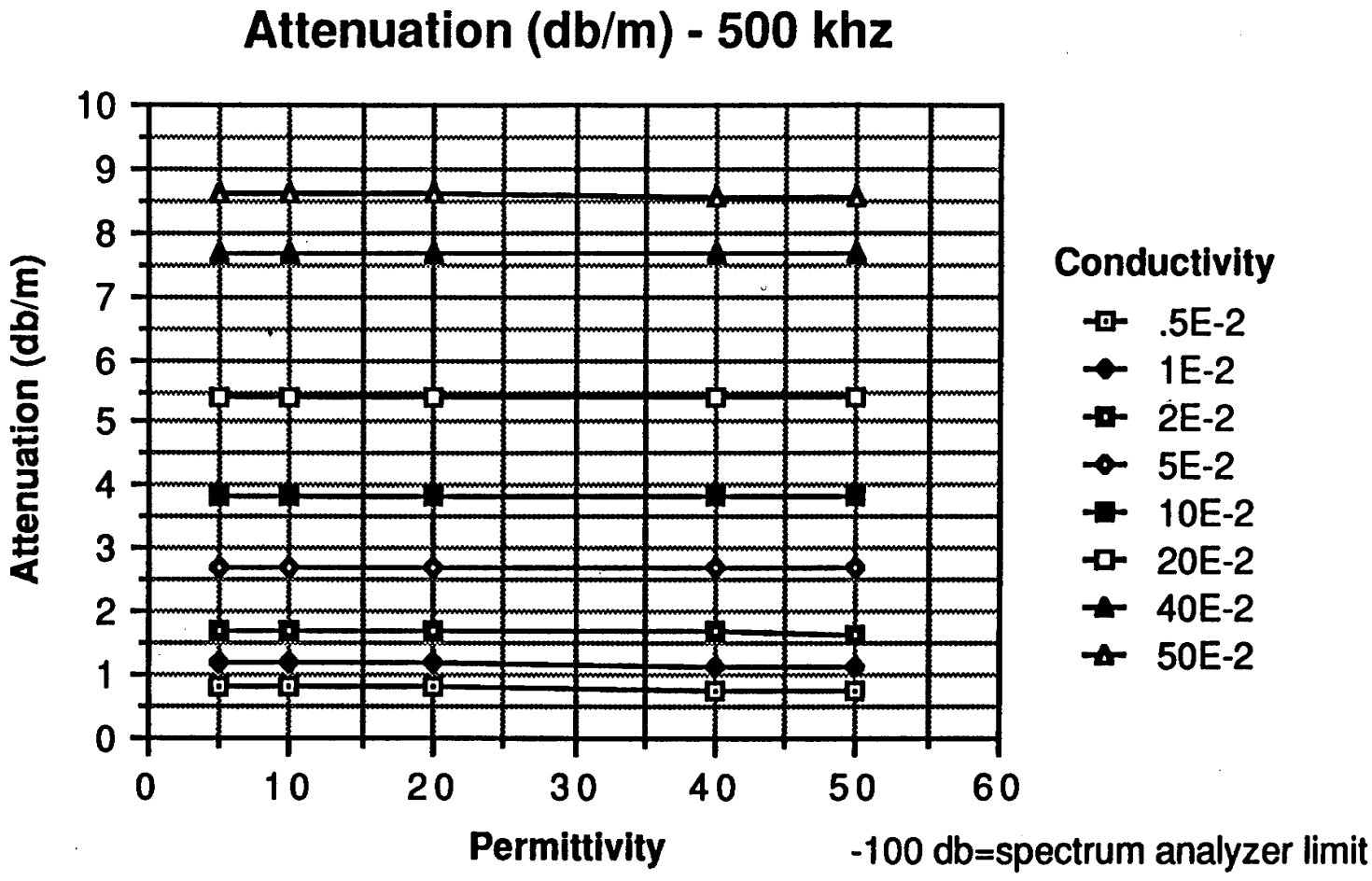

Figure 5) Attenuation curves at a fixed conductivity showing attenuation in db/meter as a function of permittivity at 500 kHz.

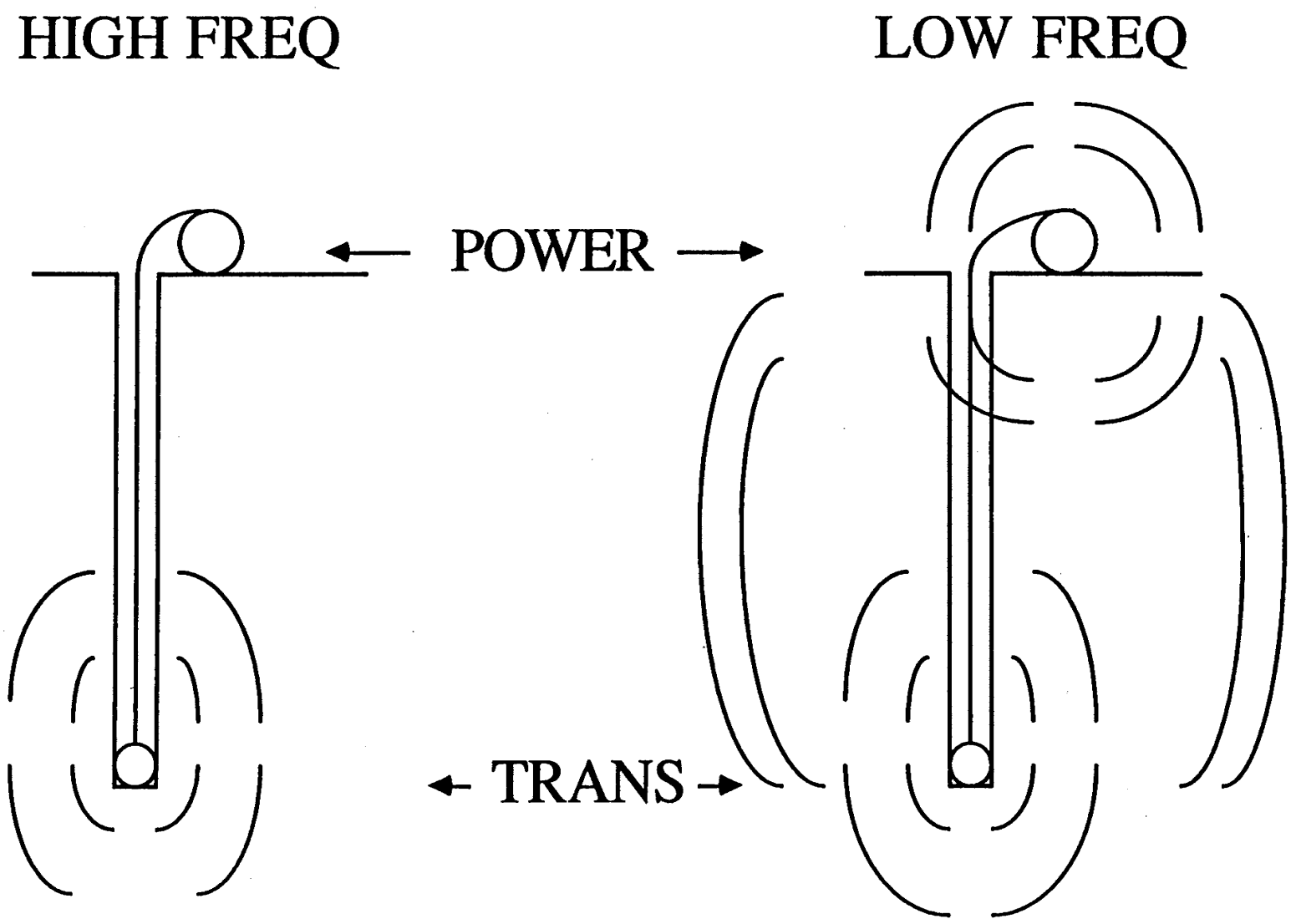

Figure 6) Diagram showing the instrument and cable radiation problems encountered when operating at low frequency.

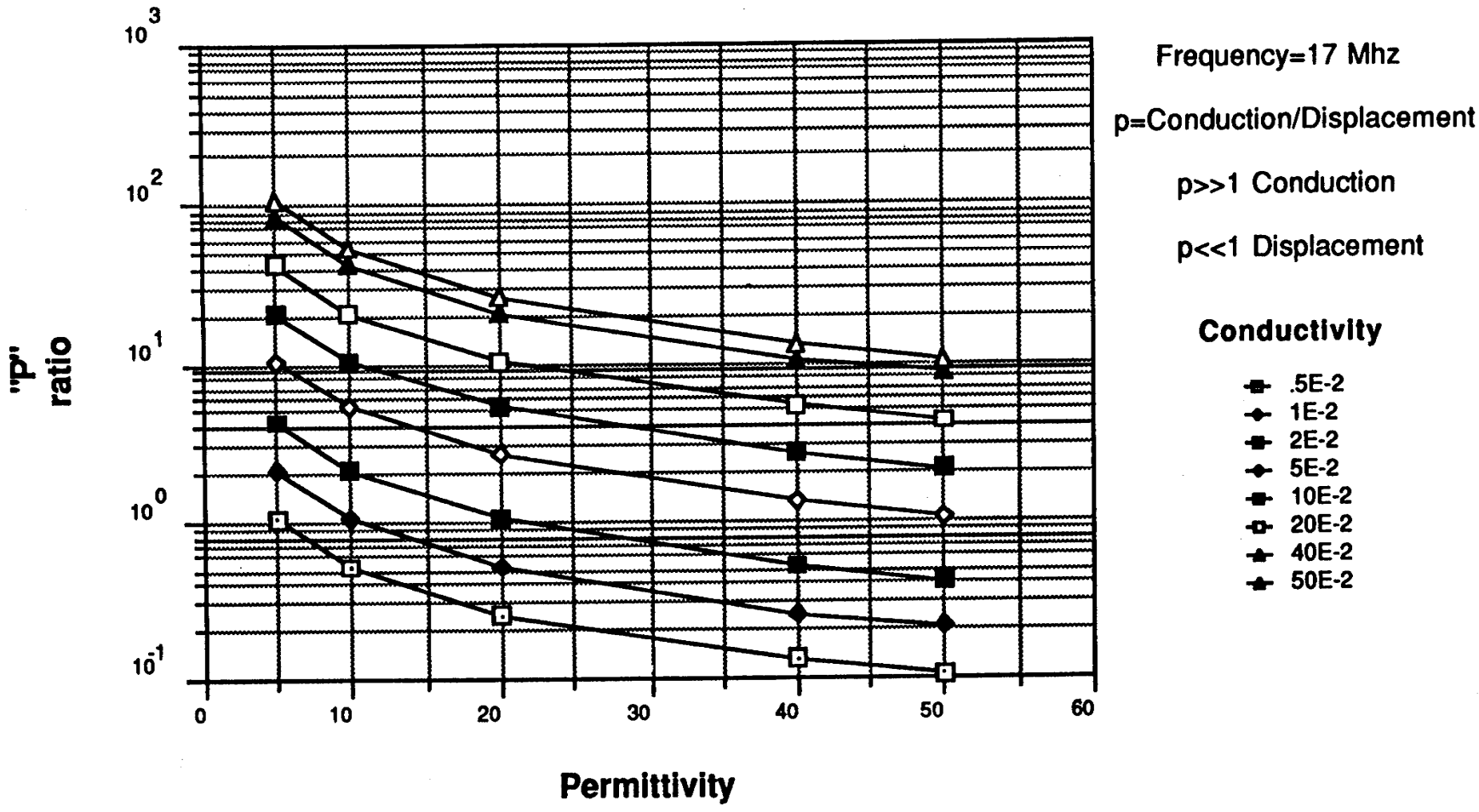

Figure 7) The ratio of conduction currents to displacement currents are shown as a function of permittivity at fixed conductivities. At 17 MHz the conduction currents dominate only at high conductivity.

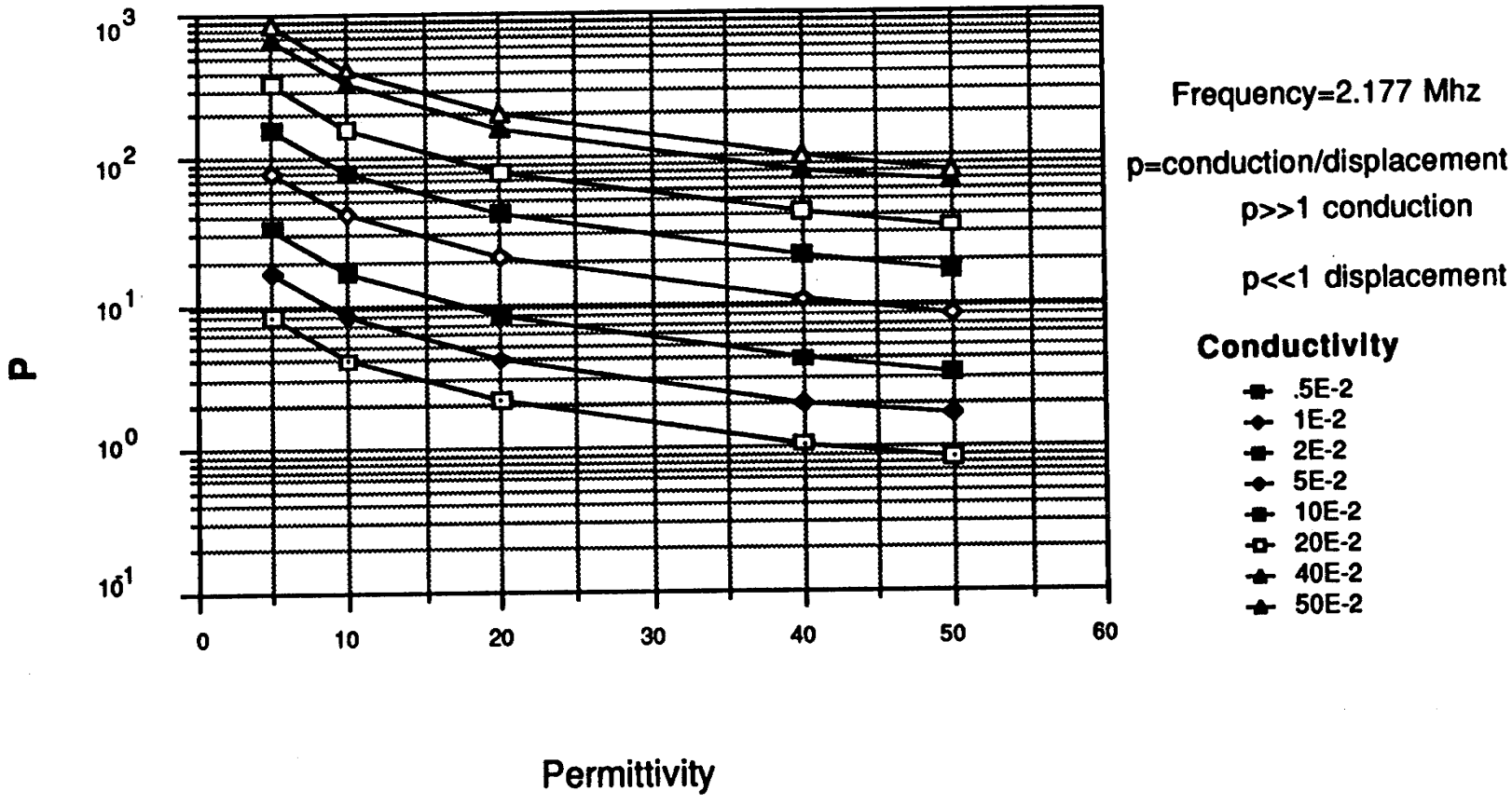

Figure 8) The ratio of conduction currents to displacement currents are shown as a function of permittivity at fixed conductivities. At 2 MHz, conduction currents dominate.

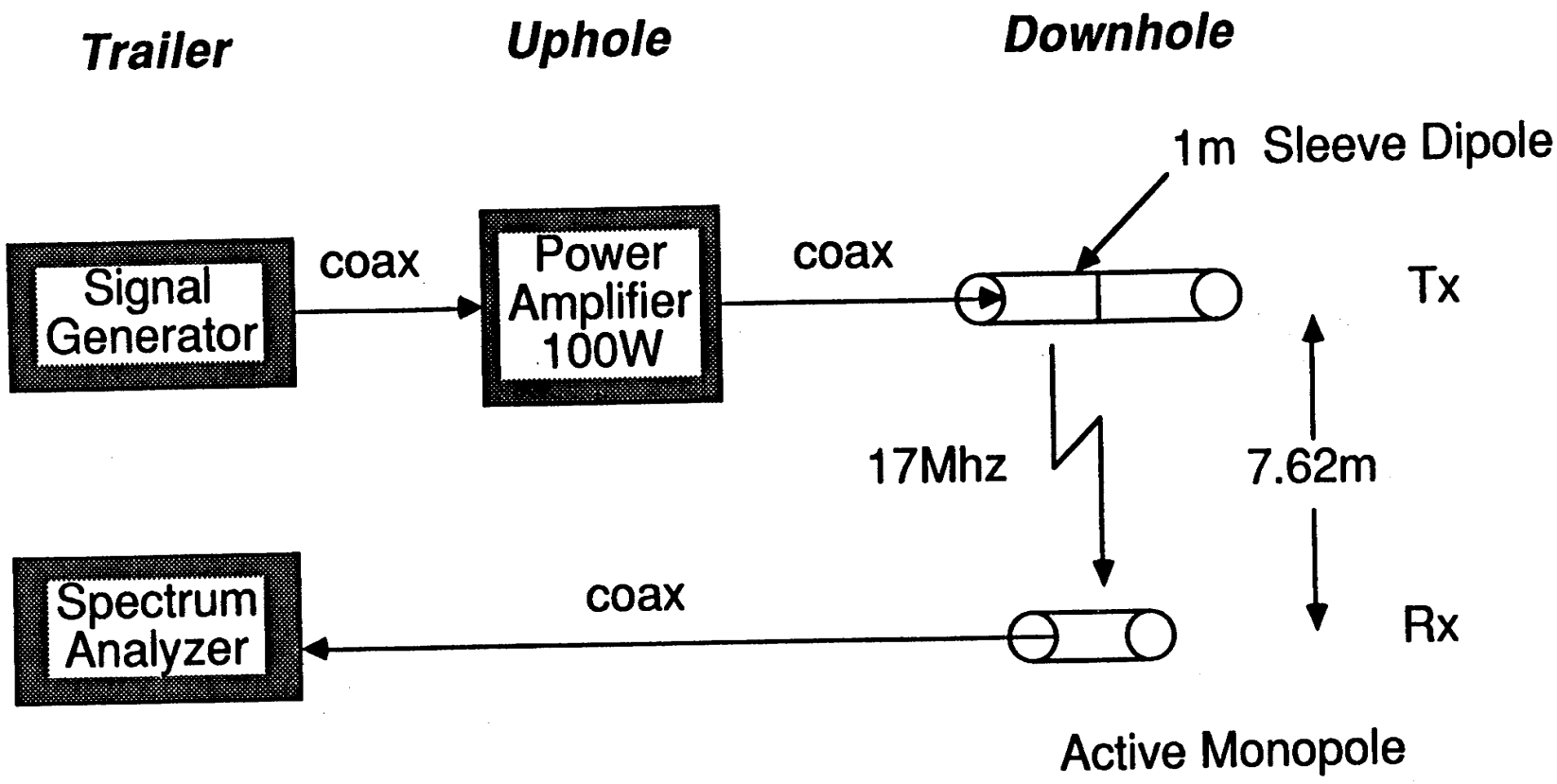

Figure 9) Block diagram showing the old cross-borehole electromagnetic data acquisition system. The system uses an uphole power amplifier to drive the downhole transmitter.

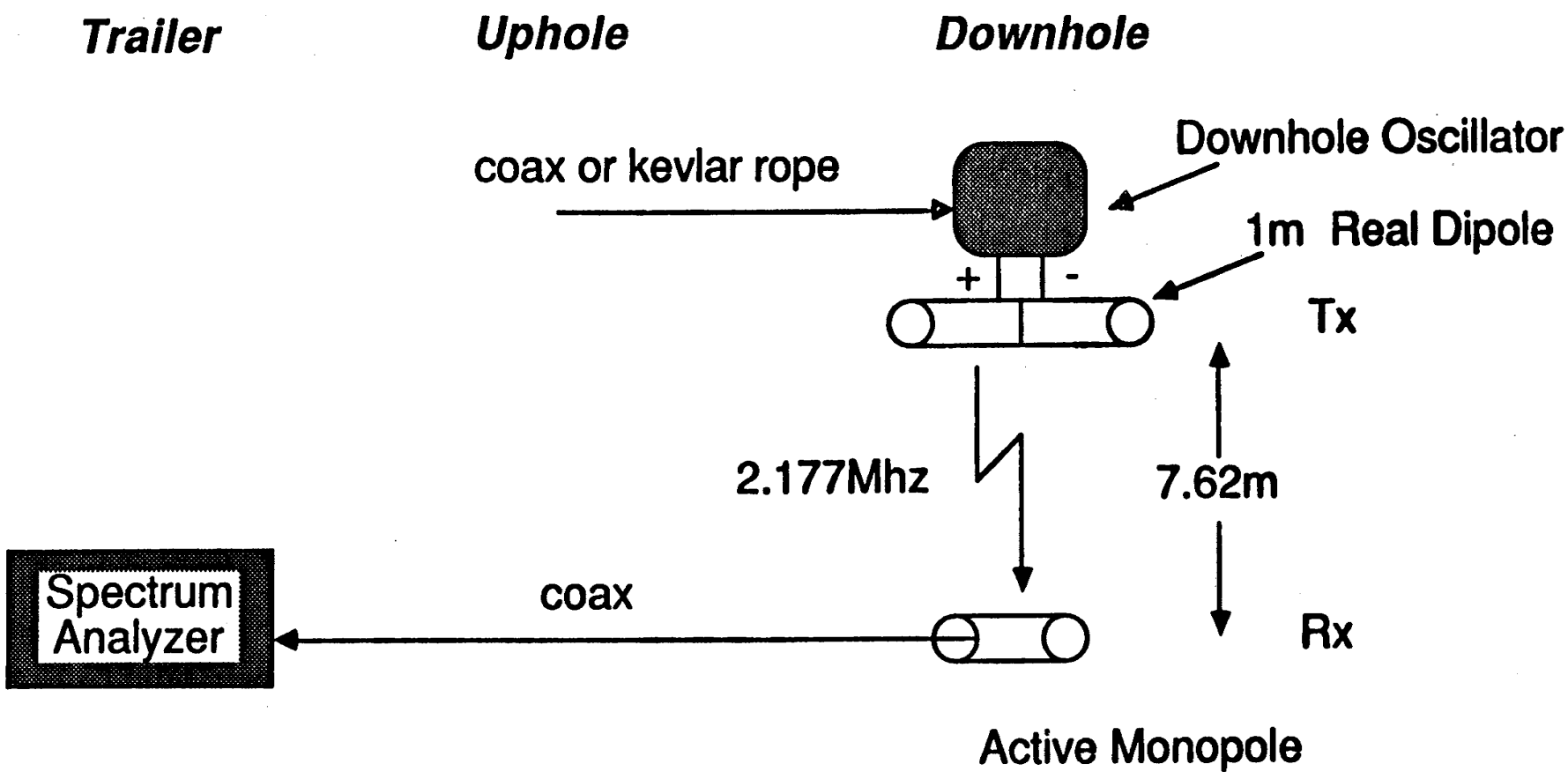

Figure 10) Block diagram showing our proposed new cross-borehole electromagnetic data acquisition system. The system uses a downhole oscillator to drive the downhole transmitter.

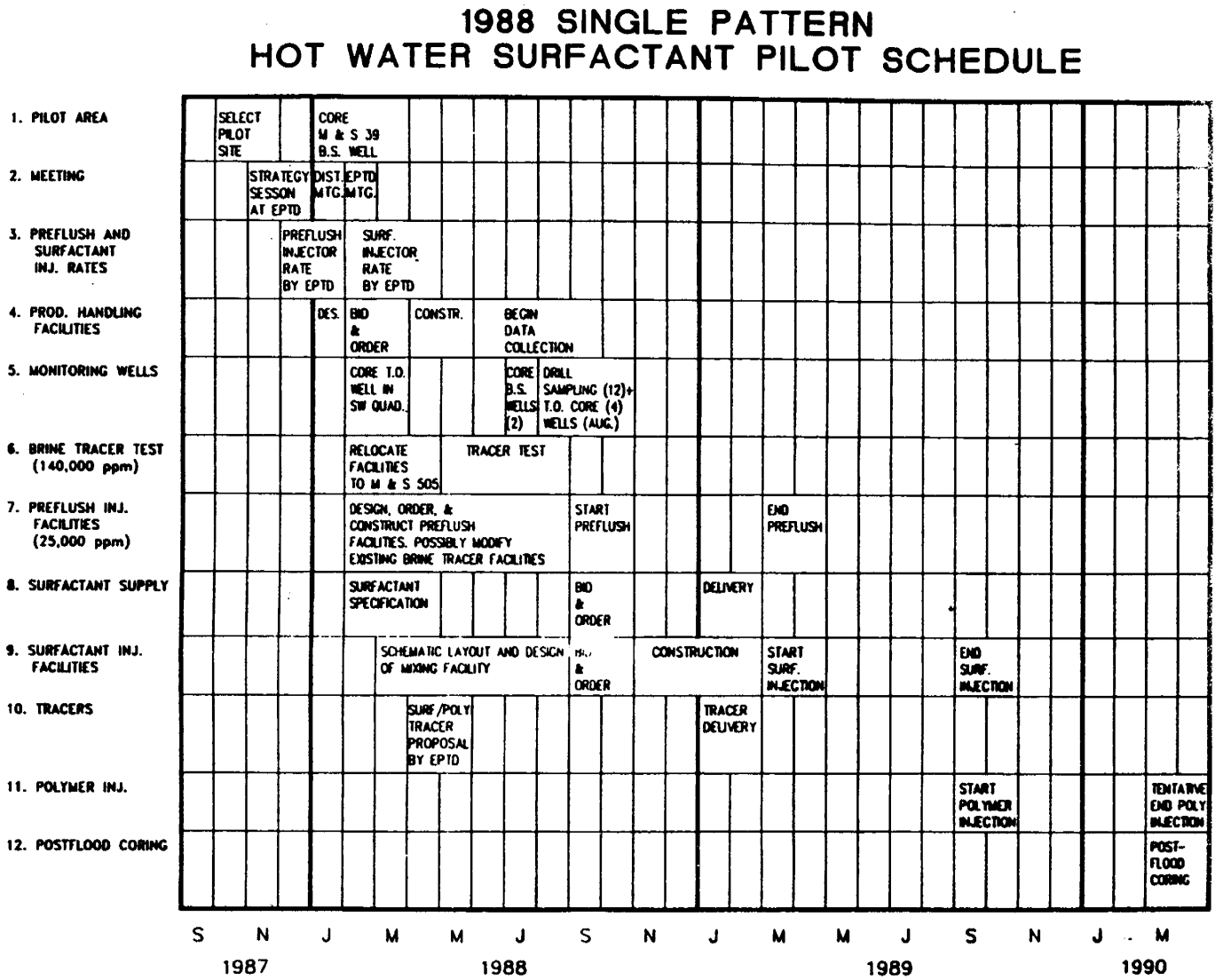

Figure 11) Schedule of the Texaco hot water surfactant pilot test. We plan to run underground imaging experiments during the pilot test.

Task 33 - INTEVEP shall provide DOE with information and results pertaining to electromagnetic properties of stratified media. Modeling of close hole arrays shall be performed to define optimun parameters for the design of surveys requiring well to well geometries.

FEASILIBITY STUDY FOR A WELL TO WELL ELECTROMAGNETIC PROSPECTING TECHNIQUE

(Task 33 of annex IV of the Implementing Agreement)

Prepared by
Herminio Passalacqua M.
INTEVEP, S.A.

Los Teques, Venezuela
February 1988

CONTENTS

	Page
ABSTRACT	33-4
LIST OF ILLUSTRATIONS	33-5
1. INTRODUCTION AND OBJECTIVES	33-7
2. INFLUENCE OF ANISOTROPY ON E.M. FIELDS	33-8
3. VERTICAL CABLE AS A SOURCE FOR E.M. FIELDS	33-10
4. ATTENUATION OF E.M. FIELDS DUE TO CASED BOREHOLES	33-11
5. CONCLUSIONS AND RECOMMENDATIONS	33-13
BIBLIOGRAPHY	33-14

ABSTRACT

A numerical modelling was carried out in order to analyse the feasilibity of well to well arrays for oil exploration or production.

Parameters like source-receiver separation, transmitter's frequency, source and receiver depth relative to the geological model, anisotropy and others, were considered.

The most practical approach seems to be the use of a vertical linear source because it produces a more homogeneous and stronger primary field.

LIST OF ILLUSTRATIONS

		Page
Fig. 1.	Geoelectrical model assumed for the calculations of the electromagnetic fields, showing the definition of the most important parameters.	33-15
Fig. 2.	Variation of the amplitude of the horizontal electric field against anisotropy of the first and third layer. Transmitter is located in the first layer.	33-16
Fig. 3.	Frequency response of the horizontal magnetic field for different values of the separation source-receiver. Transmitter at the third layer.	33-17
Fig. 4.	Frequency response of the horizontal magnetic field for different values of the separation source-receiver. Isotropic case. Transmitter at the third layer.	33-18
Fig. 5.	Amplitude variation of the horizontal electric-field with varying depth of receiver for different values of conductivity and anisotropy. Transmitter at the first layer.	33-19
Fig. 6.	Amplitude variation of the vertical electric field with varying depth of receiver for different values of conductivity and anisotropy. Transmitter at the first layer.	33-20
Fig. 7.	Amplitude variation of the horizontal electric field with varying depth of transmitter and receiver fixed at the surface for different values of conductivity and anisotropy.	33-21

Page

Fig. 8. Geometry and geological parameters for the calculations of the e.m. fields due to a vertical linear source. 33-22

Fig. 9. Amplitude plot of the magnetic field due to a linear source against frequency and horizontal separation source-receiver. 33-23

Fig. 10. Amplitude plot for the vertical electric field due to a linear source against frequency and receiver depth. 33-24

Fig. 11. Amplitude plot for the horizontal electric field due to a linear source against receiver's depth and source length. Fixed frequency. 33-25

Fig. 12. Geometry and electrical parameters assumed for the calculations of the attenuation of the e.m. fields. 33-26

Fig. 13. Variations of the amplitude of the horizontal electric field relative to the amplitude of the field in the half-space. Casing resistivity assumes six values. 33-27

Fig. 14. Variations of the amplitude of the horizontal electric field relative to the amplitude of the field in the half-space. Casing thickness assumes five values. 33-28

Fig. 15. Plot of the relative amplitude of the horizontal magnetic field showing its behaviour with horizontal distance and frequency. 33-29

1. INTRODUCTION AND OBJECTIVES

The application of electromagnetic prospecting techniques to the exploration or production of hidrocarbons has been widely treated in the literature. However, because of the practicality of data acquisition, most of this literature is concerned with source-receiver arrays located on the surface of the earth. But it is well known that the air-earth interface plays an important rol in the efficency of these techniques. This influence could be avoided, in principle, locating source and receiver underground.

INTEVEP, S.A. is carrying out a theoretical analysis of different methodologies of electromagnetic prospecting in order to understand the existing relationships between parameters like frequency of signal, source-receiver separation, depth of source and receiver, anisotropy of the medium, layer thicknesses, etc., for each component of the field. Mathematical expressions were derived and different numerical approaches were needed for the evaluation of the electromagnetic fields.

Three different aspects of the problem are considered in this report:

a) influence of anisotropy,
b) the use of a vertical conductor as a primary source for e.m. fields, and,
c) attenuation of fields due to cased boreholes;

for cases a) and b) the fields were evaluated in a common geological model of three horizontal layers with transverse anisotropy.

2. INFLUENCE OF ANISOTROPY ON E.M. FIELDS

Electrical conductivity in sedimentary rocks can be characterized by two constants which are direction dependent: longitudinal conductivity (parallell to stratification, σ_l) and transversal conductivity (perpendicular to stratification, σ_t).

A mathematical expression for each component of the field was obtained considering a three layered earth (Fig. 1) excited by a vertical electric dipole embedded in the medium. The quasi static approximation and exponentially varying fields (e^{-iwt}) were assumed.

In order to understand the influence of anisotropy on the e.m. fields calculations were carried our for different combinations of geoelectrical parameters.

For the geoelectrical model of Fig. 1, it was shown that for increasing anisotropies of the medium there is a decrease on the amplitude of each component of the field.

Fig. 2 shows the variations of amplitude for the real component of the horizontal electric field against variations of the anisotropy of the first and third layer. The uppermost curve was calculated for a value of σ_2/σ_1 = 0.1 and the lower most one for a ratio σ_2/σ_1 = 10. The thicknesses of the layers and the depth of receiver are indicated by h_1, h_2 and Z, respectively. These quantities are normalized by the transmitter's depth (h_0). The horizontal separation source-receiver (ρ) and the induction number (δ) are also normalized by h_0.

Fig. 3 shows the amplitude variation of the horizontal magnetic field against the induction number for different separations source-receiver, while Fig. 4 shows the same calculation for anisotropic medium. All the parameters are indicated in the illustrations. These two graphs are very similar in shape. The only difference being the amplitude variation.

When the receiver is moved vertically throughout the geological section, the horizontal electric field is discontinuous when the receiver crosses the interface between two layers. Notice that the amount of the discontinuity varies with conductivity and anisotropy (Fig. 5).

The conductivity contrast between two media can be quantified from the ratio of the amplitudes of the vertical electric field in each layer or medium (Fig. 6).

Also of interest is the behaviour of the horizontal electric field measured at the surface of the earth with a moving source (Fig. 7). Notice the changes of amplitude that occur when the transmitter crosses an interface and how these are related to the anisotropy of each layer.

3. VERTICAL CABLE AS A SOURCE FOR E.M. FIELDS

Expressions for the electromagnetic fields produced by a vertical cable of arbitrary length crossing a three-layered earth with uniaxial anisotropy in electrical conductivity and electrical permittivity have been derived. The fields are calculated in any point of space without considering the quasi-static approximation, so the computer modelling can be carried out for cross-hole and surface to hole arrays with not frequency limitations (Fig. 8).

A theoretical analysis, taking into account all the parameters involved in the calculation (cable length, frequency, source-receiver separation, conductivities, dielectric constants, anisotropy, field amplitudes, layer thicknesses, etc.), was carried out by means of two and three-dimensional plots in order to establish the optimum parameters for measurements of subsurface heterogeneities.

A model with Z_1 = 100 m, Z_2 = 1100 m and h = 1400 m was considered for this analysis.

Fig. 9 shows a plot of the amplitude of one of the components of the e.m. field with varying horizontal separation source-receiver. It was proved that the optimum separation is about 400 m. Eventhough this varies with the depth of the receiver.

Fig. 10 is a plot of the amplitude of the vertical electric field against depth of receiver and log of frequency. The biggest amplitude corresponds to the horizontal magnetic field and the best frequency range will be from 0,1 to 100 Hz.

Fig. 11 is the calculated variation of the amplitude of the horizontal electric field against cable length and receiver depth. Notice the big anomaly that occurs when the receiver crosses a resistive layer. These values were calculated for a frequency of 1 Hz.

4. ATTENUATION OF E.M. FIELDS DUE TO CASED BOREHOLES

Expressions for the electromagnetic fields produced by a vertical electric dipole placed on the axis of a concentrically three-layered borehole environment of infinite length with uniaxial anisotropy in electrical conductivity and electrical permittivity have been derived. The fields are calculated in any point of space without considering the quasi-static approximation, so the computer modelling can be carried out in any medium with no frecuency limitations. In order to evaluate the attenuation due to casings in cases where the well to well geometry is used these fields are compared to the ones produced by a half-space.

A theoretical analysis, considering the attenuation of the electromagnetic fields in the external medium as a function of frequency, conductivities, dielectric constants, anisotropy, thicknesses, source-receiver separation, etc., related to the field measured in an anisotropic, homogeneous and infinite medium, was carried out. Two and three dimensional plots allow us to make such analysis in a global way.

Fig. 12 shows the geometry of this problem. The most internal medium has the electrical properties of air. To the external layer was assigned a resistivity of 100 ohm-m and the second layer will have a variable resistivity. The internal radius of this layer will be 7 cm and the external will be variable in principle.

In Fig. 13 the relative amplitude of the horizontal electric field is plotted against the log of frequency. Each curve is calculated for a different resistivity of the second layer (casing) and notice that for values of this parameter bigger than 1 ohm-m the relative amplitude of any component of the field is very close to 100%.

For a casing thicker than 3 cm the relative amplitude of the horizontal magnetic field will be less than 60% of the field in a half-space (more than 40% of attenuation) for low frequency. It was assumed a resistivity of 0,001 ohm-m for the casing (Fig. 14).

Finally Fig. 15 shows the behaviour of the relative amplitude of the magnetic field as a function of the horizontal separation source-receiver and of frequency. It was assumed a thickness of 1,5 cm and a resistivity of 0,001 ohm-m for the intermediate layer. For frequencies below 1 KHz the amplitude is independent on frequency. The amplitude increases with the separation from the source. For higher frequencies the amplitude approaches to an asintotic value for higher separations from the source.

5. CONCLUSIONS AND RECOMMENDATIONS

From the numerical modeling just described the following conclusions can be drawn:

a) For a hole to hole geometry a very diagnostic information for exploration and/or production purposes can be obtained when transmitter or receiver crosses the boundary of an inhomogeneity. However, in some cases it is possible to sense such anomalies when transmitter or receiver are located at the half the depth of the target.

b) The most important effect of anisotropy can be seen on the amplitude of the fields.

c) Linear sources of current, will prove a very practical technique for the improvement of e.m. prospecting, if the following facts are considered:

- The crossing of the intermediate layer in a three layer model with a linear source is a sufficient condition for determining its geoelectrical parameters.

- Compared to dipolar sources, linear sources will generate bigger amplitudes of fields and will allow a bigger depth of penetration.

d) Magnetic fields suffer less attenuation due to a metallic casing eventhough it decays faster with the increasing of frequency.

BIBLIOGRAPHY

1. Michelena, R. and Passalacqua, H. Campos Electromagnéticos Producidos por un Dipolo Eléctrico Vertical en un Medio Estratificado y Anisótropo. INT-01726,86, INTEVEP, S.A. 1986.

2. Michelena, R. and Passalacqua, H. Campos Electromagnéticos Debido a un Dipolo Eléctrico Vertical para un Arreglo Pozo a Pozo en una Tierra Estratificada. INT-01630,86, INTEVEP, S.A. 1986.

3. Whait, J. Analysis for the Electromagnetic Fields of a Dipole Located Within a Metal-Cased Borehole, Journal of Applied Physics, v. 48, n. 3, p.1009-1012. 1976.

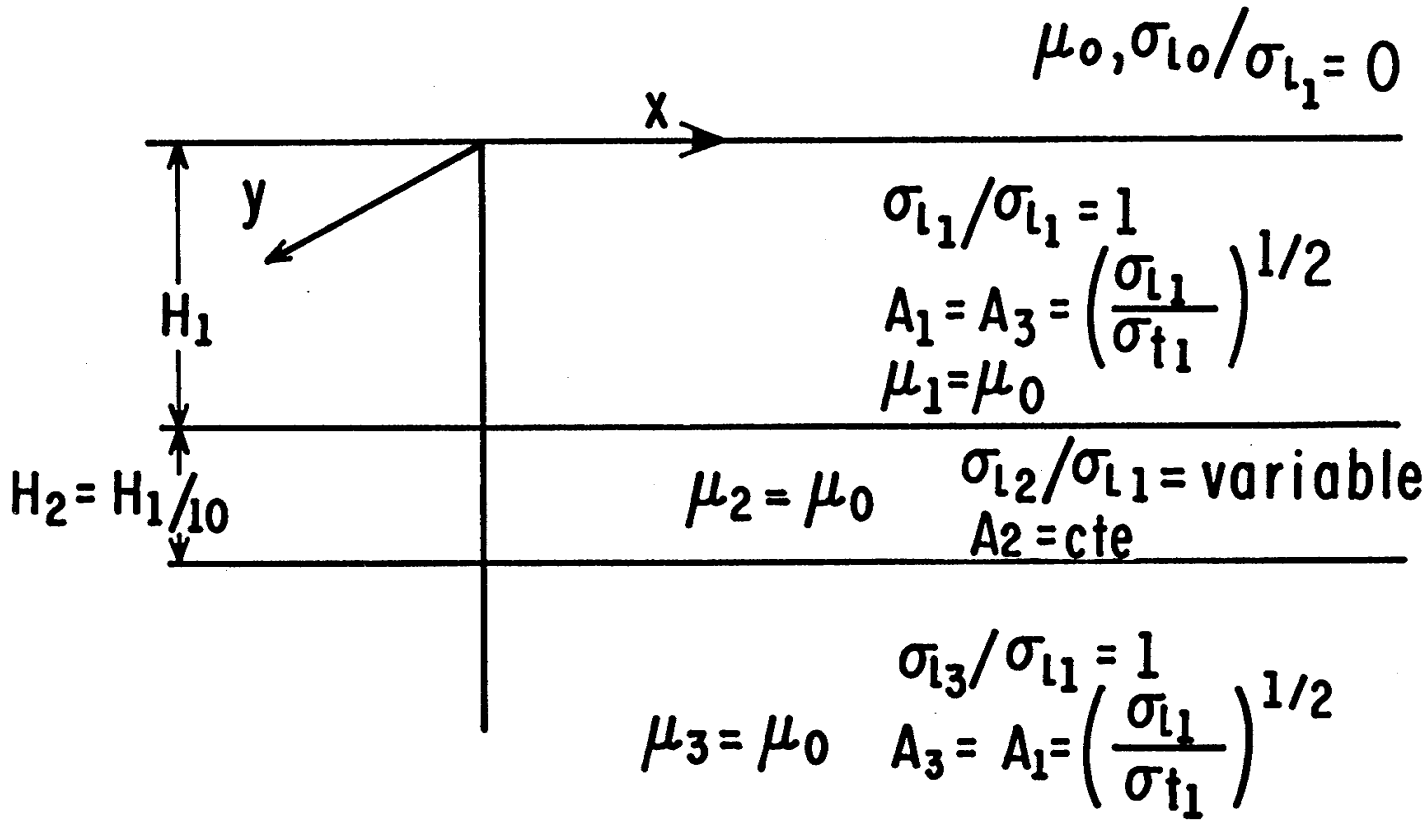

Fig. 1. Geolectrical model assumed for the calculations of the electromagnetic fields, showing the definition of the most important parameters.

Intevep, S.A. Centro de Investigación y Desarrollo, Filial de Petroleos de Venezuela, S.A.

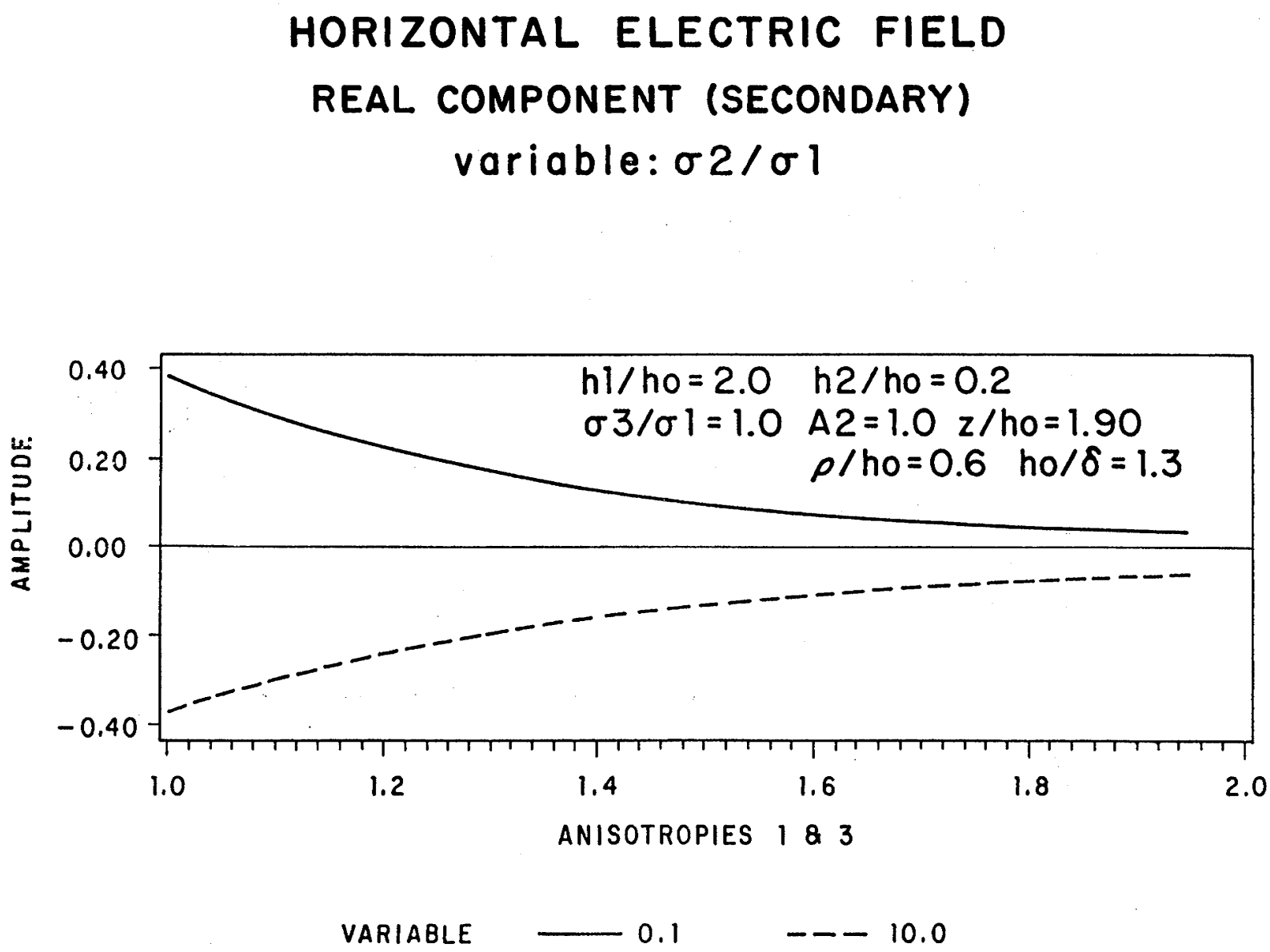

Fig. 2. Variation of the amplitude of the horizontal electric field against anisotropy of the first and third layer. Transmitter is located in the first layer.

Intevep, S.A. Centro de Investigacion y Desarrollo, Filial de Petroleos de Venezuela, S.A.

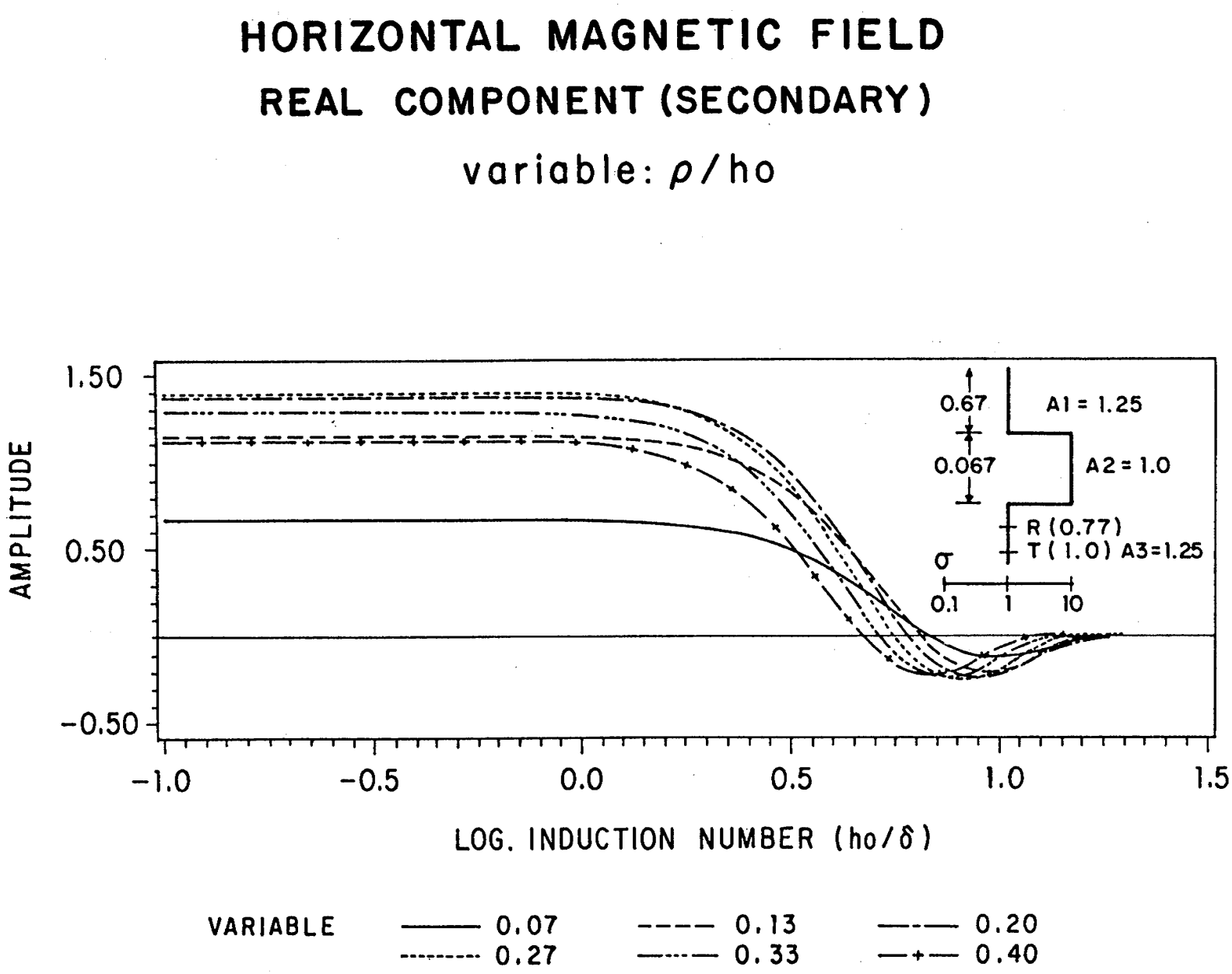

Fig. 3. Frequency response of the horizontal magnetic field for different values of the separation source-receiver. Transmitter at the third layer.

Intevep, S.A. Centro de Investigación y Desarrollo, Filial de Petróleos de Venezuela, S.A.

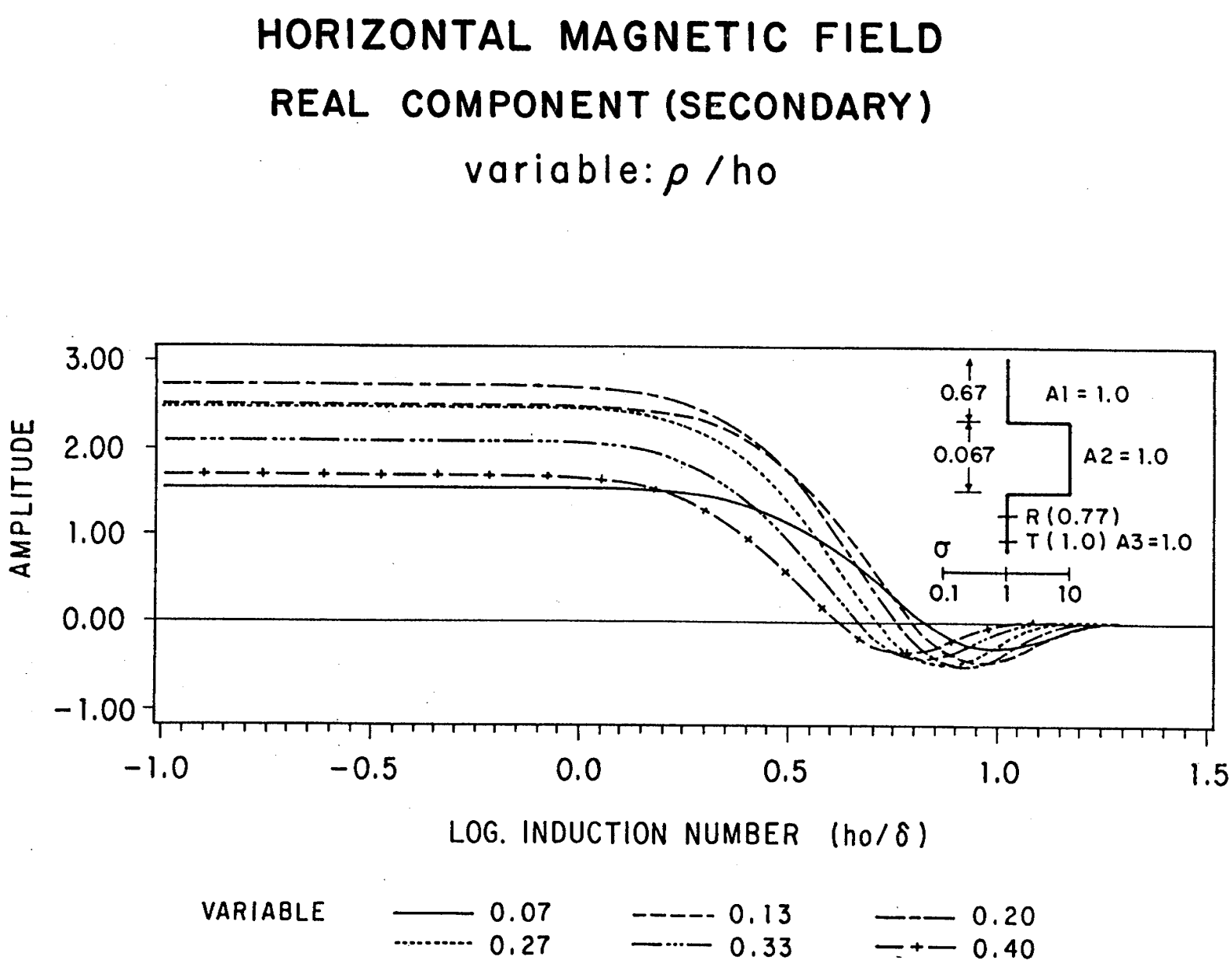

Fig. 4. Frequency response of the horizontal magnetic field for different values of the separation source-receiver. Isotropic case. Transmitter at the third layer.

Intevep, S.A. Centro de Investigación y Desarrollo, Filial de Petróleos de Venezuela, S.A.

HORIZONTAL ELECTRIC FIELD

REAL COMPONENT (SECONDARY)

variables: σ2/σ1 y A1 = A3

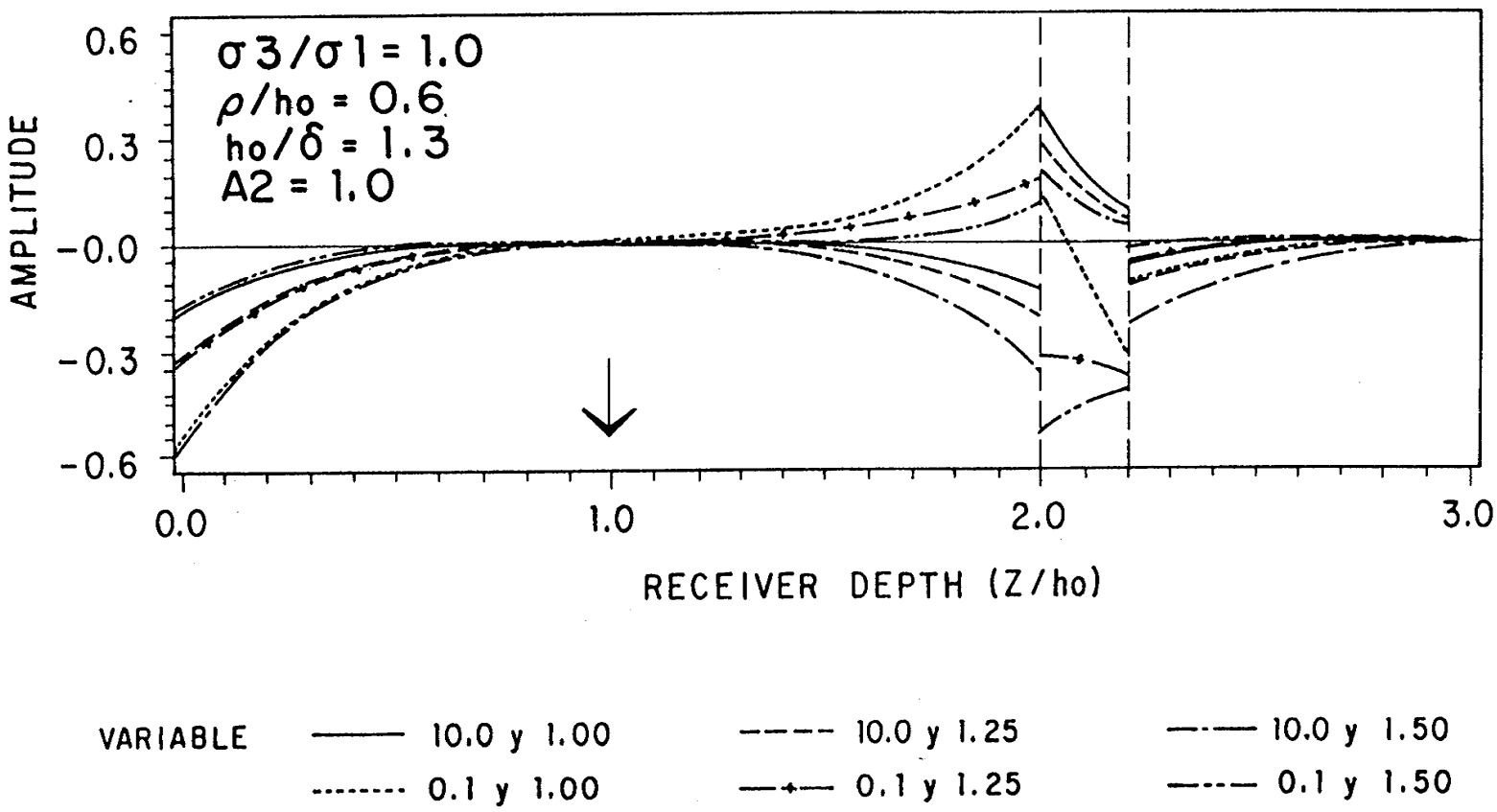

Fig. 5. Amplitude variation of the horizontal electric-field with varying depth of receiver for different values of conductivity and anisotropy. Transmitter at the first layer.

Intevep, S.A. Centro de Investigación y Desarrollo, Filial de Petróleos de Venezuela, S.A.

VERTICAL ELECTRIC FIELD

REAL COMPONENT (TOTAL)

variables: σ2/σ1 y A1 = A3

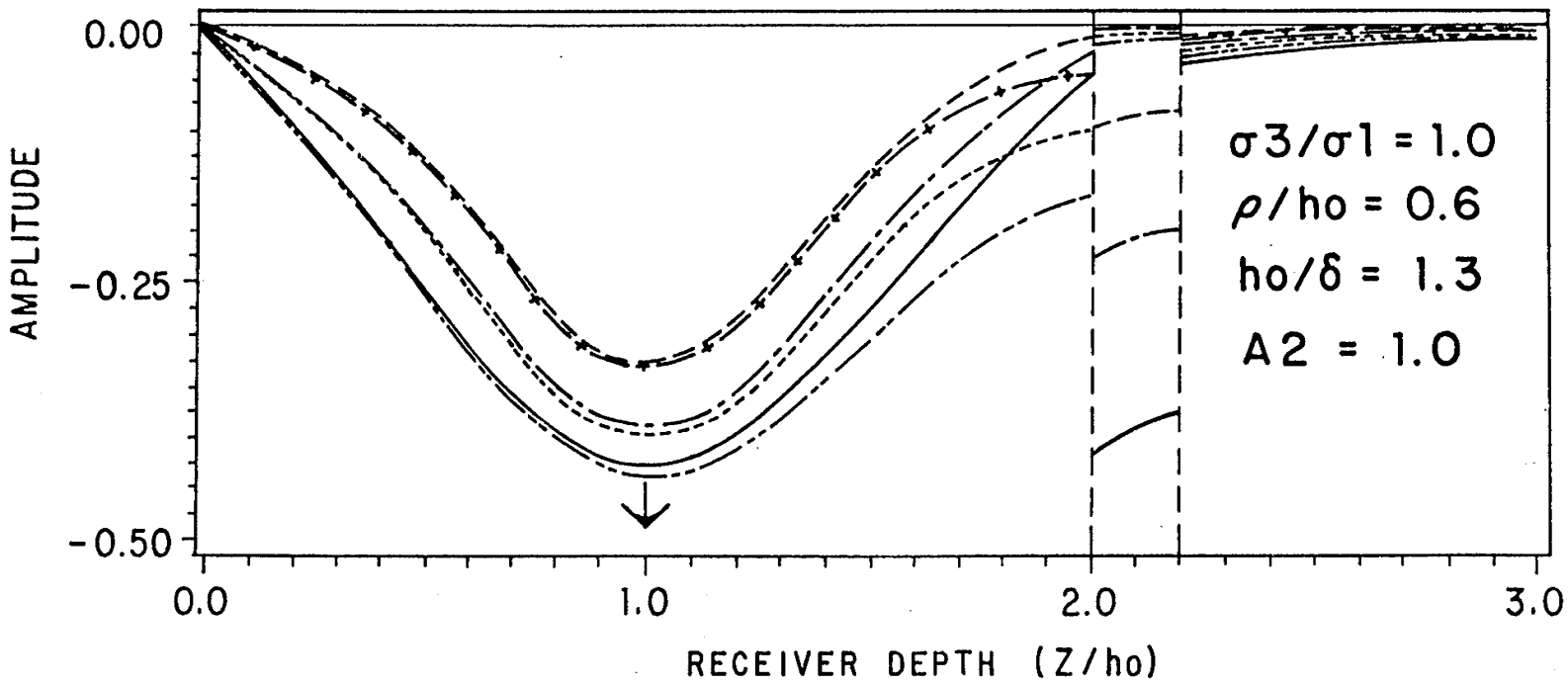

VARIABLE ——— 0.1 y 1.00 —-— 0.1 y 1.25 ---- 0.1 y 1.50

—--— 10.0 y 1.00 ------- 10.0 y 1.25 —+— 10.0 y 1.50

Fig. 6. Amplitude variation of the vertical electric field with varying depth of receiver for different values of conductivity and anisotropy. Transmitter at the first layer.

Intevep, S.A. Centro de Investigación y Desarrollo, Filial de Petroleos de Venezuela, S.A.

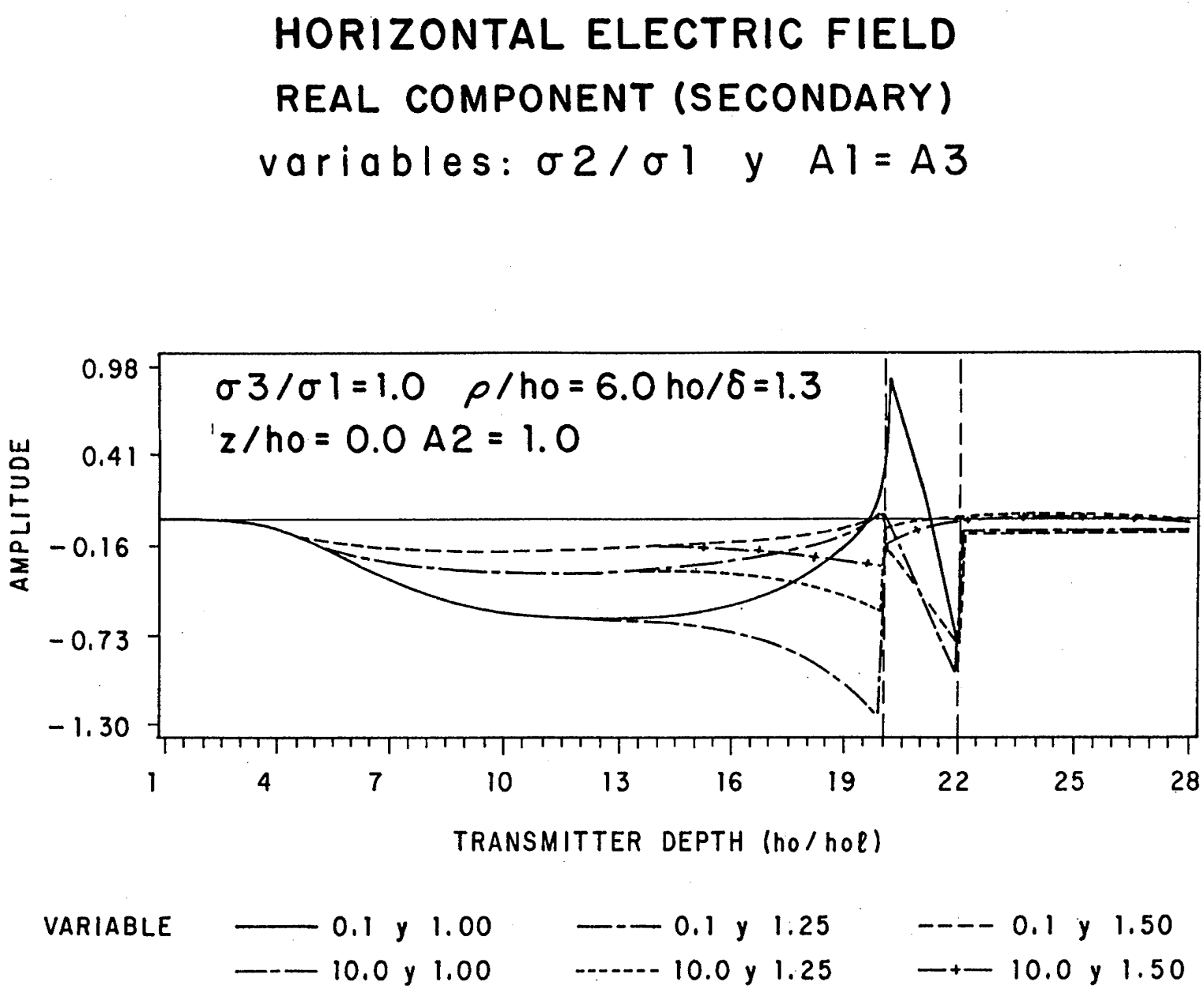

Fig. 7. Amplitude variation of the horizontal electric field with varying depth of transmitter and receiver fixed at the surface for different values of conductivity and anisotropy.

Intevep, S.A. Centro de Investigación y Desarrollo, Filial de Petróleos de Venezuela, S.A.

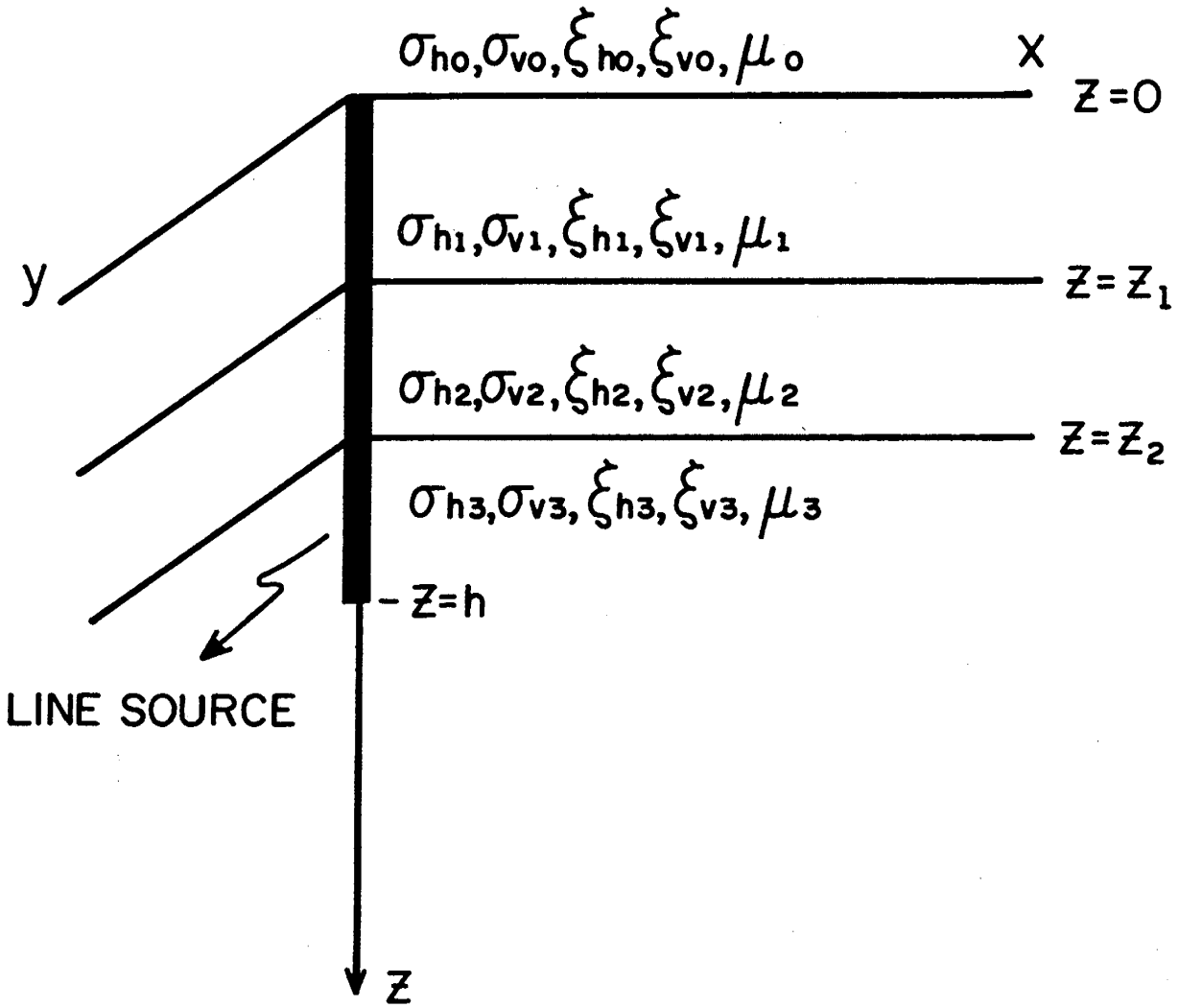

Fig. 8. Geometry and geological parameters for the calculations of the e.m. fields due to a vertical linear source.

Intevep, S.A. Centro de Investigación y Desarrollo, Filial de Petróleos de Venezuela, S.A.

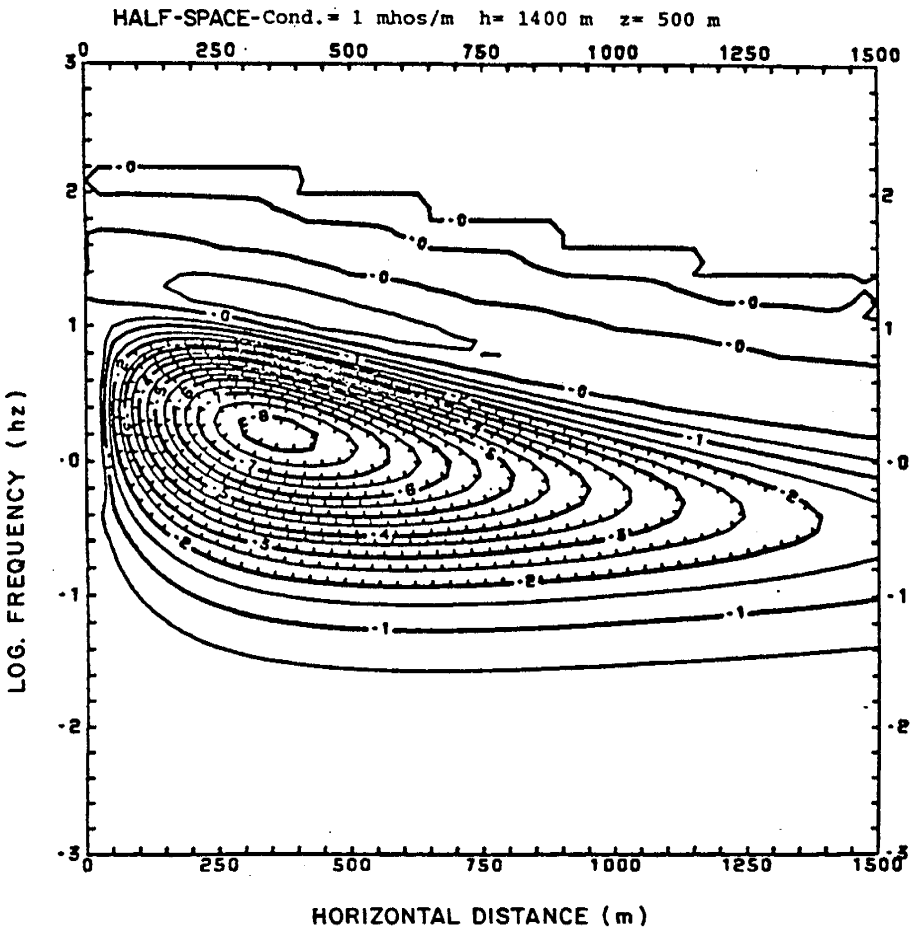

Fig. 9. Amplitude plot of the magnetic field due to a linear source against frequency and horizontal separation source-receiver.

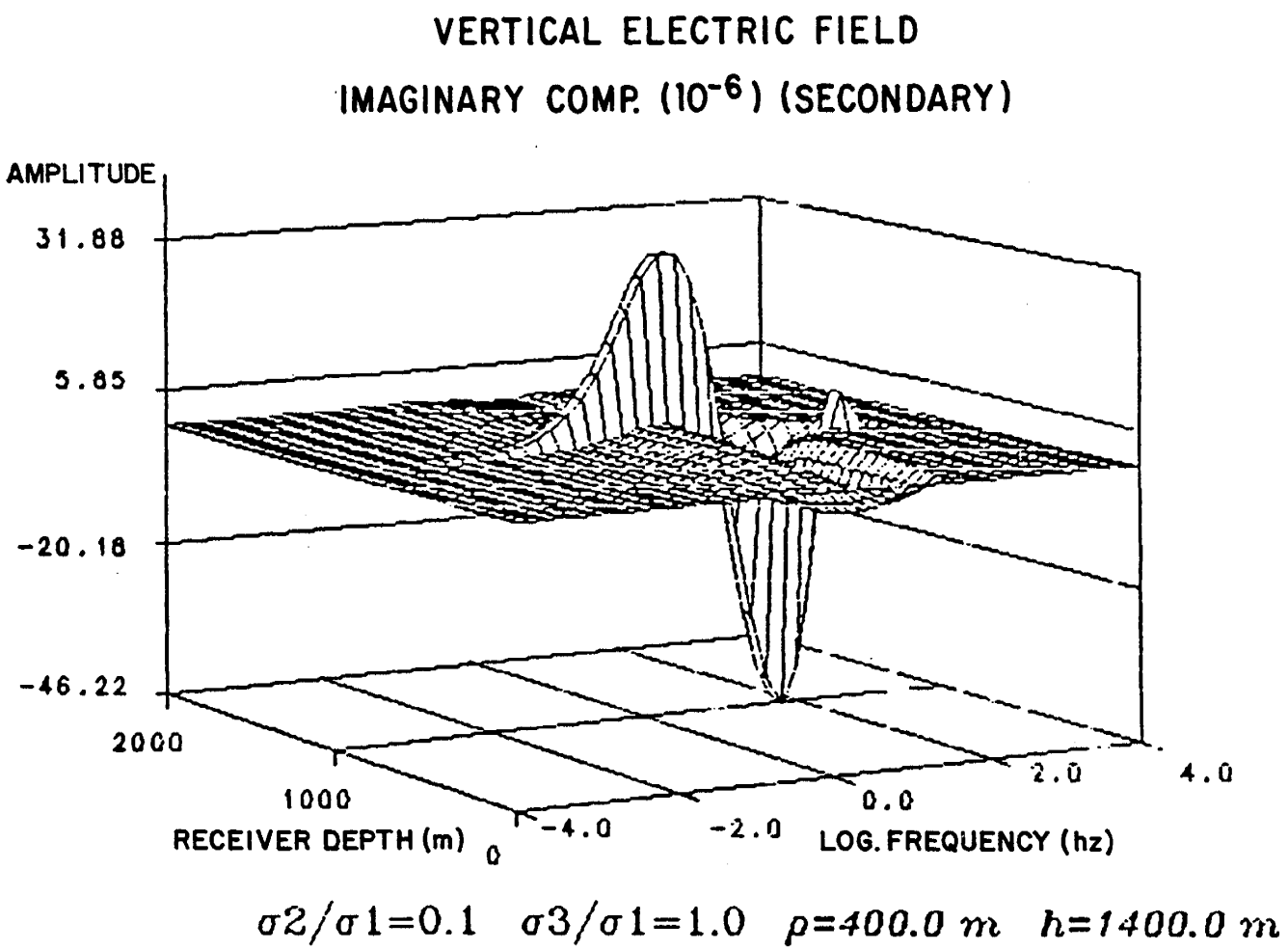

Fig. 10. Amplitude plot for the vertical electric field due to a linear source against frequency and receiver depth.

Intevep, S.A. Centro de Investigación y Desarrollo, Filial de Petróleos de Venezuela, S.A.

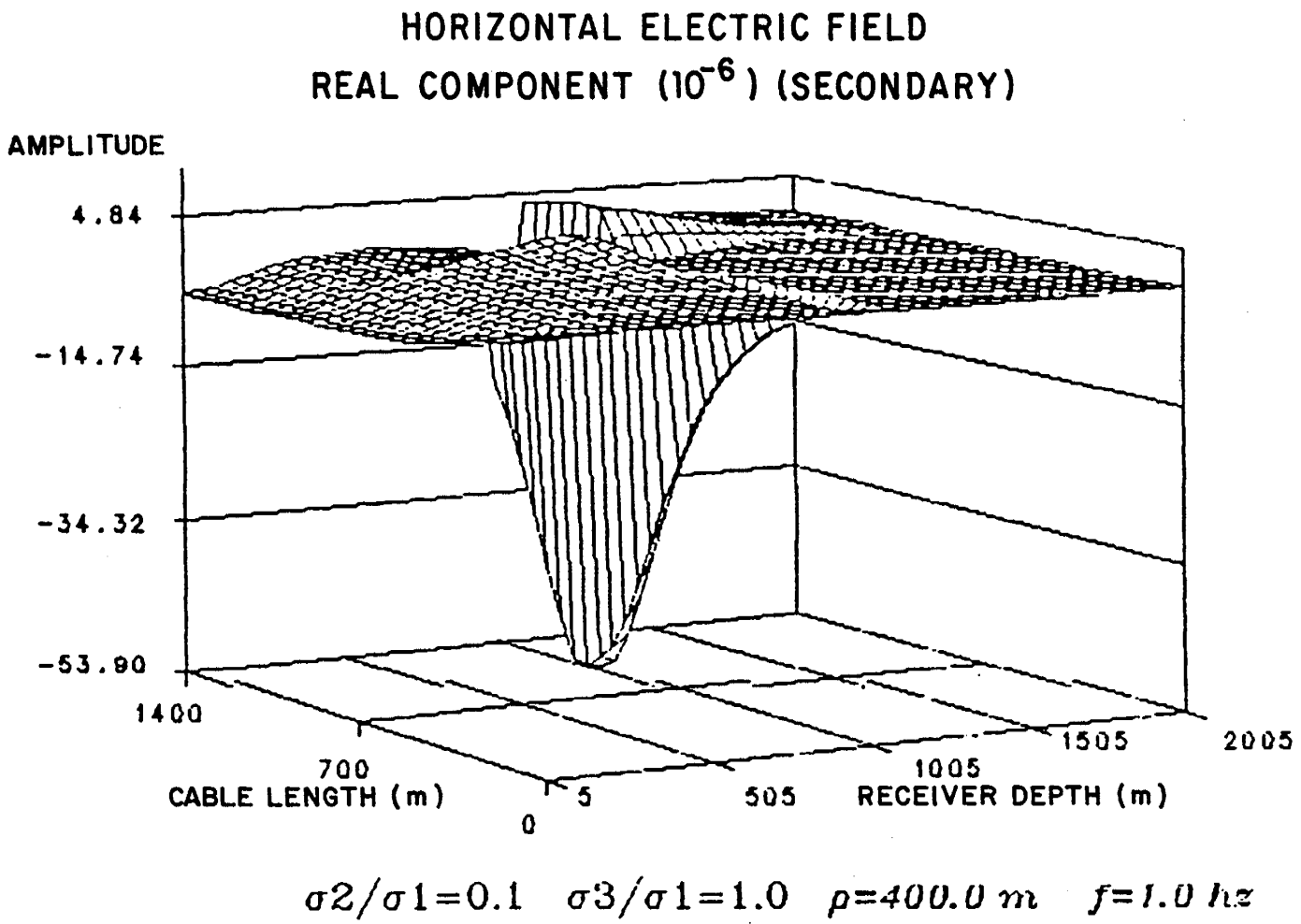

Fig. 11. Amplitude plot for the horizontal electric field due to a linear source against receiver's depth and source length. Fixed frequency.

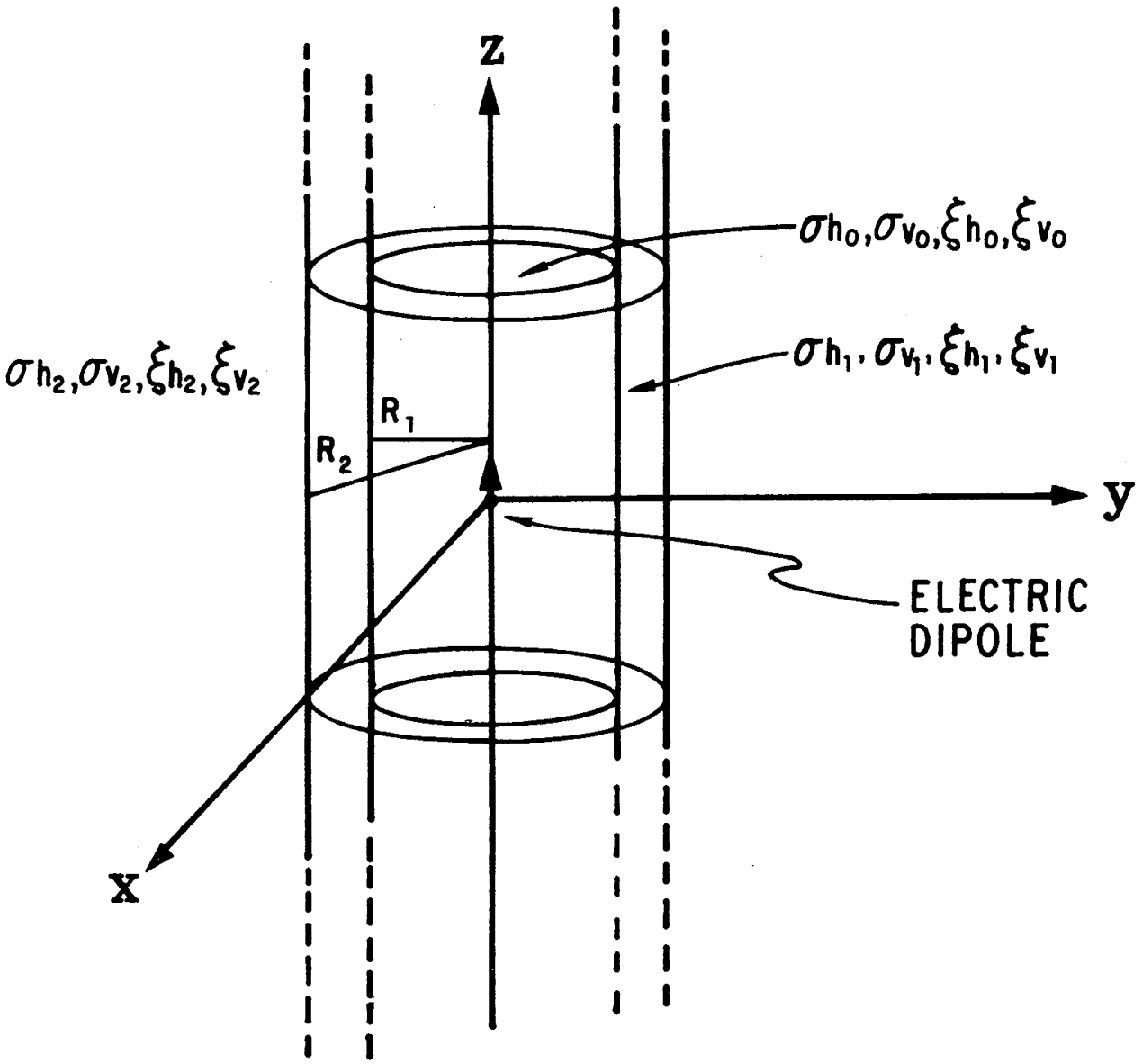

Fig. 12. Geometry and electrical parameters assumed for the calculations of the attenuation of the e.m. fields.

Intevep, S.A. Centro de Investigación y Desarrollo, Filial de Petróleos de Venezuela, S.A.

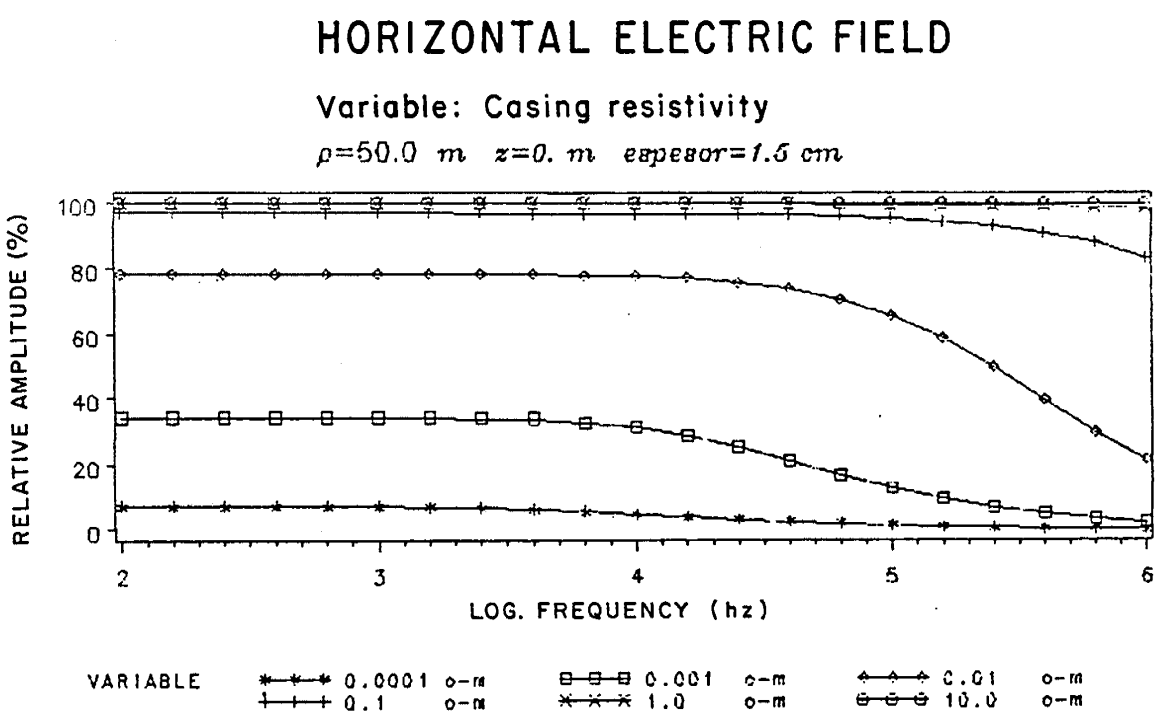

Fig. 13. Variations of the amplitude of the horizontal electric field relative to the amplitude of the field in the half-space. Casing resistivity assumes six values.

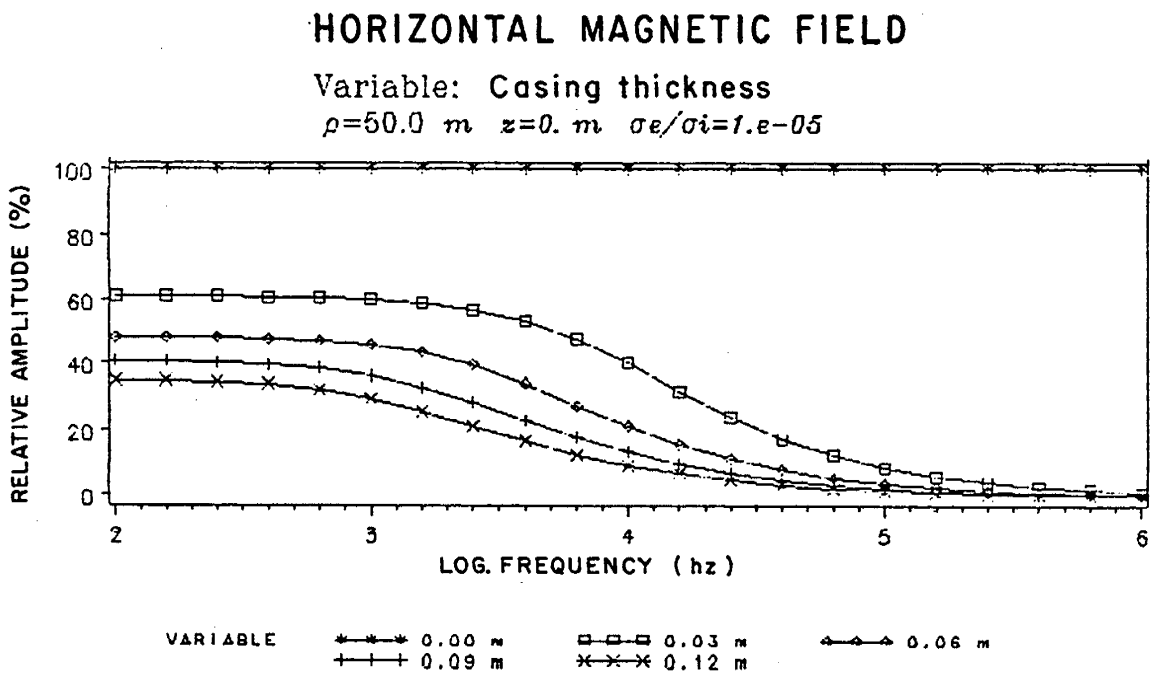

Fig. 14. Variations of the amplitude of the horizontal electric field relative to the amplitude of the field in the half-space. Casing thickness assumes five values.

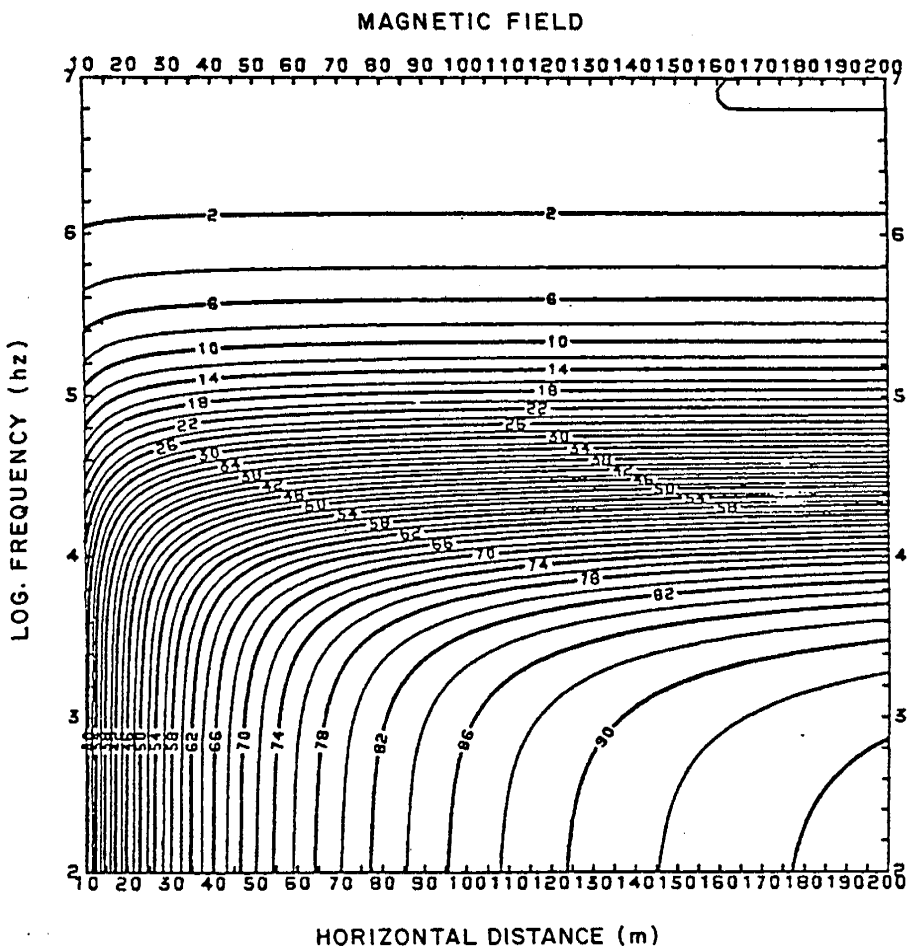

Fig. 15. Plot of the relative amplitude of the horizontal magnetic field showing its behaviour with horizontal distance and frequency.

Intevep, S.A. Centro de Investigación y Desarrollo, Filial de Petróleos de Venezuela, S.A.

Task 34 - INTEVEP shall provide DOE with information from research and screening tests performed by INTEVEP related to steam-foam displacement and cyclic stimulation. The Project Managers shall consult with one another concerning screening tests and exchange information obtained to avoid unnecessary duplication of research efforts.

INFLUENCE OF A SURFACTANT ON THE STEAM PRODUCTION CHARACTERISTIC PARAMETERS

(Task 34 of Annex IV of the Implementing Agreement)

Prepared by:
José Luis Ziritt
Guido Bresolin

INTEVEP, S.A.
Los Teques - Miranda
Venezuela

March 1988

SUMMARY

A study on the steam production characteristic parameters has been carried out to evaluate and understand the results of a cyclic steam-surfactant injection test carried out in the Bolívar Coast in Venezuela.

Through the field test performance and displacement laboratory tests it has been determined that steam diversion and oil relative permeability increase are the two main mechanisms responsible for the improved oil production observed in the field test. However, the relative contribution of these mechanisms to oil production is unbalanced, being steam diversion the most important one.

CONTENT

	Page
SUMMARY	34-3
1. INTRODUCTION	34-5
2. FIELD TEST	34-6
3. OIL/WATER RELATIVE PERMEABILITY	34-8
4. STEAM DIVERSION LABORATORY STUDY	34-10
5. CONCLUSIONS	34-12
REFERENCES	34-13
FIGURES	34-14

1. INTRODUCTION

Steam soak is the most practiced thermal recovery process in Venezuela and the world. From the start of its use in the early 60's, it has continuously developed and its application nowadays is a usual field task.

Nevertheless, steam injection is not free of problems. The performance of the process is influence by the poor vertical and areal steam distribution, as a consecuence of using a gas to heat a liquid. Thus, the low density and viscosity of steam are responsible for its tendency to override through the top of the injected formations and to channel through high permeability and/or previously heated zones.

Injection of mobility control agents has been proposed as a method to improve steam distribution (1). Accordingly, a research program on the use of foaming agents was conducted, followed by a field pilot test involving 16 cyclic steam injection wells of Tia Juana, Lagunillas and Bachaquero fields in Venezuela (2, 3). The wells were stimulated with steam and two different foaming surfactants. Production response of test wells is encouraging (4). However, a detailed evaluation and understanding of the process is needed to optimize the use of the surfactants.

Based on the field results, laboratory research has continued with the purpose of determining the effect of a surfactant on the steam production characteristic parameters. This report presents the first results of this research effort, which shows the existance of important changes in fluids distribution and flow during injection and production of the wells. These parameters should be evaluated when considering the use of a surfactant as an additive to steam.

2. FIELD TEST

The field test was carried out in 16 wells of Tia Juana, Lagunillas and Bachaquero fields in the Bolívar Coast area in Venezuela. Two different foaming surfactants, selected through laboratory tests, were used. A linear alkyltoluene sodium sulphonate (LTS) and a branched alkylbenzene sodium sulphonate (BBS).

Details of the test are presented in the chapter related to Task 36 in this same report. Therefore, following we will only mention the outstanding facts of the field test that have guided the laboratory research.

When the test wells were injected, steam distribution in the sand face was evaluated through the use of spinner surveys known as flowmeters. As an example, Fig. 1 shows the steam distribution in well LSE-2705 during steam alone and steam-surfactant injection. It is clearly observed that the surfactant diverts steam from the top most zone of the reservoir to other sands which were not previously steam stimulated. Steam diversion due to the presence of the added surfactants was observed in all the wells, through in various degrees.

Well head injection pressure was another parameter monitored during the tests. An initial small pressure increment was observed as steam was injected during the first 5 days (Fig. 2). On the other hand, when a surfactant was added to the injected steam, a substancial injection pressure increase was observed. This phenomenon is caused by the blocking properties of the steam-surfactant mixture as reported in our previous laboratory works (5, 6).

Once the wells were injected they were put on production. Most of the wells have shown an oil production increment with respect to the expected production of a conventional cycle if only steam had been injected. As reported in Task 39, the incremental oil production correlates with the steam diversion achieved during injection. However, other production mechanisms influenced by the added surfactants are involved.

In all the wells treated with LTS surfactant, the initial oil production was associated with very high water-cuts (90%) which lasted for several months (aprox. 8 months) before they decreased to normal 20%-30% cuts. On the contrary to the wells stimulated with LTS, when using BBS water-cuts where similar to those of a conventional steam soak.

The field test injection and production information digest lead to evaluate the influence of the surfactants on the oil/water relative permeability curves and the injection profile.

3. OIL/WATER RELATIVE PERMEABILITY

Displacement tests in Berea cores were performed to determine the influence of the surfactants on the relative permeability curves. Tests were performed by displacing oil both with water and 0.5% w/w active matter surfactant solutions. The relative permeability curves were calculated using Welge's method (7) corrected for the end effects through Odeh and Dotson's theory (8).

The influence of LTS on the water/oil relative permeability curves is presented in Fig. 3. First, we can observe that LTS shifts the oil relative permeability curve to a lower residual oil saturation (end point) and to slightly higher relative permeability values.

The change in the oil relative permeability curve will be responsible for part of the incremental oil production observed in the field test. Moreover, if the residual oil saturation is shifted to a lower value, as it seems to be the case, then higher oil recoveries will be achieved with the use LTS.

The second phenomenon observed in Fig. 3 is that LTS dramatically increases relative permeability to water. This increment, in over 6 times its original value, supports the inconventional high water-cut observed in the wells stimulated with LTS. The later reduction of water-cut is probably associated to desorption of the surfactant from the porous medium and/or to simply water desaturation.

The influence of the change in water relative permeability on the water-cut production was corroborated with the results observed using BBS surfactant. As shown in Fig. 4, BBS seems not to influence the water relative permeability curve and in this case, field production water-cuts were normal.

Here again as for LTS surfactant, BBS apparently increases oil relative permeability values. However, the shift in the two cases are too small to completely support the average 24% oil production increment reported for the field test. The relative contribution of oil relative permeability increase

and steam diversion to oil production is unbalanced, being steam diversion in this case the most important mechanism.

4. STEAM DIVERSION LABORATORY STUDY

Through the field test results it has been shown that the performance of a steam stimulation process can be enhanced by using an additive to divert steam. Yet, oil production can still be improved by using a foaming surfactant that will also favorably change the oil/water relative permeability curves.

To study the importance of steam diversion and the possibility of combining this mechanism with changes in the permeability parameters, a two-dimensional high pressure displacement cell has being design. The experimental equipment consists of a two-dimensional sand pack prepared in a thin wall stainless steel cell measuring 60 cm in length, 30 cm in height and 7 cm in width. The cell has a 54 thermocouples grid in the vertical plane along the flow direction, which allows to continously monitor the heat front when steam is injected. As shown in the schematic representation of the equipment in Fig. 5, the experimental cell is placed insulated in a pressure vessel and thermocouples, balances and pressure transducers are branched to a computarized data gathering system.

Fig. 6 shows a straight to the flow cross-section of the experimental cell placed inside the pressure vessel. Two different materials are used to insulate the cell. First, the cell is wrapped in a 4 cm Fiberfrax blanquet and then the annulus is filled with expanded clay. Several thermocomples were placed within the insulating material to evaluate heat loss during a steam injection test (see Fig. 6).

Fig. 7 presents the temperature profile evolution in the insulating media starting at one point on the wall of the experimental cell and towards the pressure vessel wall placed at a distance of 23 cm. As it can be observed the insulating media behaves as a semi-infinite material towards which heat from the experimental cell is transfered.

A simple mass and heat balance model was developed to calculate the heated volume (steam zone volume) in the experimental cell. The insulating material

was characterized asuming heat transfer to a semi-infinite medium. For a set of experimental tests carried out at a pressure range of 300-500 psi and injection rates of 20-40 cc/min, the model adequately fits the experimental results as shown in Fig. 8.

Up to date, laboratory work has been focussed to evaluate the performance of the equipment by steaming the sand pack to displace water. Fig. 9 shows the heat efficiency of several tests carried out under different experimental conditions. It was found that the experimental set-up is more efficient when steam is injected at 30 cc/min (cold water equivalent). At this rate, small pressure variations will have little or no influence on the results. This optimum rate is due to the steam override phenomenon combined to the heat loss. High steam rates produce early steam breakthroughs and, on the other hand, if steam rate is too low then heat losses become too important.

The effect of a surfactant on the injection profile can be easily visualized on Figs. 10 and 11. They respectively present the steam front profile as a function of time when injecting steam and steam-surfactant. The foaming agent clearly ameliorates the vertical sweep efficiency of steam. As shown in Fig. 12, heat efficiency is also improved due to the reasons mentioned before.

Future work will be carried out on oil saturated sand packs and will be focussed to evaluate the performance of foaming surfactants that also increase oil relative permeability curves.

5. CONCLUSIONS

Two different mechanisms are responsible for the improved oil production observed in the Bolívar Coast steam-surfactant pilot test: steam diversion and oil relative permeability increase.

However, the relative contribution of these mechanisms to oil production is unbalanced, being steam diversion in this case the most important one.

The best surfactant additive for steam soak processes will probably be one which adequately combines the two mechanisms that improve oil production. Hence, research in this sense will be continued by using the two-dimensional displacement cell set up for this purpose.

REFERENCES

1. DILGREN, R.E.; HIRASAKI, G.J.; HILL, H.J. and WHITTEN, D.G.: U.S. Patent 4,086,964.

2. D'ORAZIO, F.; ZIRITT, J.L.; RONDON, L.; RUBIO, R.; PAZ. E.; RIVAS, O. and PAZ, F.: "Pruebas Piloto de Inyección Alternada de Vapor con Surfactantes" Paper Presented at the II Simposio Internacional sobre Recuperación Mejorada de Crudo, Maracaibo, February 1987, Proc. Vol. II, pp. 245-273.

3. ROBAINA, R. and ZIRITT, J.L.: "Evaluation of a Surfactant-Steam Soak Pilot Test in the Bolívar Coast, Venezuela", Paper SPE/DOE 17386, Presented at the SPE/DOE Sixth Symposium on EOR, Tulsa, April 1988.

4. ZIRITT, J.L. and RIVAS, O.: "Evaluation of a Cyclic Steam-Surfactant Injection Pilot Test in the Bolívar Coast, Venezuela", IV European Meeting on Improved Oil Recovery, Hamburg, 27-29 October 1987, Proc. pp 611-622.

5. ZIRITT, J.L.; RANCEL, C. and PAZ, F.: "Properties of Anionic Surfactants and their Use as Diverting Agents", EOR Thermal Processes, DOE/BC-86/2/SP, March 1986, pp 18.1-18.63.

6. ZIRITT, J.L.; PAZ, F. and RANCEL C.: "Steam-Surfactant Process - A Laboratory Research and a Field Application", Paper Presented at the 3rd European Meeting on Improved Oil Recovery, Rome, April 1985, Proc. Vol. I, pp. 341-348.

7. WELGE, H.J.: "Simplified Method for Computing Oil Recoveries by Gas or Water Drive", Trans. AIME (1952) 195, pp. 91-98.

8. ODEH, A.S. and DOTSON, B.J.: "A Method for Reducing the Rate Effect on Oil and Water Relative Permeabilities Calculated from Dynamic Displacement Data". J. Pet. Tech. (Nov. 1985) pp. 2052-2058.

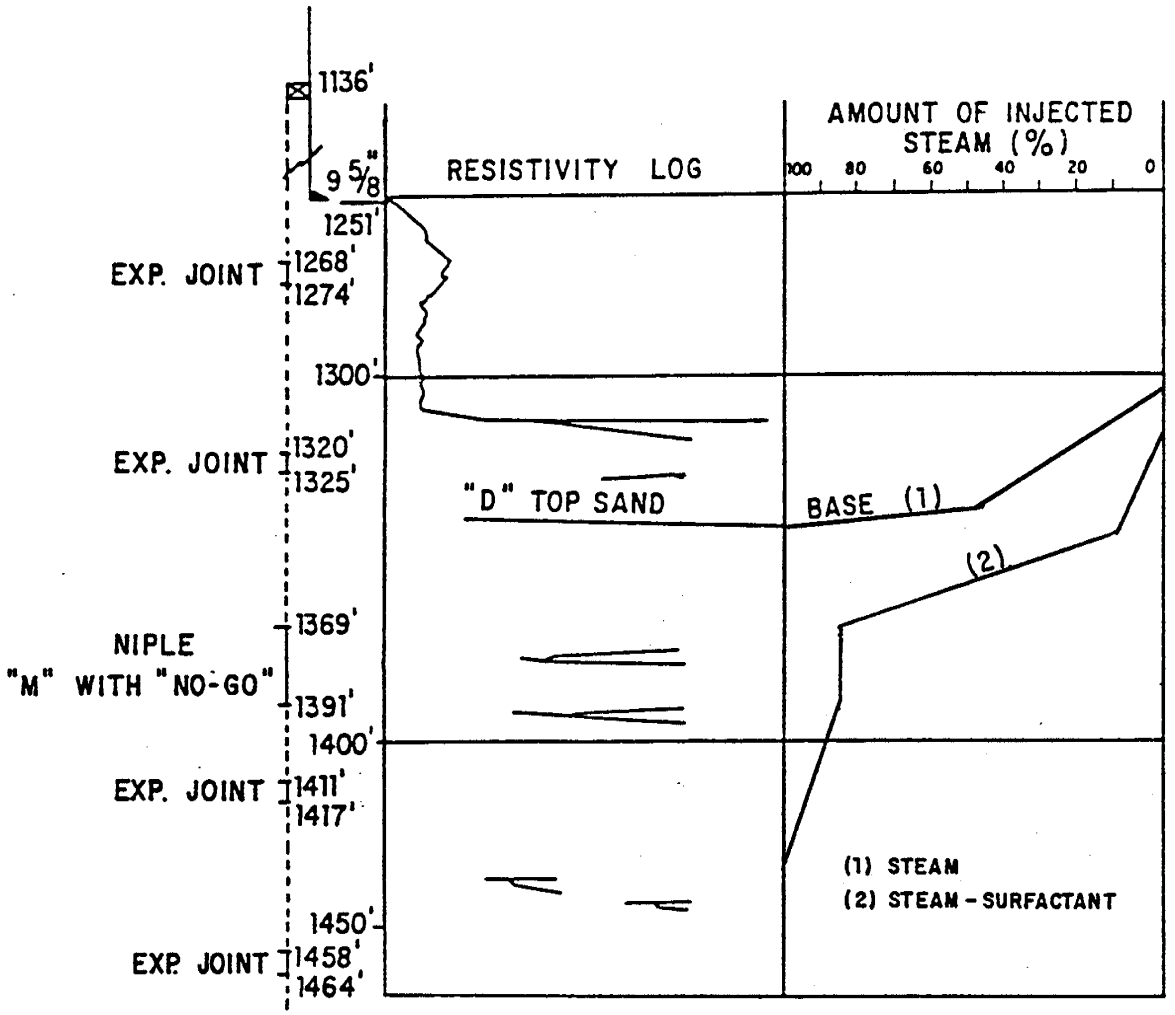

FIG. 1 INFLUENCE OF LTS SURFACTANT ON THE STEAM INJECTION PROFILE IN WELL LSE-2705

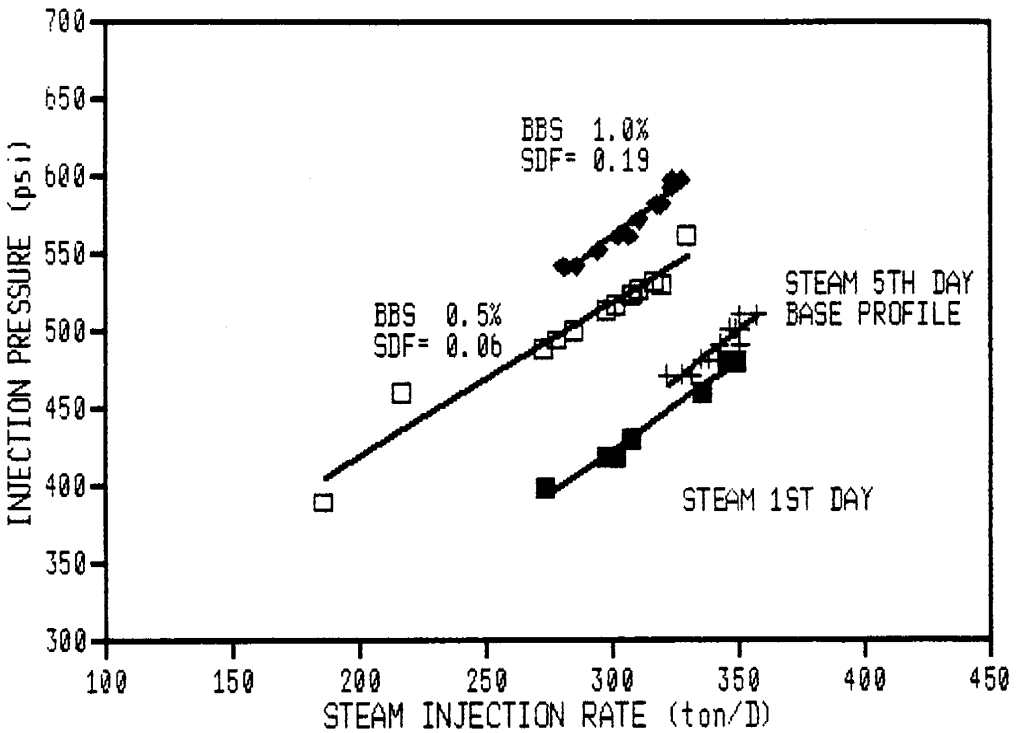

FIG. 2 INFLUENCE OF SURFACTANT CONCENTRATION ON THE WELL HEAD INJECTION PRESSURE OF WELL LSE-3116

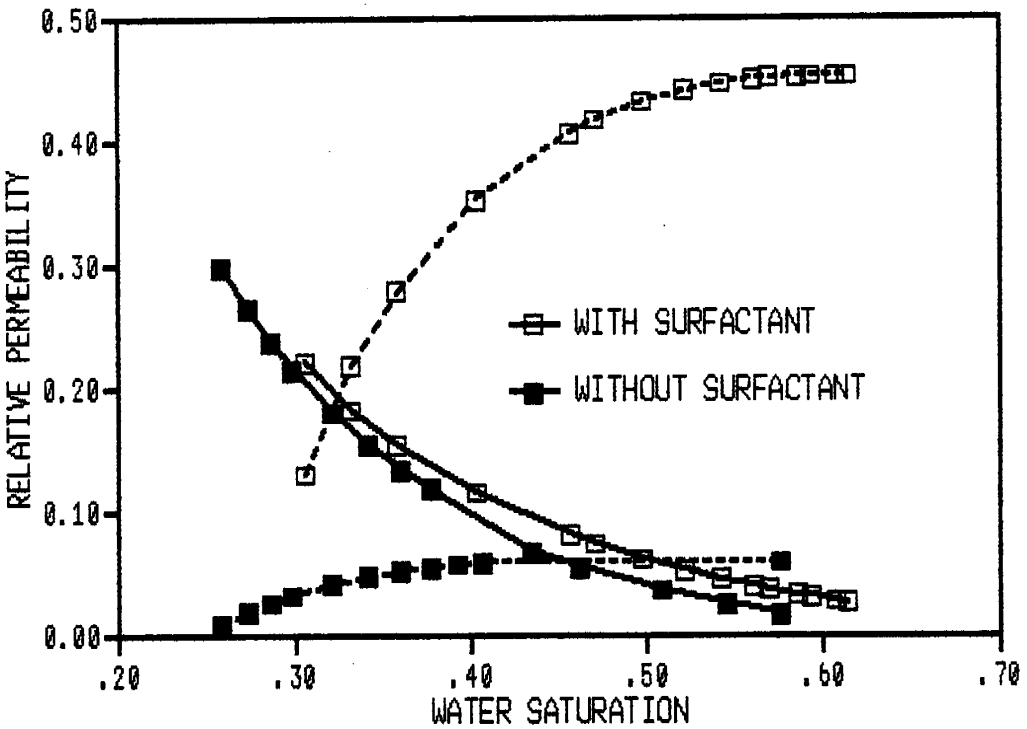

FIG. 3 INFLUENCE OF LTS SURFACTANT ON THE OIL/WATER RELATIVE PERMEABILITY CURVES

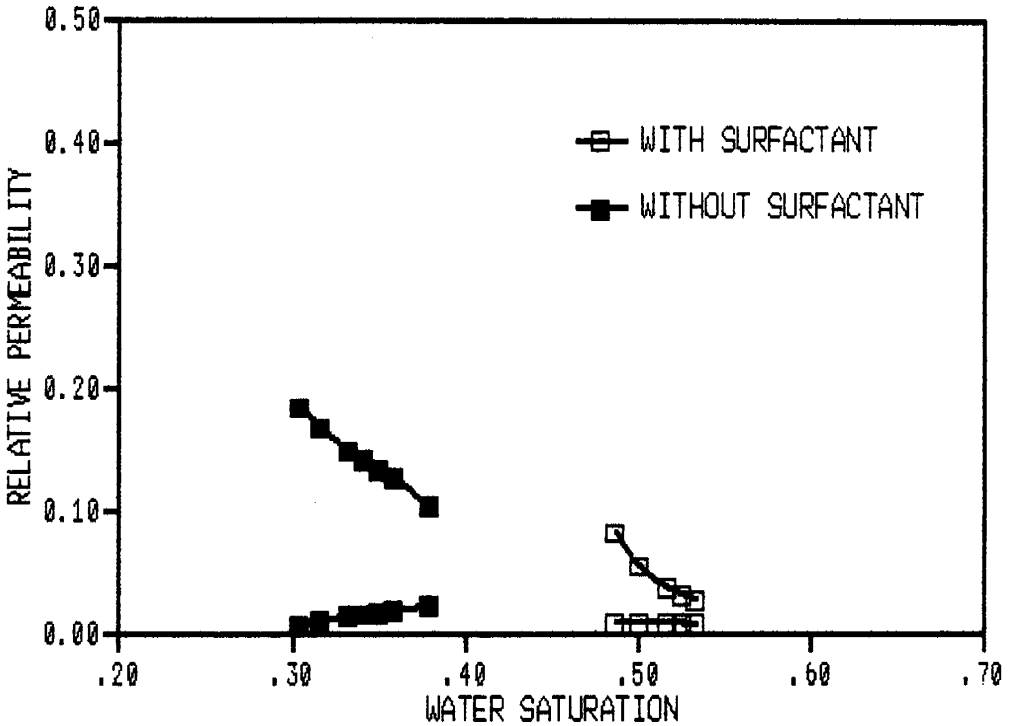

FIG. 4 INFLUENCE OF BBS SURFACTANT ON THE OIL/WATER RELATIVE PERMEABILITY

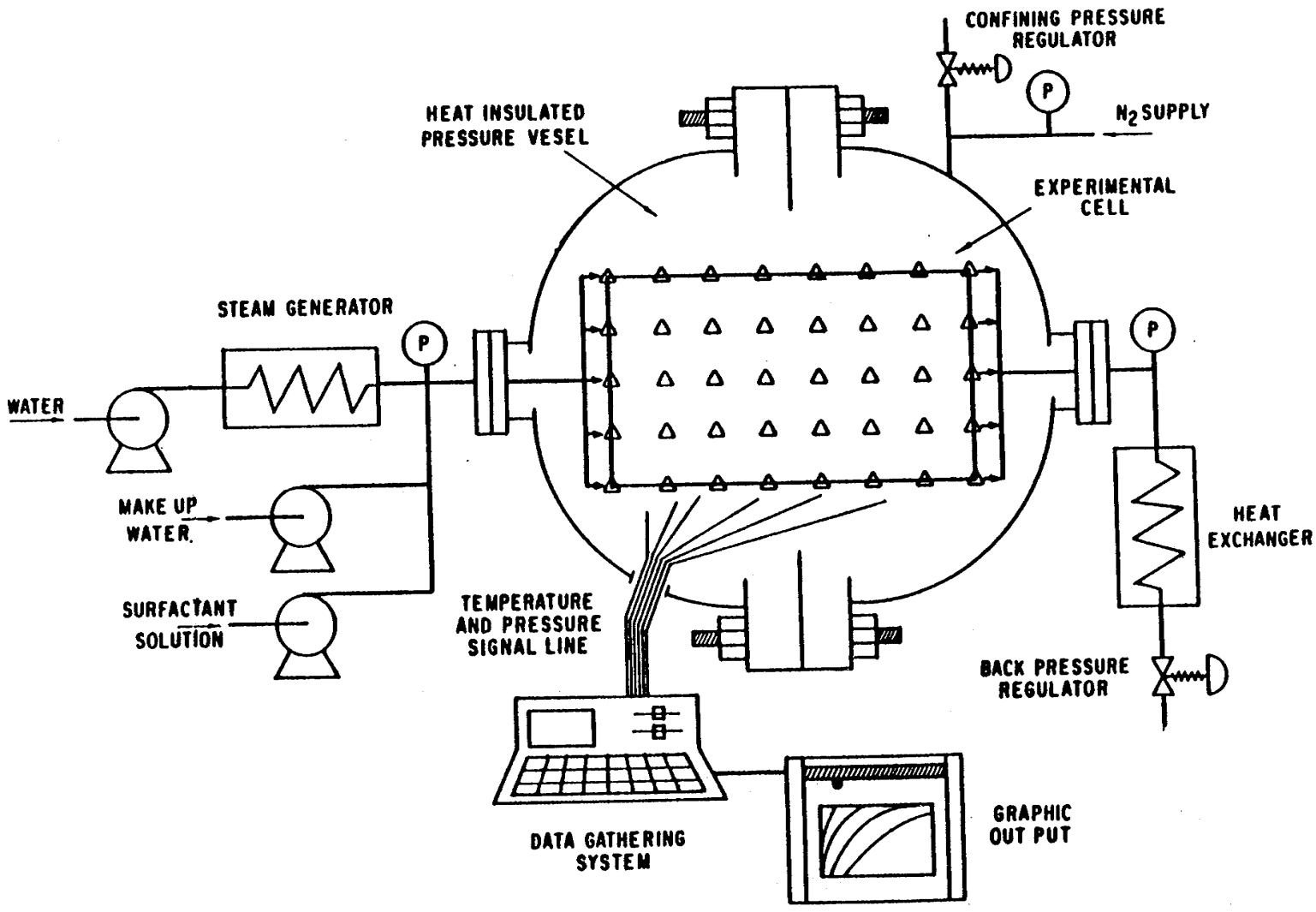

Fig. 5 TWO DIMENSIONAL HIGH PRESSURE DISPLACEMENT CELL

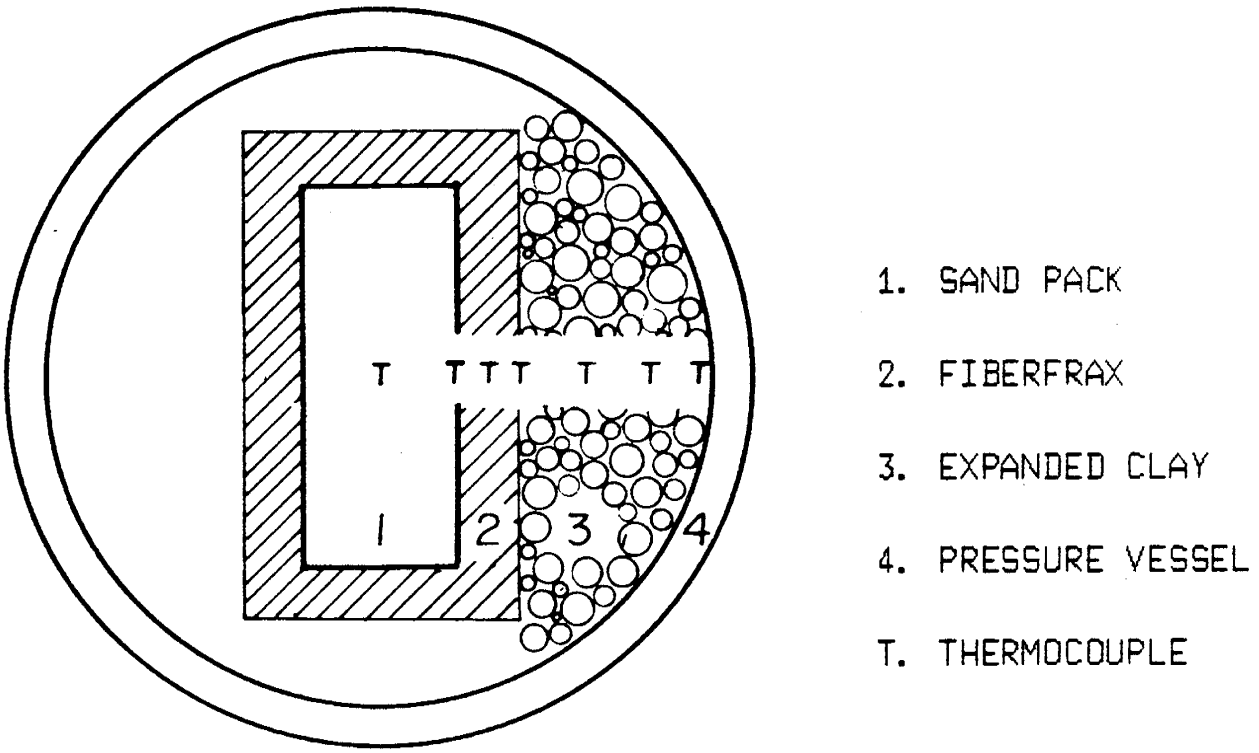

FIG. 6 CROSS SECTION OF THE EXPERIMENTAL CELL PLACED INSIDE THE PRESSURE VESSEL

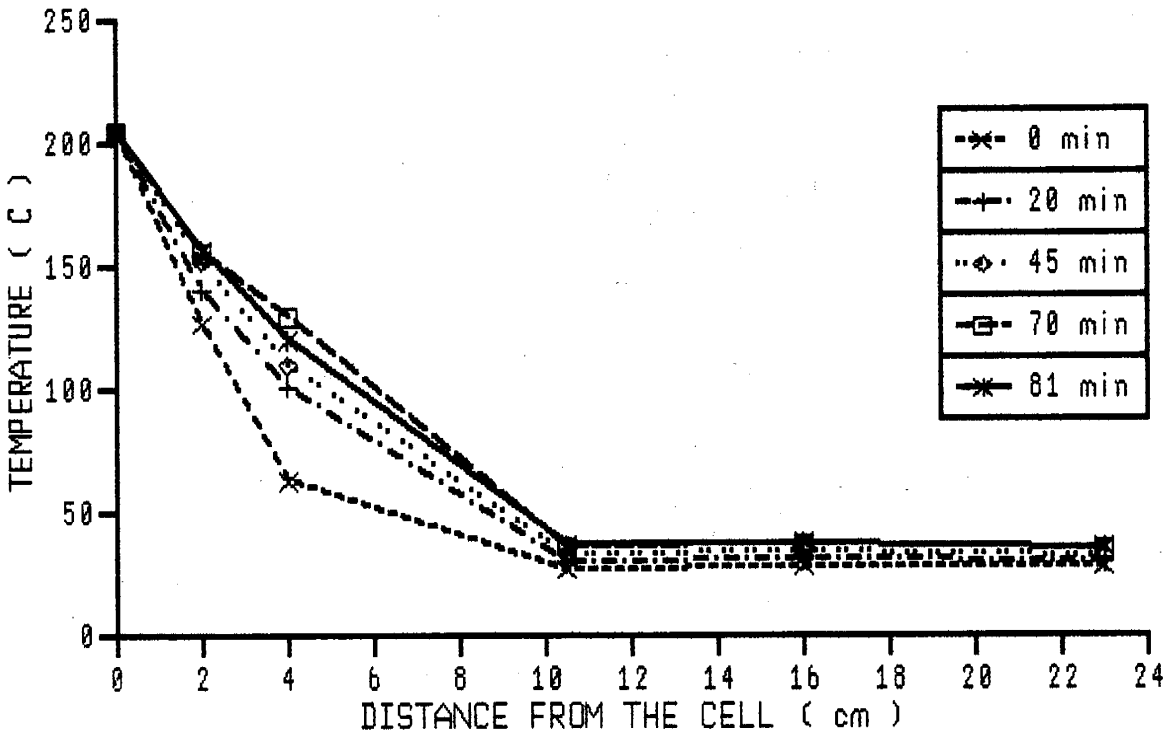

FIG. 7 TEMPERATURE PROFILE EVOLUTION IN THE INSULATING MEDIA

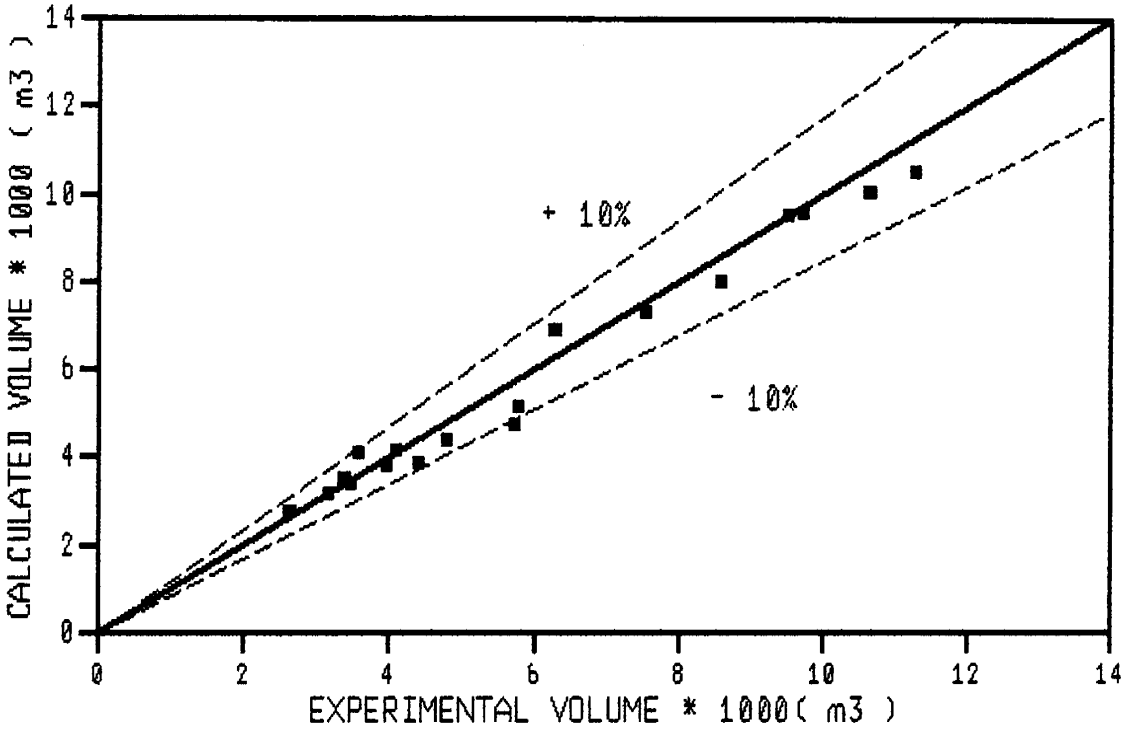

FIG. 8 EXPERIMENTAL vs. CALCULATED STEAM ZONE VOLUME

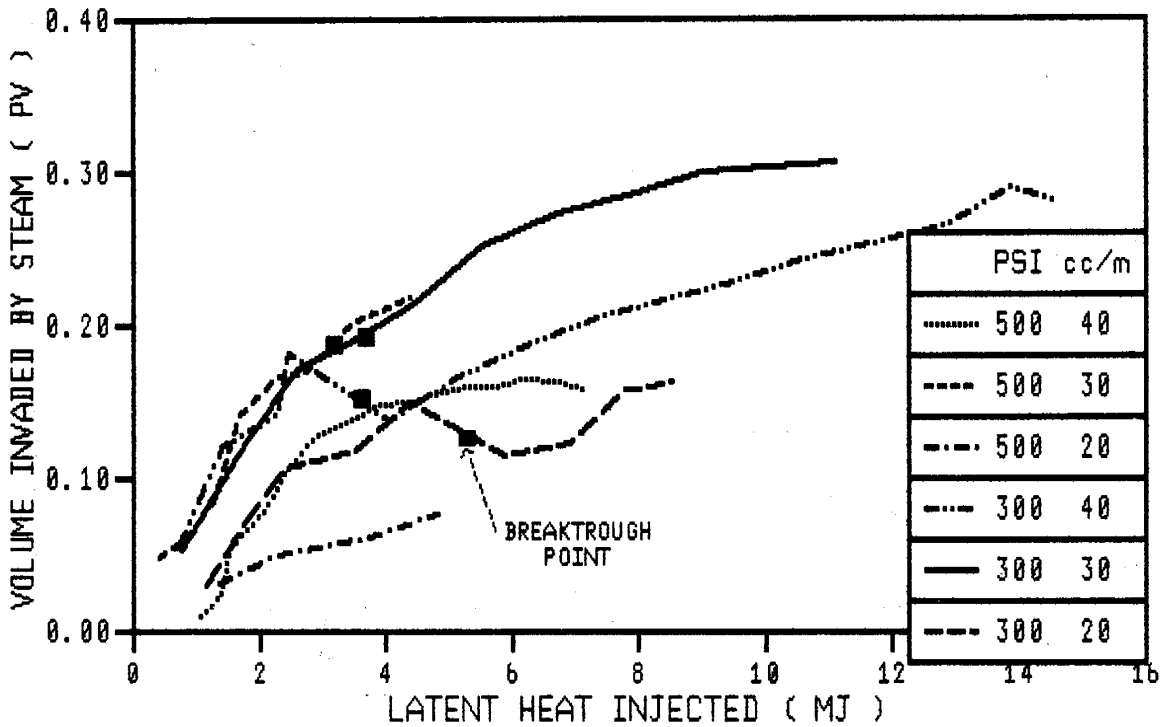

FIG. 9 STEAM ZONE VOLUME AS A FUNCTION OF THE INJECTED HEAT

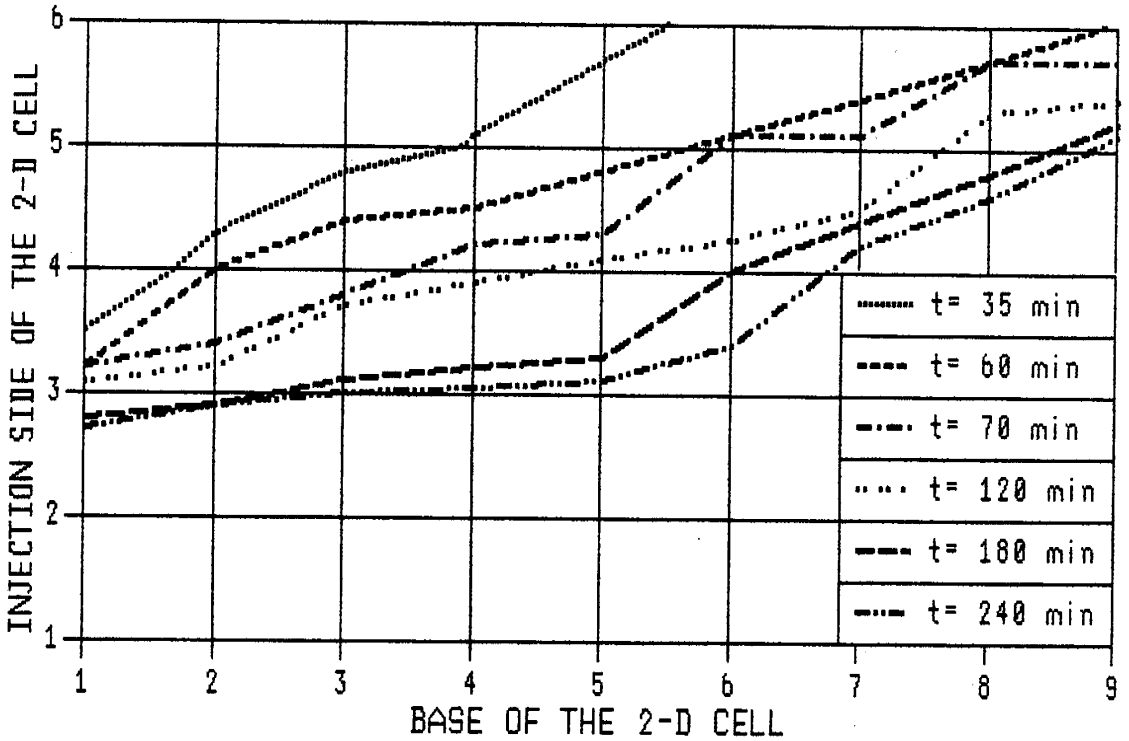

FIG. 10 STEAM FRONT PROFILES FOR STEAM INJECTION AT 300 PSI AND 30 CC/MIN

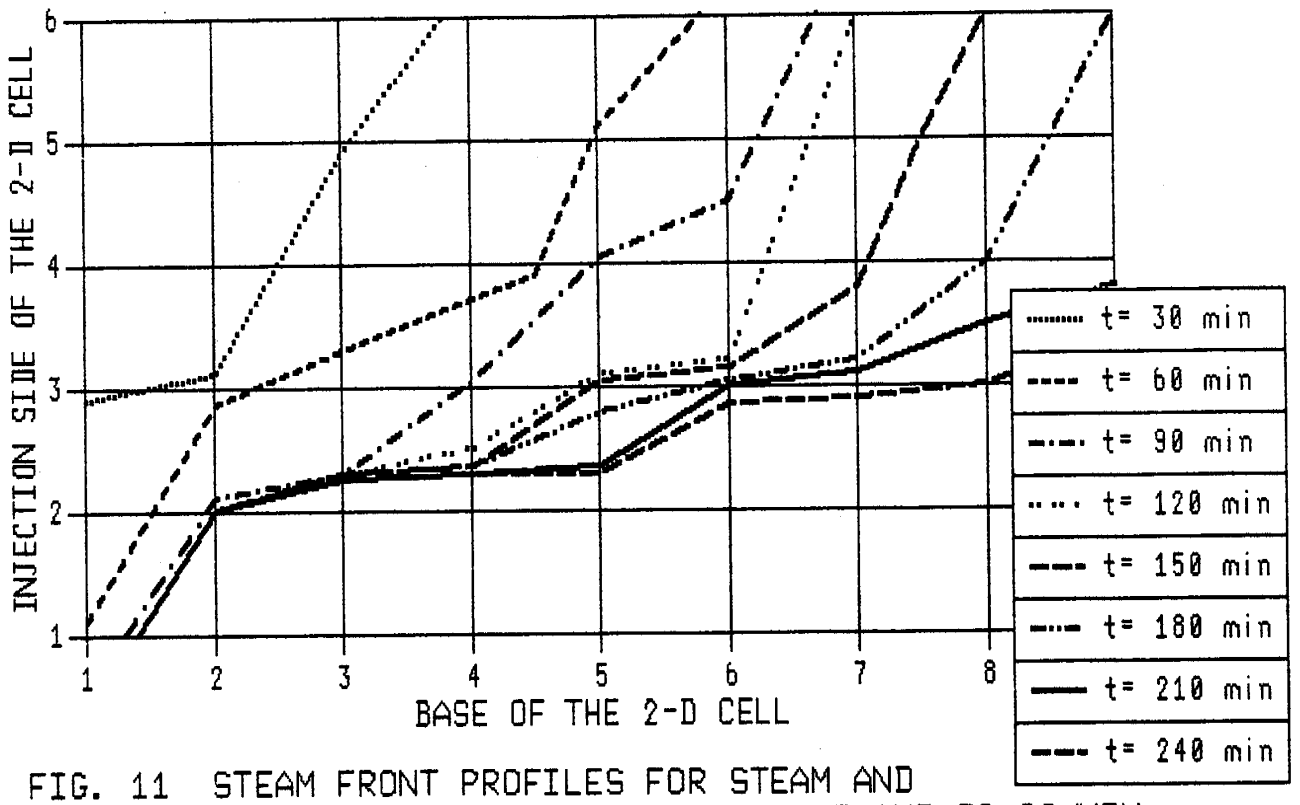

FIG. 11 STEAM FRONT PROFILES FOR STEAM AND SURFACTANT INJECTION AT 300 PSI AND 30 CC/MIN

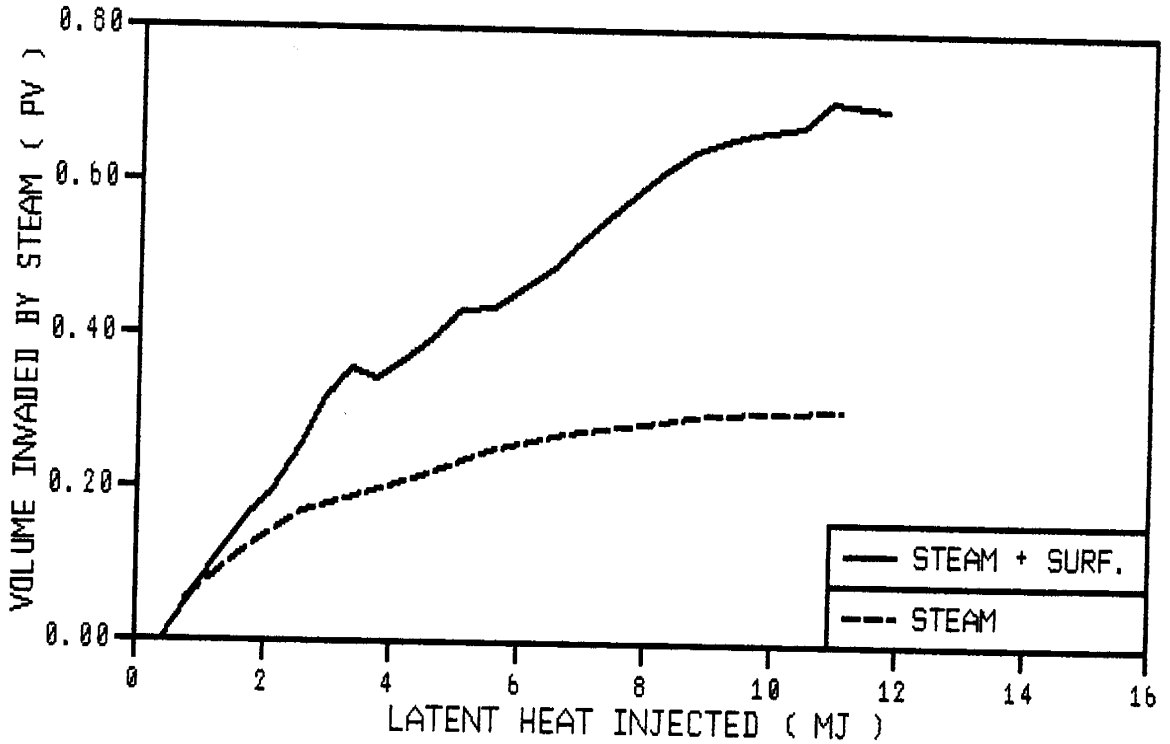

FIG. 12 STEAM ZONE VOLUME AS A FUNCTION OF THE INJECTED HEAT AT 300 PSI AND 30 CC/min

Task 35 - DOE shall provide INTEVEP with information from the foam diversion research and steam additive modeling conducted by DOE contractors. The Project Managers will consult with one another on foam diversion research and modeling conducted by DOE and INTEVEP laboratories with a view toward avoiding duplication of effort and enhancing the respective research efforts.

CONTENTS

Transient Behavior of Foam Flow in 1-D Porous Media 35-3

Steam Foam 1-D Model 35-6

Foamers and Emulsifiers 35-22

One-Dimensional Steam Flood Experiments 35-23

3.1 TRANSIENT BEHAVIOR OF FOAM FLOW IN 1-D POROUS MEDIUM (D. Liu)

3.1.1. INTRODUCTION

This work is a continuation of Erickson's (1986) work on the transient behavior of foam flow in a one-dimensional porous medium. The equipment used is a modified version of that used by Treinen *et al.* (1985). Most studies have dealt with steady state foam injection, but true steady state conditions are rarely achieved for a field project. Few experimental data are available for transient foam flow. The ultimate goal of this work is to develop a predictive model for foam flow in porous media. The first step in creating such a model is to accumulate basic experimental data on transient foam flow. The system studied is a one-dimensional, low temperature, low pressure environment.

3.1.2. EXPERIMENTAL PROCEDURE

For a detailed description of both the experimental apparatus and the procedures, the reader is referred to Erickson (1986). The following is a brief summary. It includes, however, some modifications to previous proceedings.

Foam is generated through a foam generator by introducing surfactant solution and nitrogen simultaneously. The quality of the foam is controlled by the constant rate pumps. Then the foam is flowed through an transparent observation cell so that one can be assured that the foam was indeed generated. After that, the foam is injected into a sandpack which is a 1-in. diameter and 24-in. long acrylic tube which contains unconsolidated Ottawa sand of a predetermined range of mesh sizes. Each experimental run uses a new sandpack. The sandpack was first saturated with distilled water. During the displacement, the pressures are recorded by pressure transducers at the pressure taps mounted along the sandpack. Effluents are collected and analyzed for concentrations of surfactant to study adsorption.

Prior to each experimental run, the pressure transducers were calibrated with the aid of a computer program, which was written on an Apple PC to facilitate reading and storing the pressure data. It should be pointed out that the calibration should be carried out at the expected experimental conditions instead of at low pressure. This was found to be important, for the differential transducers are sensitive to the absolute pressure level.

Another important point is the measurement of porosity. Previously, the porosity was calculated by knowing the weight of the sand and dividing it by 2.65 g/cc to get the grain volume. This is found to be somewhat inaccurate. A more accurate way is to saturate the sandpack with a fluid of known density (e.g. distilled water) and measure the weight before and after saturating to calculate the pore volume.

One important defect of the equipment was the pressure regulator. In the previous design, the same pressure line was connected to both the backpressure regulator and the transducer constant pressure. But the pressure at which the backpressure regulator allowed fluids to pass was two to three psi less than the regulator's pressure. Since the pressure drop in the sandpack is about five psi, this difference could be fatal. This problem was remedied by placing a small metal spring in the regulator to eliminate this discrepancy.

3.1.3. RESULTS AND DISCUSSION

Effort was made to salvage the data obtained by Erickson (1986). We will take one example to illustrate the experience. Since the pressure versus distance curves were rather erratic (Erickson, 1986), we attempted a plot of the pressure gradients over the four sections vs pore volumes of foam injected (Fig. 3.1.1). However, these curves also do not follow any definite trends. It was finally concluded that new experiments will be needed which give more reliable data. A new run was performed in the updated equipment.

Prior to the run, work was focused on:

- Modifying the software program to give more accurate data.
- Calibrating the pressure transducers at high pressure.
- Calibrating the gas and water pumps.
- Modifying the back-pressure regulator to allow flow to be at the same pressure as in the transducers.
- Preparing sand and making a new sandpack.
- Making trial runs at elevated pressure to check the accuracy of the apparatus and assure that there is no leakage.

Foam was then injected to the sandpack for 14 days using 0.1% surfactant concentration at a flow rate of 0.1 cc/min. The pressures at the pressure taps were recorded at different time intervals. The effluents were collected for later analysis of surfactant concentration by the titration method. After 11 days with the hope that the transient flow of the gas/surfactant mixture could be visualized, the surfactant solution was dyed blue with food color and injection was continued. Because the color was too light, no significant color changes were observed in the inlet until three days later, when the experiment had to be stopped due to a power shutdown.

In this experiment, no foam was observed at the outlet. It was believed that the foam was destroyed in the sandpack. It appears that we will need to either increase the surfactant concentration or the flow rate. In addition, we have considered dying the original water with food color in the sandpack without altering the wettability. In so doing, the transient behavior could be better visualized.

New sandpacks are presently being fabricated. Once these are built, we intend to make and analyze additional runs.

3.1.4. REFERENCES

Erickson, A.: "The Transient Behavior of Surfactant Foam Flow in Porous Media," MS Report, Stanford U., Stanford, CA (1985).

Treinen, R.J., Brigham, W.E., and Castanier, L.M.: "Apparent Viscosity Measurements of Surfactant Foam in Porous Media," SUPRI TR-48, Stanford University [DE-ACO3-81SF1564] (1985).

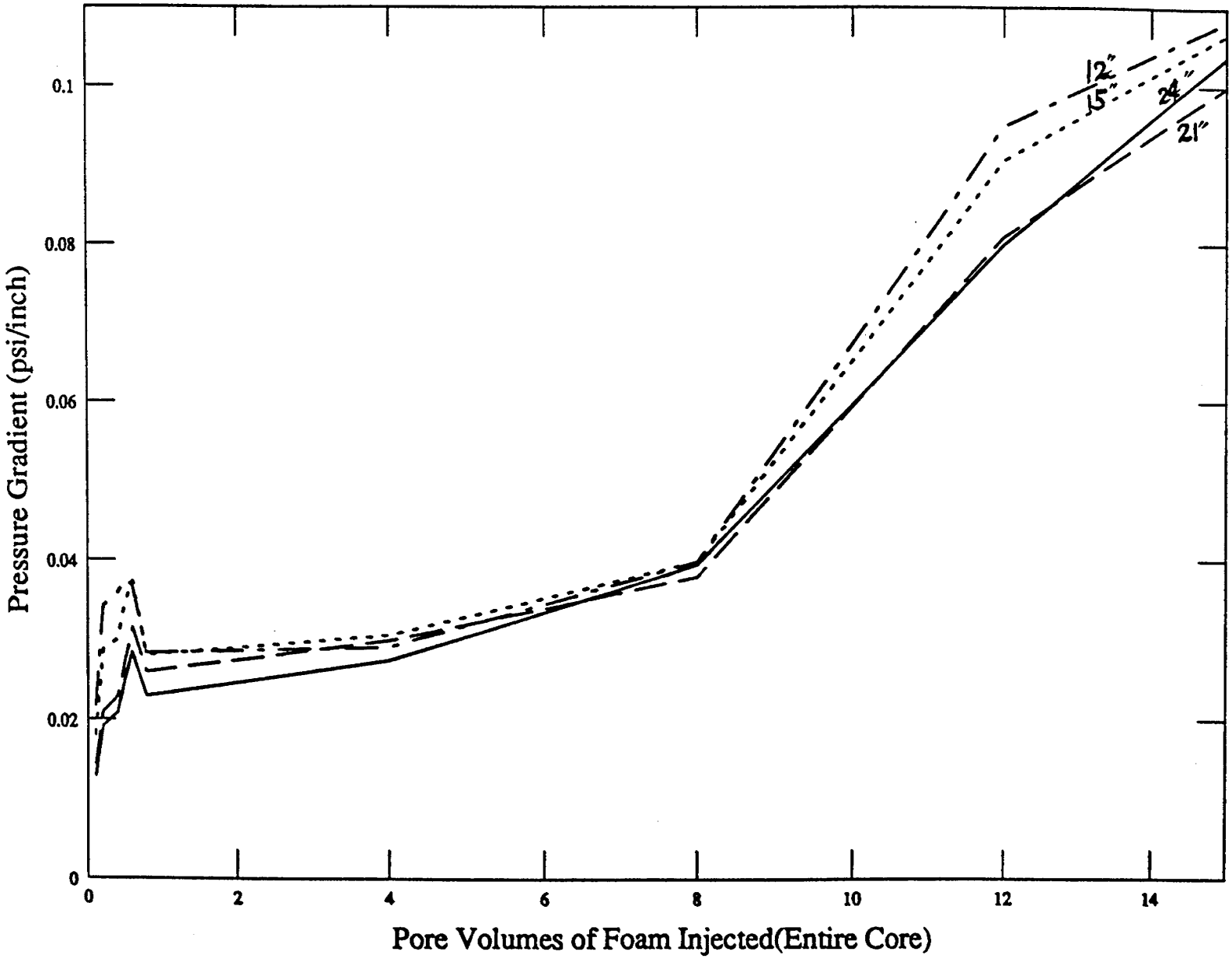

Fig. 3.1.1. Pressure Gradients Over Four Sections.

3.2 STEAM FOAM 1-D MODEL
(M. Maneffa)

3.2.1. INTRODUCTION AND SUMMARY

The foam diverting capabilities of the surfactant Chaser SD1000 were measured in a linear sandpack at steam conditions. The effects of nitrogen and surfactant concentration were investigated.

Ottawa sand, 170 to 200 mesh, was packed into a 6 ft stainless steel tube. In the two sandpacks used, the porosities ranged from 35.3 to 36.2 % and the permeabilities ranged from 5 to 6.2 darcys. The sandpacks were originally saturated with water and then flooded with oil to residual water saturation. Afterwards, the sandpack was steamed to residual oil saturation to represent a steam channel.

Two types of runs were made, one with no nitrogen injection, and the others with continuous nitrogen injection. In both cases, slightly superheated steam was injected concurrently with slugs of surfactant or water. The temperature and pressure profiles along the sandpack were measured. A system backpressure of 70 psig was applied.

Results showed that the SD1000 slugs at concentrations from 0.1 wt % to 1.0 wt % performed no better than slugs of water. This was observed whether or not nitrogen was injected. For the runs with nitrogen, it was also observed that the largest pressure gradient increases were in the last 20 in. of the sandpack, and the second SD1000 slug performed slightly better than all other slugs.

The purpose of this study was to observe the effects of continuous nitrogen injection and surfactant slugs at steam conditions. Nitrogen and surfactant were injected at various concentrations and the pressure profiles along a sandpack were measured. This report also intended to compare the diverting capabilities of the commercial surfactants Chaser SD1000 and Enordet LTS 18 manufactured by Chevron and Shell, respectively. However, because of equipment problems and time limitations, only the Chevron product was included at the time of this writing.

3.2.2. EXPERIMENTAL APPARATUS

The equipment used in this report can be grouped into four parts: an injection system, the sandpack itself, a data acquisition system, and a fluid production system. Figure 3.2.1 is a schematic diagram of the apparatus and Table 3.2.1 lists properties of the sandpack. A more detailed description of this equipment was given by Wang (1986).

A constant rate of mass injection of oil, water, and/or steam was handled by two Constametric Model III pumps with two pistons each at 180 degree phasing to reduce pulsing. One pump was soley used for pumping water for steam generation, and the other pump was used to inject oil, or slugs of water and surfactant solution. Steam was generated by a tubular furnace (Marshall Model #1046) that could achieve steam injection temperatures in excess of 600°F. Nitrogen injection was controlled by a Matheson Model 8240 flow controller consisting of a flow transducer, a flow control valve, and a power supply/readout box.

TABLE 3.2.1

PROPERTIES OF SANDPACKS

	Sandpack No. 1	Sandpack No.2
Porosity	$\Phi = 35.3\%$	$\Phi = 36.2\%$
Permeability	K = 4.97 Darcys	K = 6.22 Darcys
Residual oil saturation	$S_{or} = 18.7\%$	$S_{or} = 19.2\%$
Porous medium	Ottawa sand (mesh 170-200)	
Sandpack length	L = 6 ft	
Sandpack inside diameter	ID = 2.15 in.	

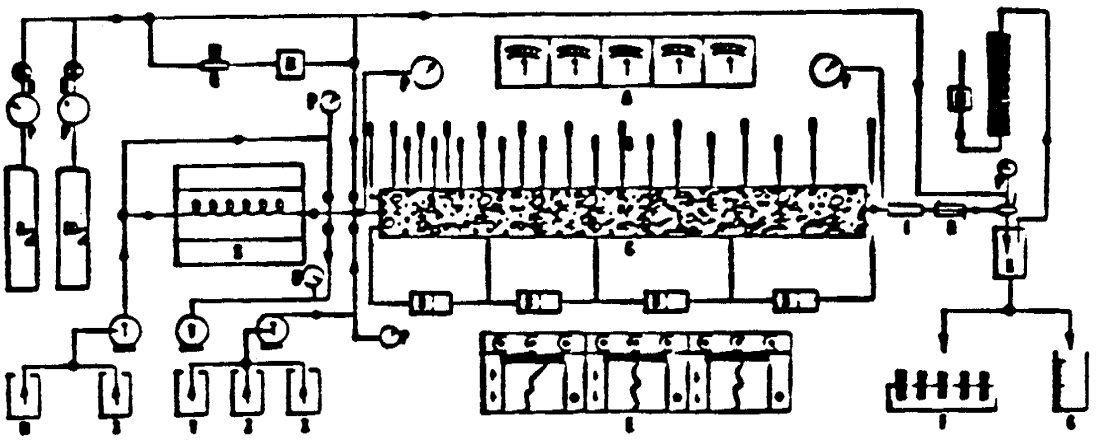

A: temperature controllers
B: thermocouples
C: sandpack
D: pressure transducers
E: recorders
F: fraction collector
G: graduated cylinder
H: heat exchanger (condenser)
I: sight glass
J: backpressure regulator
K: gas/liquid separator
L: moisture drier
M: gas flow meter
N: nitrogen cylinder
O: carbon dioxide cylinder
P: pressure gauge
Q: gas flow controller
R: gas flow regulator
S: steam generator
T: pump
U: vacuum gauge
V: vacuum pump
W: water container
X: cleaning fluid
Y: oil container
Z: surfactant solution container

Fig. 3.2.1. Steam Foam 1-D Model.

A 6 ft stainless steel tube (SS #321, 2.25 in. O.D., 2.15 in. I.D.) with flanges at each end made up the sandpack. Both flanges had a fluid intake, a pressure tap, and a thermocouple. Along the tube, 21 thermocouples (1/16 in. O.D., from Conax) were mounted at various distances to measure the temperature profile. Five pressure taps located 0, 16, 32, 52, and 72 in. from the inlet divided the sandpack into four sections. Fiberfax insulation (a fibrous aluminum-silica mixture) was used to reduce heat losses along the tube.

Temperatures along the sandpack were recorded by a 24 channel strip chart recorder (Leeds and Northrop, Speedomax). Pressure data from the five pressure taps were measured by Celesco Model #KP-15 transducers. Celesco Model CD10B carrier demodulators converted the signals from the transducers to 0-10 volt DC outputs and were recorded by two Soltec Model #1243 three-pen strip chart recorders.

The temperature and pressure output were also recorded by computer. An Esterline Angus Model PD-2064 data logger converted the analog data into digital form and transmitted them to a Compaq computer where the data was stored on floppy disk. Later this data was transferred to a VAX 11/750 computer for analysis. A small program written in Fortran 77 was used to develop various graphs.

The fluid production system consisted of an 60 micron filter at the outlet flange, a sight glass to see the produced fluids, a condenser, a backpressure regulator, and a fraction collector.

Slight modifications to the backpressure regulator (Grove Valve and Regulator Co., Model 591 W) were made to control fluctuations when two phases were being produced. The backpressure regulator originally had a paper-thin plastic diaphragm which held the backpressure within 0.7 psi of the desired pressure when a single phase was produced. However, the pressure was found to fluctuate rapidly by as much as 5 psi when two phases were being produced, and the pressure often drifted by as much as 100 psi. Thus, modification of the backpressure regulator was critical to achieving stable operation of the equipment.

Treinen (1985) had modified a similar backpressure regulator by replacing the plastic diaphragm by a thin Neoprene diaphragm. It is believed that the brittle plastic diaphragm could not open and close the outlet port as easily and quickly as the flexible Neoprene diaphragm. A brass pin was placed in the outlet port to reduce diaphragm fluctuation and grooves were made on the regulator near the outlet port to prevent the diaphragm from sealing the outlet.

The backpressure modifications made in this experiment were very similar to that described by Treinen (1985) except that a thicker Neoprene diaphragm (3/8 in.) was used with a "thumbtack like" pin placed in the outlet port of the regulator. The pin was dimpled on the underside, rather than making grooves on the regulator, to prevent sealing the outlet (Fig. 3.2.2). With these modifications, the regulator was able to hold the backpressure to within 0.5 psi of the desired pressure when nitrogen and water and/or surfactant were produced.

The produced liquids were collected by Buchler Model Fractomette Alpha 200 collector. This gave a constant volume of production (30 cc) for each test tube. A Matheson Model 8160 flow indicator consisting of a flow transducer and a power supply/readout box was available to measure the produced nitrogen rate.

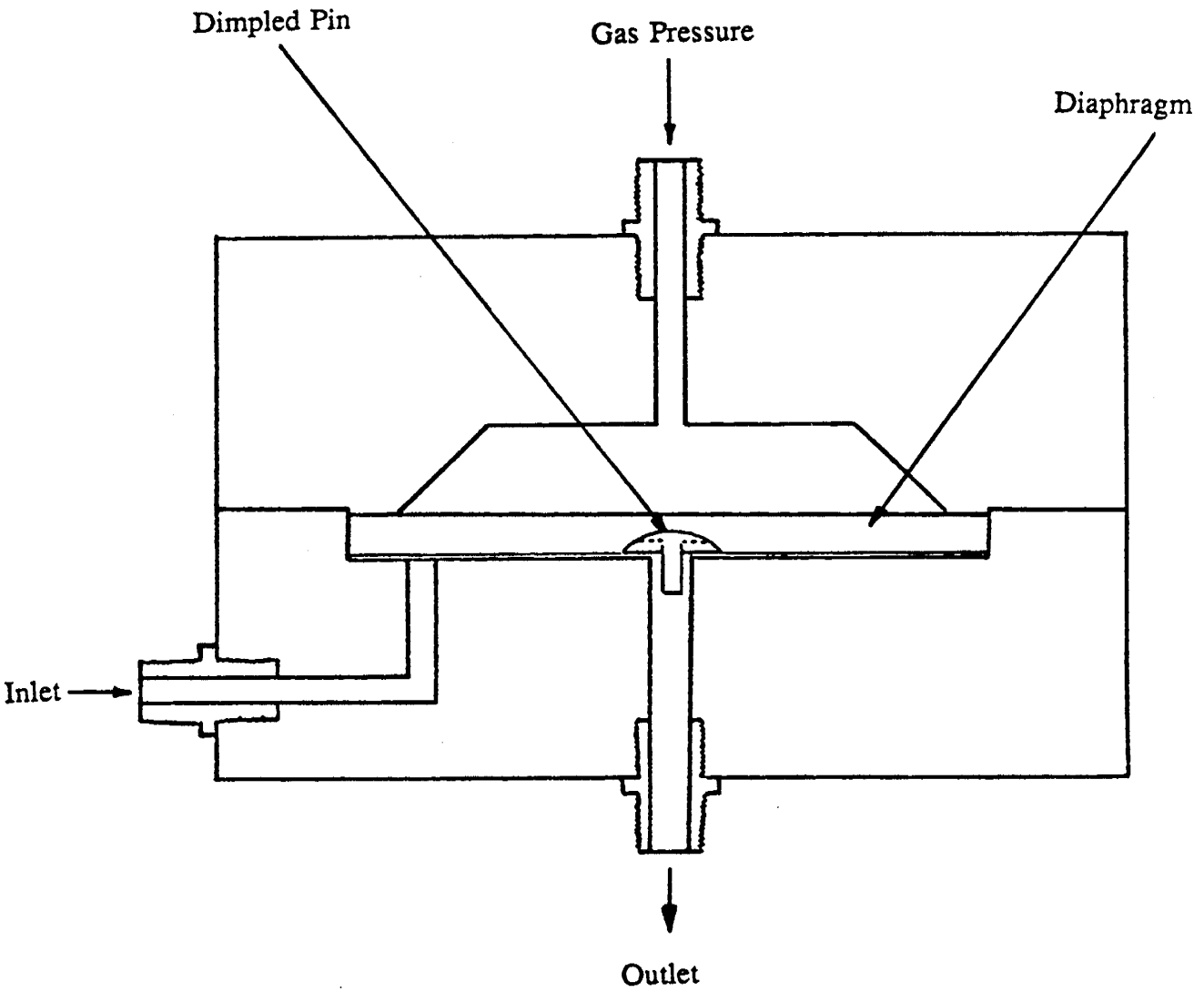

Fig. 3.2.2. Backpressure Modification.

3.2.3. EXPERIMENTAL PROCEDURE

In all the experiments, the sandpack was first steamflooded until breakthrough. This steam-out condition was meant to simulate steam channels in the field. Slightly superheated steam was injected at 4.0 cc/min of equivalent water with a 70 psig backpressure held on the system. The heating tape and band heater were set at 450°F. Breakthrough usually occurred 4-1/2 hours after initiating steam injection.

The first four runs consisted of water or surfactant, and steam injection with no nitrogen. After steam breakthrough, steam injection was continued and 0.1 pore volume slugs of water or surfactant solution were injected at 4 cc/min. Anywhere from one to five slugs were injected in a run (Table 3.2.2). Subsequent slugs were not injected until the pressure gradients in the sandpack dropped to levels prior to slug injection (usually 1-1/2 hours between slugs). The quality of the injected steam/liquid mixture was estimated by an enthalpy balance to be 40%. Concentrations of Chevron's Chaser SD1000 ranged from 0.1 to 1.0 wt % (Table 3.2.2). Steam injection continued after injection of the water or surfactant slug had ceased. During the injection of the slugs, the in-line heating tape and the band heater at the inlet flange where shut off.

Runs 5 through 11 were conducted in a similar manner except that nitrogen was concurrently injected with the steam and water/surfactant slugs. Also, after the injection of each of the water/surfactant slugs stopped, nitrogen and steam injection were continued. Nitrogen concentrations were 1.0 or 5.0 mole % of the injected steam (Table 3.2.2).

3.2.4. RESULTS AND DISCUSSION

The experimental runs performed in this report can be divided into three groups. The first group (Run Set 1) includes Runs #2, #3, and #4. In these runs, steam and water/surfactant slugs were simultaneoulsy injected with no nitrogen. Run #1 was not included because it was performed at zero backpressure and inexperience with the equipment gave erratic results. The second group (Run Set 2) includes Runs #5 through #8. Nitrogen was injected concurrently with steam and water/surfactant slugs in these runs. However, due to backpressure control problems and a clogged filter at the outlet, the results from these runs are suspect. The last set of runs (Run Set 3) includes Runs #9, #10, and #11. The procedure used in this run set was the same as Run Set 2 but the backpressure control problems had been solved and the previously clogged filter was replaced after each run. Table 3.2.2 is a summary of Runs #2 through #11.

Run Set 1

Run #2 consisted of two surfactant slug injections and a third water slug injection. The surfactant concentration used was 0.1 wt % and the size of the all the surfactant slugs were 0.1 pore volume. The mass injection rates of steam and water/surfactant slugs were 4.0 cc/min. Figure 3.2.3 shows the pressure gradient versus time for the four sections of the sandpack and the average pressure gradient along the entire pack. The starting points of surfactant and water injection are marked. Each slug injection lasted approximately 39 minutes. Subsequent slugs were not injected until the pressure gradients dropped to levels prior to slug injection.

The first SD1000 slug gave an unexpectedly large pressure gradient along the entire sandpack, whereas the second SD1000 slug and the water slug showed only minor pressure gradient increases. It is not known why this large increase occurred for the first slug only. However, the succeeding slugs and later runs indicate that this large increase was not

TABLE 3.2.2

SD1000 SURFACTANT RUNS

Run No.	Nitrogen (mole %)	Water/Surfactant Injection (wt%)				
		slug 1	slug 2	slug 3	slug 4	slug 5
2	0.0	0.1	0.1	water	--	--
3	0.0	water	1.0	1.0	--	--
4	0.0	water	1.0	1.0	--	--
5	5.0	water	1.0	1.0	--	--
6	5.0	1.0	--	--	--	--
7	1.0	1.0	--	--	--	--
8	5.0	1.0*	--	--	--	--
9	5.0	water	water	0.1	0.1	--
10	5.0	water	water	0.5	0.5	--
11	5.0	water	water	1.0	1.0	1.0

*Suntech IV was used for this run.

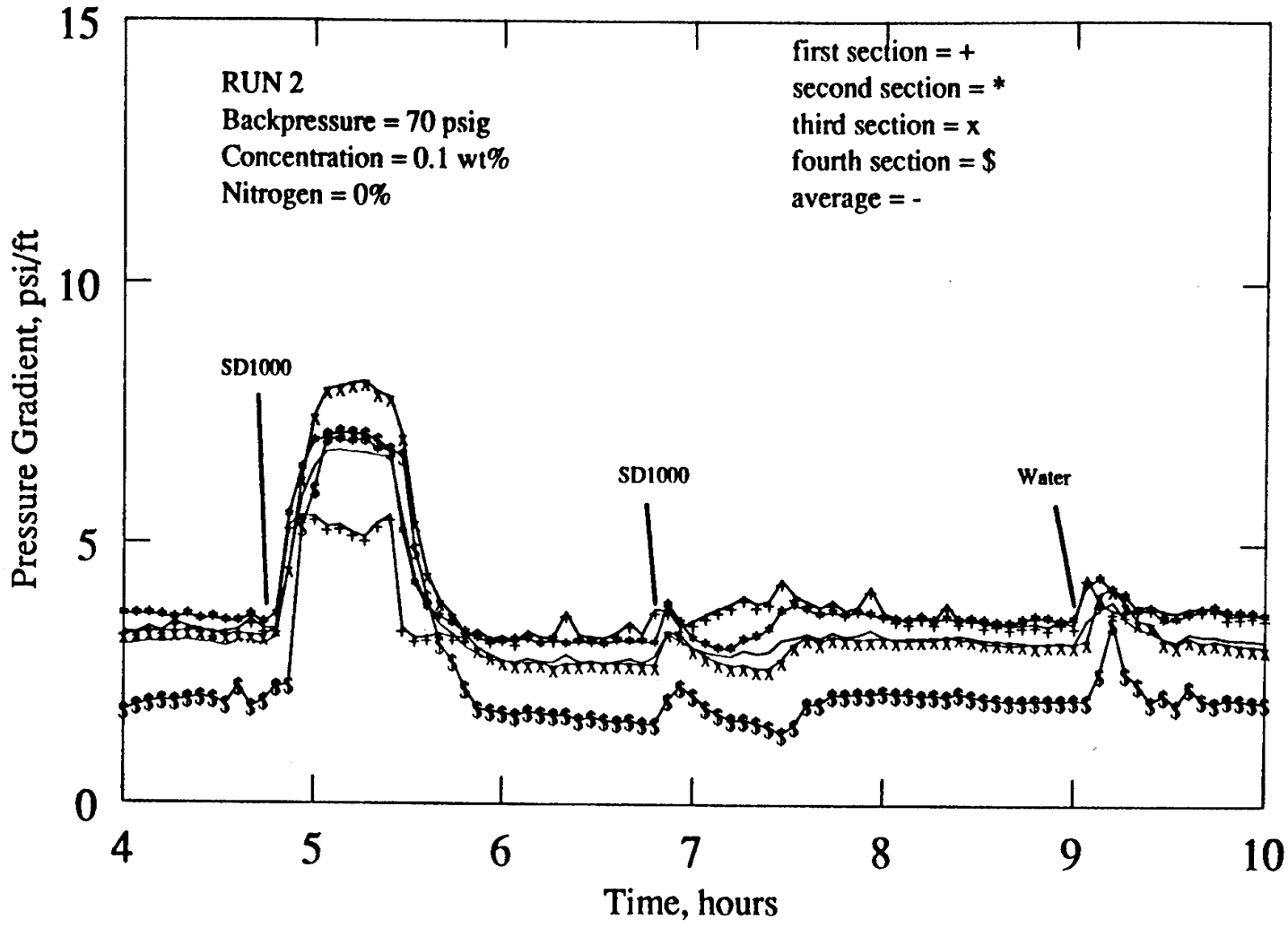

Fig. 3.2.3. Pressure Gradient Profile for Run No. 2 Using 0.1 wt% SD1000.

representative of the surfactant's blocking capability. The second SD1000 slug performed no better than the water slug.

Run #3 consisted of three slugs as did Run #2, but the order of injection was reversed and the concentration was increased. A water slug was injected first followed by two slugs of 1.0 wt % SD1000. The water slug was injected first because it would not be influenced by residual surfactant concentrations. Both surfactant slugs showed a 10% increase in the pressure gradients in all sections. The second surfactant slug performed slightly better than the first, but neither surfactant slug had a marked effect on the pressure drop compared to the water slug.

Run #4 was a repeat of Run #3 to check on the accuracy and reproducibility of the results. Pressure gradients from the two SD1000 slugs were 10% below that of the initial water slug. From Runs #3 and #4, it was concluded that the SD1000 at 1.0 wt % showed little or no improvement in steam blocking capability as compared to water.

Run Set 2

In this set of runs nitrogen was concurrently injected with steam during and after the water/surfactant slug injection. Run #5 consisted of three slugs; a water slug followed by two slugs of 1.0 wt % SD1000. After steam breakthrough and prior to injection of the slugs, nitrogen was injected at a rate of 5 mole % until the pressure gradients levelled off in the sandpack. The last section, however, did not level off and gave no indication that it would. Figure 3.2.4 shows the pressure gradient versus time for Run #5. The two surfactant slugs showed no improvement over the initial water slug. Approximately 11 hours into the run and three hours after the first surfactant slug injection, the backpressure increased dramatically to 95 psig followed by high quality foam production and an exponential decline in the backpressure (Fig. 3.2.5). Nitrogen injection was stopped at 11 hours and 20 mins because of excessive foam production.

The variation in the backpressure due to poor pressure regulation was reflected in the pressure gradient within the sandpack. Note that when the backpressure was rising rapidly (10.8 hrs to 11.4 hrs), the pressure gradient within the sandpack was dropping. Later, when the backpressure dropped, the pressure gradient in the sandpack rose dramatically. It is clear that these erratic results were due to poor backpressure control.

No water slug and only one surfactant slug was injected in Run #6. The nitrogen rate was still 5 mole %. For this run and all succeeding runs, nitrogen injection was started at the same time as the first slug. Figure 3.2.6 shows the results from Run #6. The large pressure gradients at the beginning of the surfactant slug injection are partially due to the initiation of nitrogen injection. However, based on the results of the previous run most of the early pressure gradient increase appears to be due to the sudden drop in backpressure (Fig. 3.2.7). Again, three hours after the surfactant injection the backpressure increased to 125 psig (Fig. 3.2.7) with a consequent drop in pressure gradient (Fig. 3.2.6). Then the backpressure declined exponentially with the production of high quality foam and at the same time the pressure gradient rose dramatically.

Run #7 was a repeat of Run #6 except that the nitrogen injection rate was cut back to 1.0 mole %. The initial pressure gradient increase during surfactant and nitrogen injection was considerably less than that in Run #6 because of the lower nitrogen rate. The backpressure control problems were less dramatic than the previous two runs, but the backpressure still gradually increased to 120 psig). Three hours after the initial surfactant injection, (at about 8 hours) a low quality foam was produced. Again, it can be seen that the rises in pressure

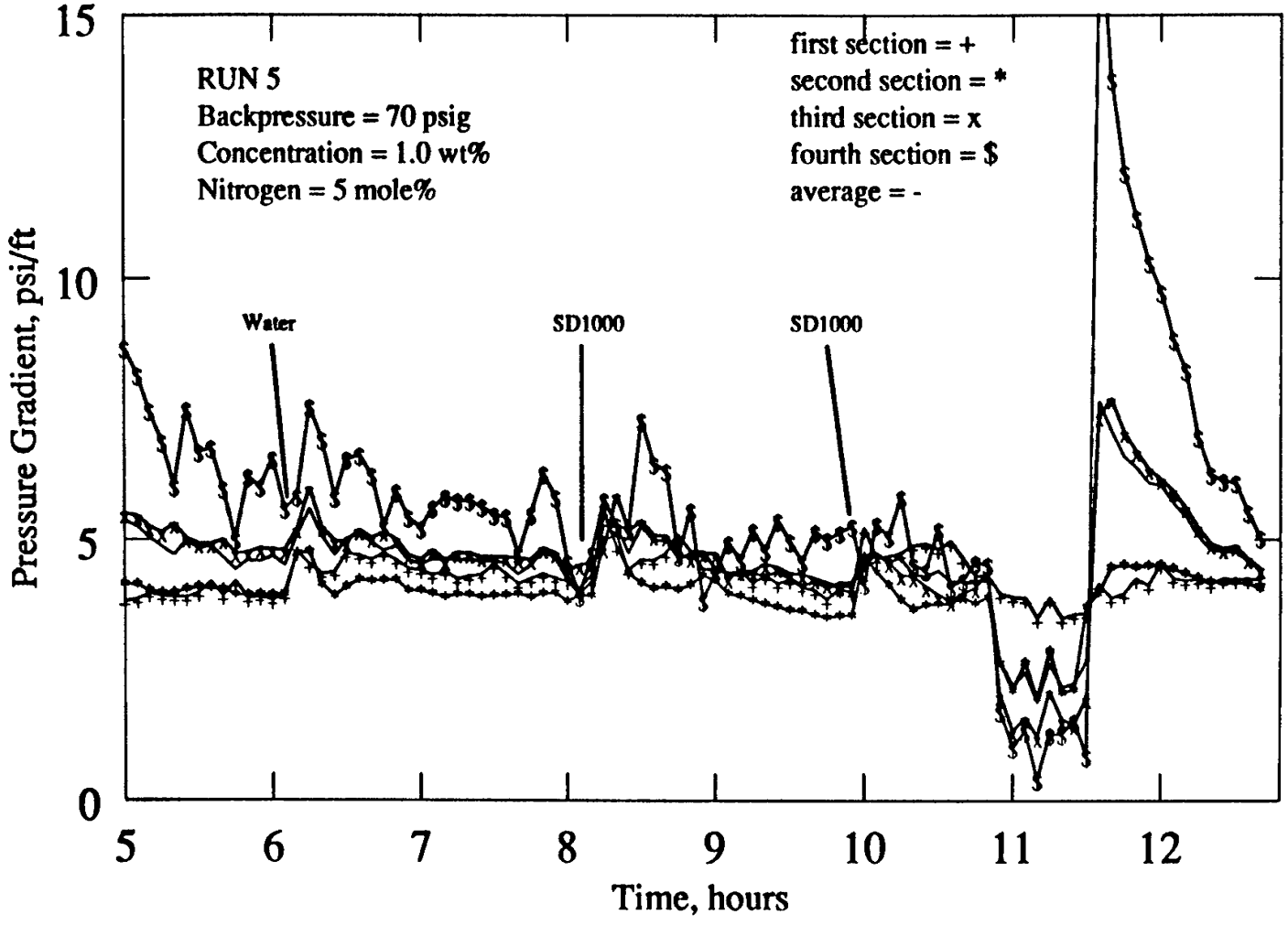

Fig. 3.2.4. Pressure Gradient Profile for Run No. 5 Using 1.0 wt% SD1000.

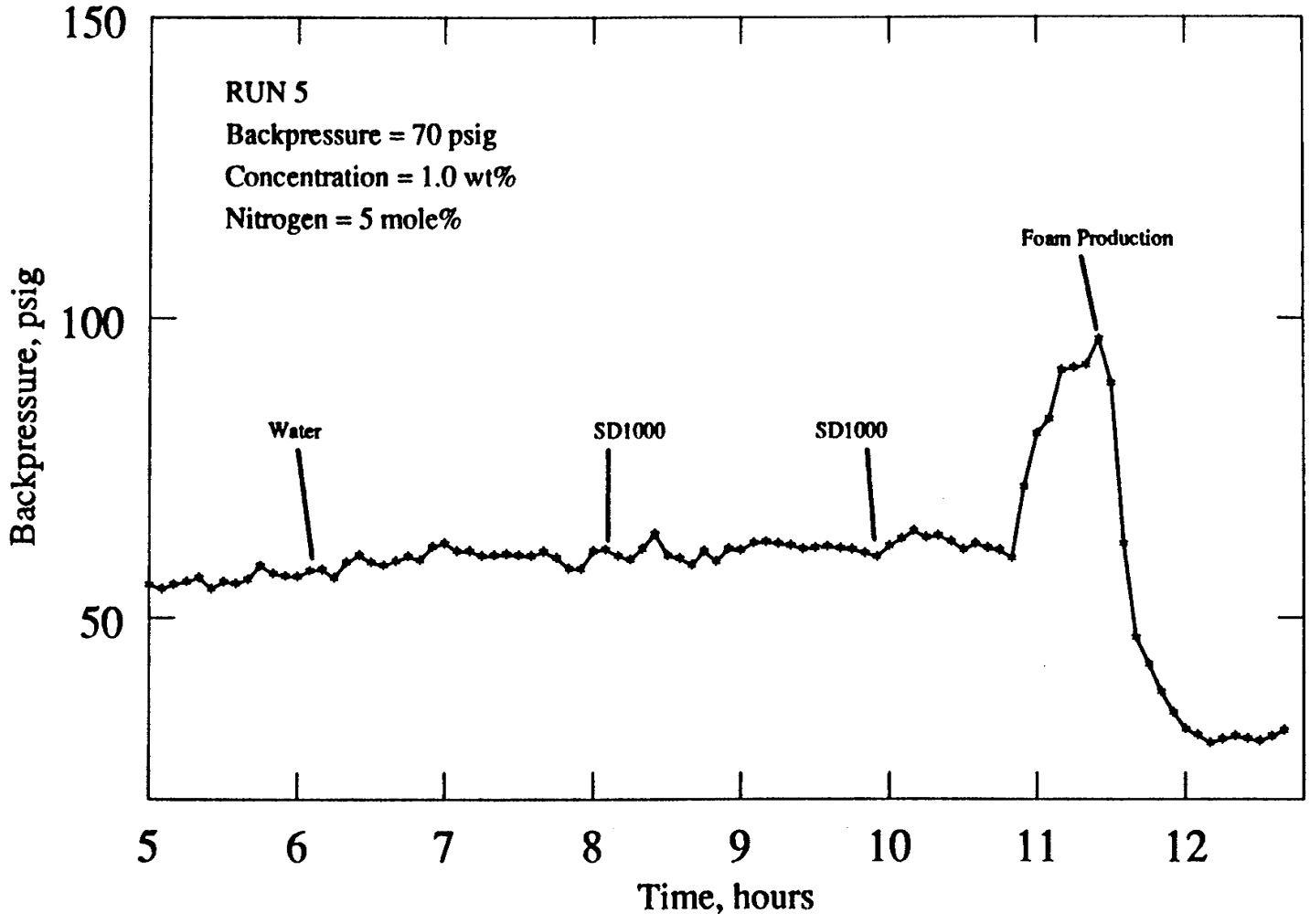

Fig. 3.2.5. Backpressure Profile for Run No. 5 Using 1.0 wt% SD1000.

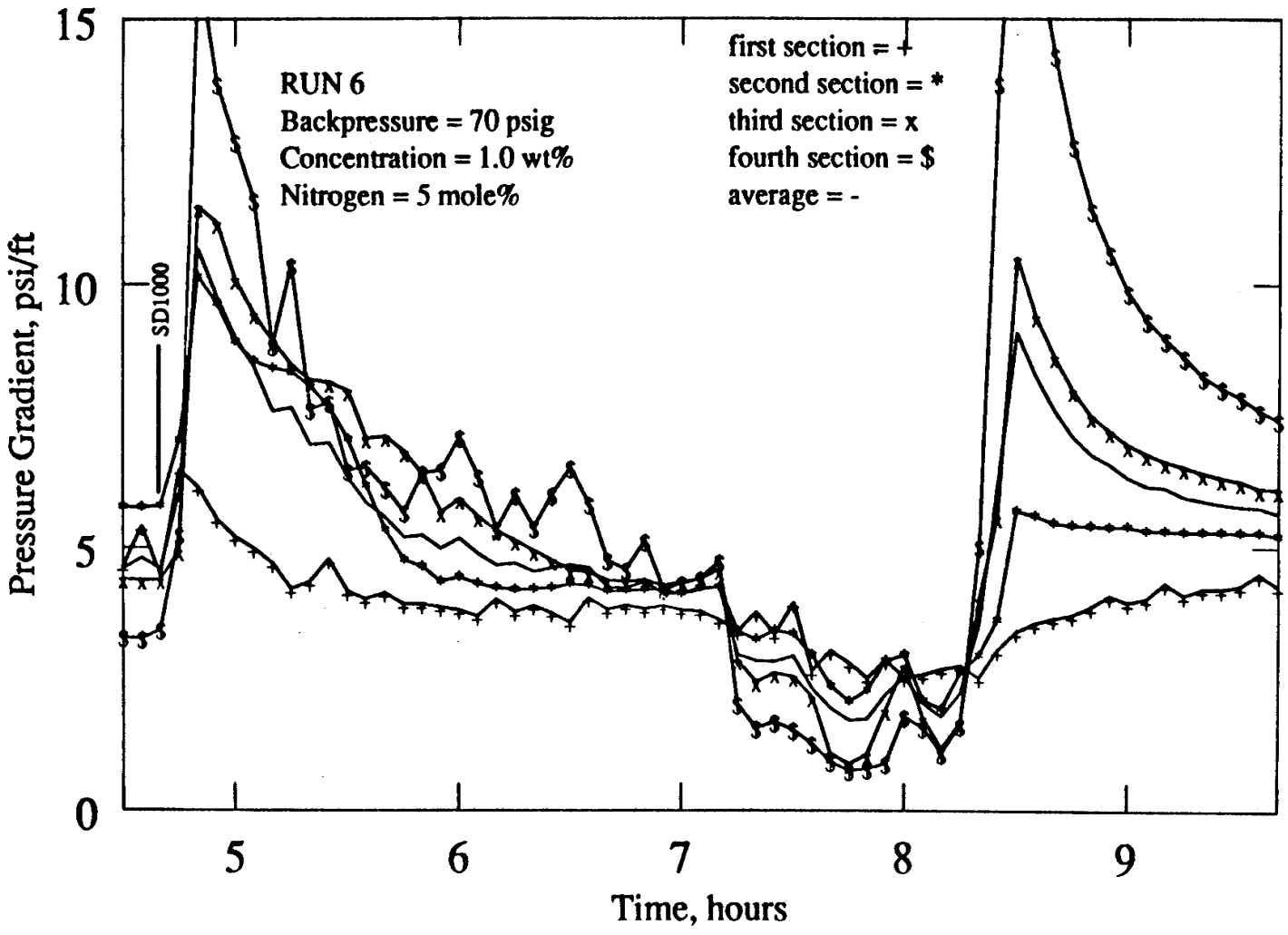

Fig. 3.2.6. Pressure Gradient Profile for Run No. 6 Using 1.0 wt% SD1000.

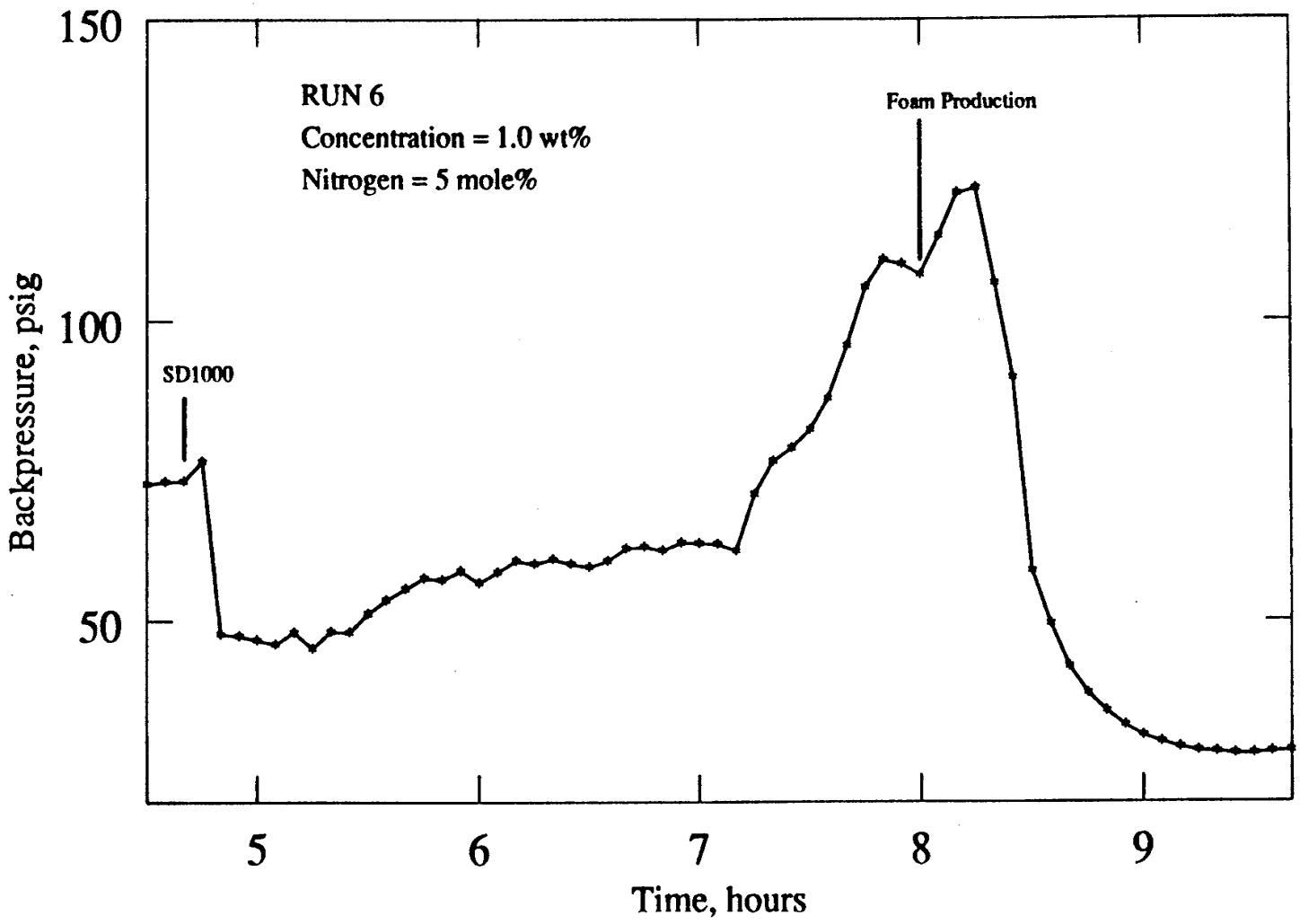

Fig. 3.2.7. Backpressure Profile for Run No. 6 Using 1.0 wt% SD1000.

gradient are the result of drops in backpressure. In the three runs mentioned above, foam could be seen through the sight glass ahead of the backpressure regulator.

To find out for certain whether the above behavior was possibly due to the surfactant rather than due to backpressure or other problems, Suntech IV was used in Run #8. Extensive work had been done by Wang (1986) with Suntech IV and its behavior with this equipment was well documented. One slug of 1.0 wt % Suntech IV at 4 cc/min was concurrently injected with steam a 4 cc/min equivalent water and 5 mole % nitrogen. The largest pressure gradients were observed in the first and second sections. This agreed with the results observed by Wang. However, the backpressure control problems were still present. The backpressure rose so high (over 175 psig) that pressure needed to be bled off the pack at 7 hrs 53 mins and at 8 hrs 10 mins into the run. Afterwards, the backpressure continued to rise and the run was subsequently stopped to prevent damage to the equipment. No foam was produced, however, soapy water was observed after bleeding the pressure from the system.

After the strange results from these four runs, it was decided to repack the tube and modify the backpressure regulator to better accomodate two phase flow. The sandpack itself showed no signs of clogging. However, a 60 micron filter attached to the outlet flange was severely clogged. From the time behavior of these runs it is believed that after the initial surfactant slug injections, it took three hours for the surfactant to move to the end of the sandpack and build up enough pressure to "blow" the clogged filter free resulting in foam production and an exponential decline in the backpressure. Backpressure modifications were described earlier, and these changes henceforth maintained the backpressure within 0.5 psi of the desired setting.

Run Set 3

A new sandpack was used for Runs #9, #10, and #11 with the properties listed in Table 3.2.1. In this last set of runs, nitrogen was concurrently injected with steam during and after the water/surfactant slug injection as in Run Set 2, but the backpressure control problems had been solved and the filter at outlet was replaced.

Run #9 consisted of four slugs; two water slugs followed by two slugs of 0.1 wt % SD1000. Nitrogen injection rate was 5 mole %. Since nitrogen injection was initiated with the injection of the first water slug, the measured pressure gradients were higher than normal until a stable saturation profile could be established. The first water slug for Runs #9, #10, and #11 should thus be ignored, and the second water slug should be used as the base case for comparison. The two surfactant slugs performed no better than the second water slug. After the modifications to the backpressure regulator, the backpressure was maintained at a constant level. This profile was characteristic for all runs in this run set.

In Run #10, the surfactant concentration was increased to 0.5 wt %. The SD1000 pressure gradient profiles were slightly higher than the base case of water, with the last SD1000 slug being the highest. In general, however, no significant improvement by foam blocking was seen at this concentration. It was also noticed that the largest pressure gradient increase occurred in the last section (the last 20 in.) of the sandpack. Remember that this also occurred in Run Set 2 but to a higher degree. Therefore, the large pressure gradient increases in Run Set 2, although due mostly to backpressure control problems, were also due partly to the behavior of the surfactant.

Five slugs were injected in the final run (Run #11). Two water slugs were followed by three slugs of 1.0 wt % SD1000. The nitrogen injection rate was again maintained at 5 mole %. The second surfactant slug showed some increase in pressure gradient in all sections so a third SD1000 slug was injected to see if some trend was developing. However, the third

surfactant slug performed worse than the second SD1000 slug and about the same as the base slug of water. It was noticed again that the largest pressure gradient increase occurred in the last section for all surfactant slugs and that the second surfactant slug had the highest pressure gradient profile.

In brief, the surfactant SD1000 did not cause appreciable pressure gradient increases in any of the run sets. However, Chevron claims that the surfactant SD1000 selectively foams in zones of low oil saturation but not in zones containing mobile oil. In the experiments made in this report, the oil was not mobile, however, the residual oil saturation was high (approximately 19 %). It is possible that the saturation was too high for the SD1000 to form a foam in the sandpack.

3.2.5. CONCLUSIONS TO DATE

Based on the results in this report, the following conclusions were made:

1. Backpressure control problems were significantly reduced by modifying the regulator to better handle two phase flow. Prior to modifying the backpressure regulator, the pressure fluctuated by as much as 5 psi and drifted by as much as 100 psi when two phases were being produced. The modifications included replacing the existing thin plastic diaphragm with a 3/8 in. Neoprene diaphragm and by placing a tack like pin at the outlet port. The Neoprene diaphragm can open and close the outlet port more quickly and easily than the brittle plastic diaphragm. The dimpled brass pin prevented the diaphragm from sealing the outlet port and reduced diaphragm fluctuation. After these modifications, the regulator was able to hold the backpressure within 0.5 psi of the desired setting when two phases were being produced.

2. The results from Run Set 2 should be ignored because of backpressure control problems and a clogged filter at the outlet flange. Variations in the backpressure due to poor pressure regulation were reflected in the pressure gradient within the sandpack. When the backpressure rose, the pressure gradient within the sandpack dropped, and vice versa. The clogged filter at the outlet caused the surfactant to accumulate in the last section of the sandpack. When the pressure in the sandpack built to a high enough pressure, the clogged filter blew free and resulted in foam production and an exponential decline in the backpressure.

3. In general, the SD1000 slugs at concentrations from 0.1 wt % to 1.0 wt % performed no better than the water slugs. This was observed whether or not nitrogen was injected continuously at 5 mole %. Run Set 1 consisted of only water or surfactant slug injection with no nitrogen injection. Run Set 3 consisted of water or surfactant slug injection with continuous nitrogen injection at 5 mole %. In both run sets, the surfactant slugs caused pressure gradients within the sandpack equal to their base case of water or water plus nitrogen, respectively.

4. The largest pressure gradient increases were observed in the last section of the sandpack for Run Set 3. In this run set, nitrogen was injected at 5 mole % and the last sections for all the SD1000 slugs showed a 10% increase in the pressure gradient as compared to the base case of water plus nitrogen.

5. For each run in Run Set 3, the second SD1000 slug performed better than the base case of water, and better than the first and third SD1000 slugs at concentrations from 0.1 wt % to 1.0 wt %. However, the increase in pressure gradients for these second slugs within the sandpack were not significant.

3.2.6. REFERENCES

Treinen, R.J., Brigham, W.E. and Castanier, L.M.: "Apparent Viscosity Measurements of Surfactant Foam in Porous Media," SUPRI TR-48, Stanford University [DE-AC03-81Sf1564] (Dec 1985).

Wang, F.P. and Brigham, W.E.: "A Study of Heat Transfer During Steam Injection and Effect of Surfactants on Steam Mobility Reduction," SUPRI TR-55, Stanford University [DE-AC03-81SF11564] (Oct 1986).

3.3 FOAMERS AND EMULSIFIERS
(J. Farrell)

A technical report titled, "Foam and Emulsion Effects on Gas Driven Oil Recovery," by J. Farrell and S.S. Marsden was sent for publication. The following is a summary of this work.

The aim of this research was to investigate the gas mobility reducing effects that a gas driven surfactant slug has on enhanced oil recovery (EOR). Three chemically similar surfactants whose properties graded from foaming agent to emulsifying agent were used to study the relative effects that foam and emulsion formation have on gravity override and enhanced oil recovery in an unconsolidated Ottawa sand model at room temperature. Both the foam lamellae and the emulsion droplets can act to reduce the mobility of the injected gas in the swept zone thus increasing the vertical sweep efficiency. Shell's Enordet series of alcohol ethoxylate surfactants were used in the study at three different concentrations of, 0.01%, 0.03% and 0.10% (wt.).

The experimental procedure consisted of displacing oil from a two-dimensional (x, z slice) porous medium at residual water saturation by injecting carbon dioxide, followed first by the injection of a 0.20 pore volume slug of surfactant solution, then by carbon dioxide gas at low pressure. At these low pressures, carbon dioxide acts as an inert gas. Measurements were made of the cumulative produced gas and liquids.

The main conclusion to be drawn from this study is that combining the foam and emulsion mechanisms may lead to more efficient oil recovery than either mechanism alone. Also the differences between the surfactants are small but consistent.

Although the conditions of this study are not representative of actual field conditions, it is believed that the recovery mechanisms in real situations are substantially the same. The fact that the displacement process with or without the surfactants is inefficient, should not detract from the overall conclusions. The findings here may make it possible to improve the effectiveness of processes that have been shown to be economically feasible such as steam-foam operations.

3.4 ONE-DIMENSIONAL STEAM FLOOD EXPERIMENTS
(D. Shallcross)

3.4.1. INTRODUCTION

The existing one-dimensional sandpack was used to continue the steam flooding experiments of Wang and Maneffa. Steam and nitrogen were simultaneously injected into the sandpack that contained oil at a residual saturation. Aqueous slugs of either water or surfactant solutions were then injected while the pressure gradient along the tube was monitored. An increase in the gradient would indicate the formation of foam. Before equipment failure delayed the experimental program, three surfactants were tested: Chevron Chaser SD1000, Dowfax and Shell Enordet LTS18.

3.4.2. EXPERIMENTAL APPARATUS AND PROCEDURE

The equipment used is essentially that employed by Wang (1986) and Maneffa (1987). A steel tube 183 cm (6 ft) long and 5.7 cm (2 ¼ in) in diameter is packed with commerically-graded sand. The sand contains oil at a residual saturation of approximately 18 percent. Superheated steam is continuously injected into the tube at a rate of 4 ml/min, cold water equivalent. After breakthrough of the steam front, nitrogen is injected at 163 std ml/min. The nitrogen serves as a noncondensable gas. The tube is surrounded by a layer of insulation to reduce heat losses from the system. Once steady state has been attained, a series of aqueous slugs are injected into the tube. Either water or surfactant solution slugs are injected. Having a size of typically 10 percent of the pack pore volume, the slugs take approximately 40 minutes to be injected at a rate of 4 ml/min. During a run the backpressure of the system is maintained at 480 kPa (70 psi), and all produced fluids are collected.

3.4.3. EXPERIMENTAL RESULTS

Only two successful experimental runs were performed using the equipment before the data logger failed. Both were conducted using a sandpack left in place by Maneffa.

In the first experiment a series of four surfacant slugs followed the injection of a water slug. Figure 3.4.1 shows the pressure gradients observed within each of the four tube sections during the run. At $t = 5.75$ hr, nitrogen injection began simultaneously with the injection of the first water slug. In all four sections an increase in the pressure gradient was observed. This increase was caused by the increased flowrate of fluids within the tube. After two hours this slug was followed by a succession of two slugs of 1.0 percent by weight SD1000 surfactant. On both occasions increases in the pressure gradients observed corresponded with the injection of the slugs. The limited extent of the increase in the gradients indicate that the changes in those gradients were probably caused solely by the increase in the flowrate of the injected fluids, rather than the formation of foam within the tube. As a consequence of this observation, the concentration of the SD1000 surfactant was increased to 2.5 percent in the next slug. No significant increase in the pressure gradients were observed. A 1 percent slug of Dowfax was then immediately injected, but to no effect. Halving the nitrogen injection rate at $t = 11.2$ hr, caused the gradients to decrease significantly. These observations confirm those of Maneffa that suggest that SD1000 does not foam in the presence of oil.

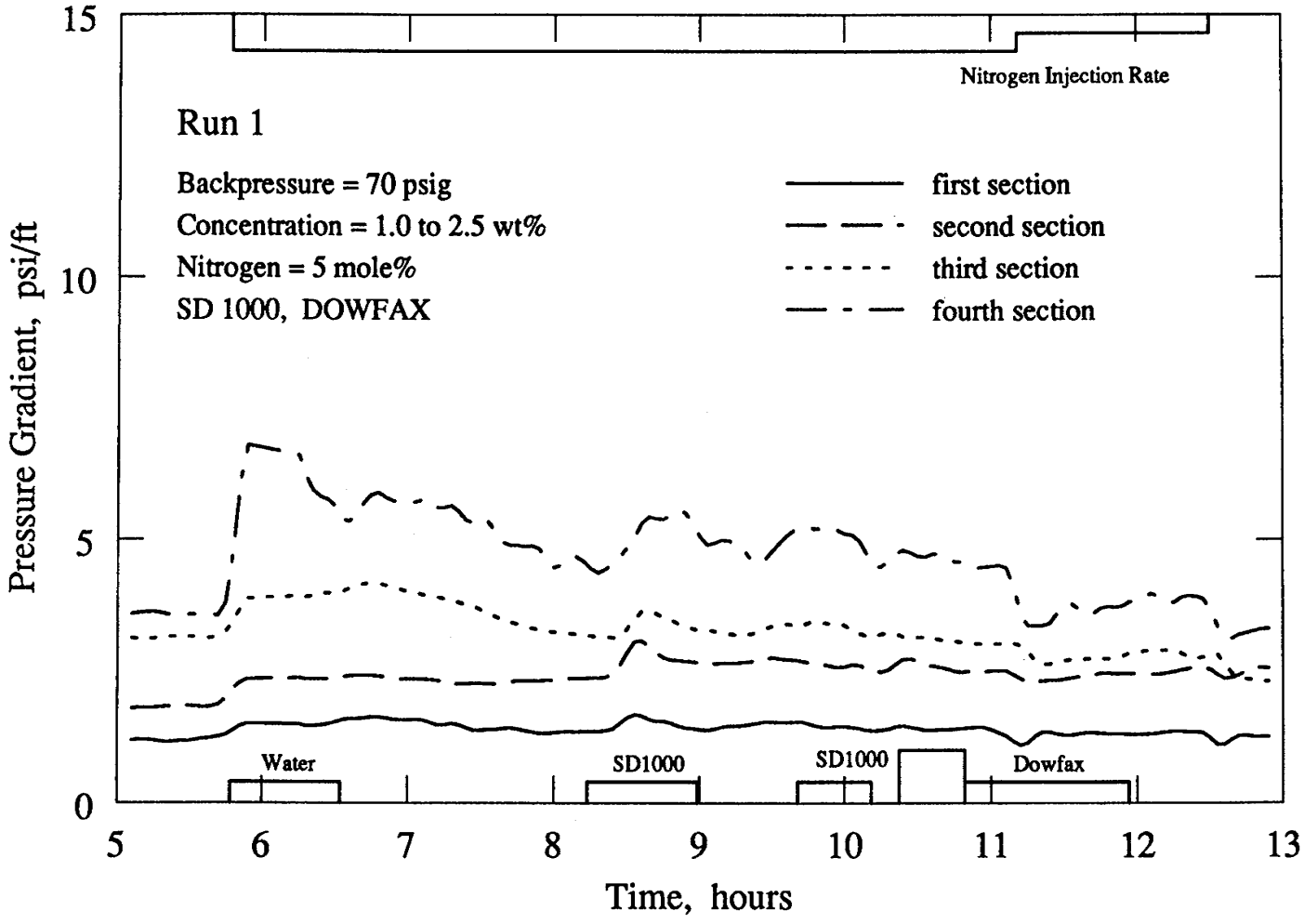

Fig. 3.4.1. Experimental Results for Run 1.

The second experiment began with the injection of nitrogen at $t = 4.9$ hr (Fig. 3.4.2). After a stabilization period a slug of distilled water was injected. This slug was followed at $t = 8.1$ hr by a 1.0 weight percent solution of Shell Enordet LTS 18 surfactant. The significant increase in the pressure gradients corresponding to this slug indicates that some foaming may have occurred. Successive slugs also indicated the possible presence of foam. Foam was not produced from the tube however.

A steady decrease in the gradient traces between each slug may have been caused by the drying action of the injected nitrogen. A third experimental run to study this phenomenon was underway when the data logger failed.

3.4.4. FAILURE AND REPLACEMENT OF THE DATA LOGGER

During the third experimental run the Esterline Angus data logger suffered a catastrophic failure that rendered it inoperable. Due to its age it was not possible to have it repaired at a reasonable cost. As a result it became necessary to replace the unit.

After an extensive survey of the available systems, a Hewlett Packard HP3497A data logging system was chosen for its versatility and ease of operation. As ordered the system would be capable of monitoring up to 80 channels at a continuous rate of 17 readings per second. These channels can be of any mixture of thermocouple, pressure transducer, or other signals. The system has the capability to be expanded into a controller unit. It may be controlled using an existing IBM XT personal computer.

At conclusion of the period covered by this report, the delivery of the system was being awaited.

3.4.5. FUTURE WORK

As well as continuing the work of Maneffa to study the foaming ability of a range of surfactants, it is hoped to extend the heat transfer work of Wang. The aim is to test and improve Wang's theoretical model. One assumption made by Wang is that the rate of heat lost from the tube to the surroundings is uniform around the tube. To test this assumption a series of heat flux sensors will be attached to the surface of the tube to directly measure the rate of heat loss. By detecting small variations in the heat transfer rates it may be possible to detect the presence of steam channeling within the tube if that occurs. It would be most useful to be able to do this without having to unpack the core.

The heat flux sensors that have been ordered are manufactured by the RdF Corporation (Part Number 20457-2). The sensor essentially consists of forty pairs of thermocouples. Each thermocouple is separated from its mate by a thin film of plastic. Each pair is connected such that a potential difference is generated proportional to the minute temperature difference existing between the two thermocouples. Because the potential difference is so small, forty of these thermocouple pairs are connected in a series in order to increase the magnitude of the signal generated. Thus forty pairs of thermocouples are placed side-by-side measuring the temperature difference across a single film of plastic. This temperature difference is proportional to the heat flux passing through the sensor. Figure 3.4.3 is a simplified diagram showing key features of the sensor [Shallcross (1986)].

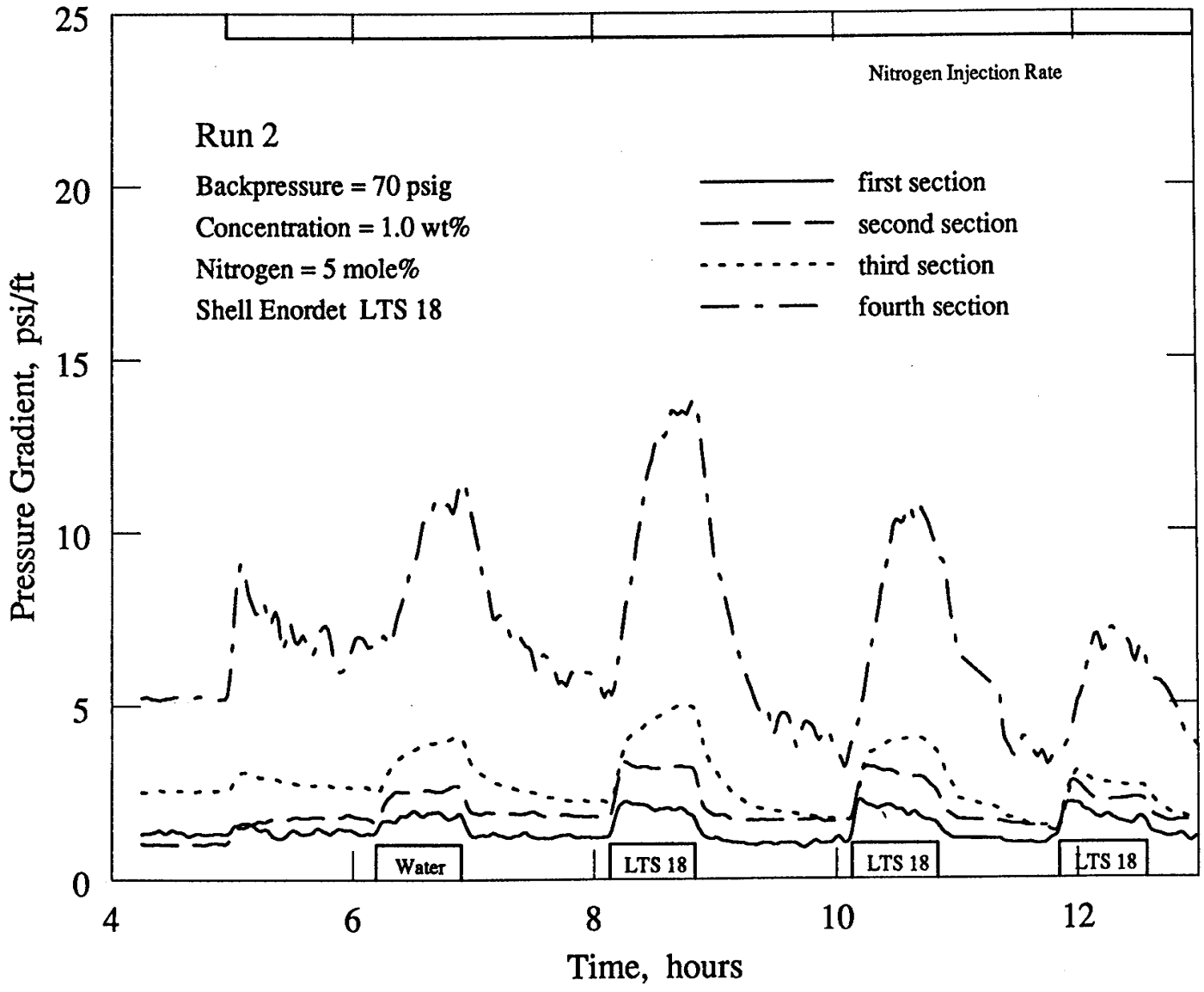

Fig. 3.4.2. Experimental Results for Run 2.

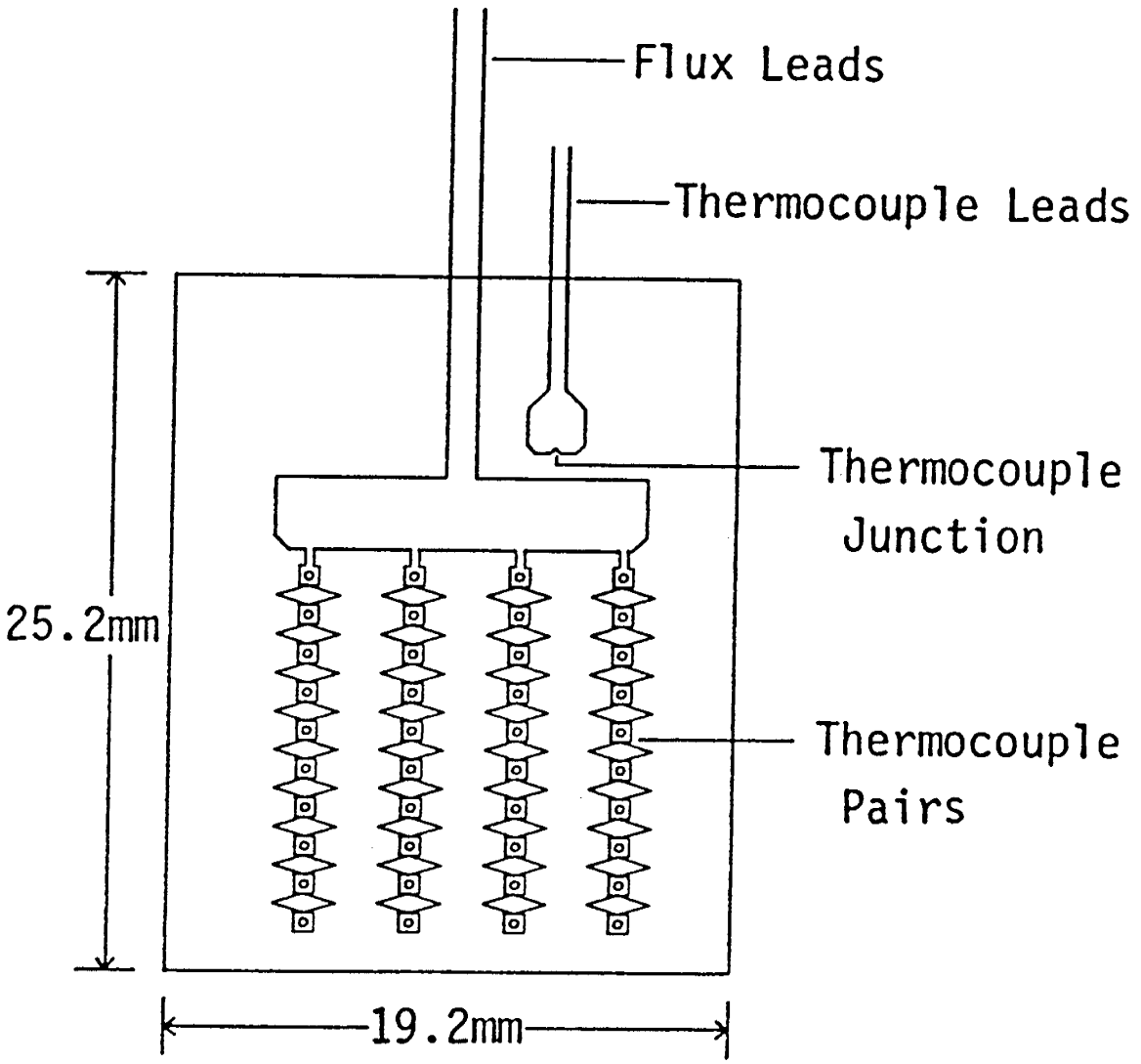

Fig. 3.4.3. Simplified Diagram of the Heat Flux Sensor.

These thermocouples are placed between additional layers of plastic to protect them from the environment. The total thickness of the sensor is approximately 0.2 mm, its width is 19.2 mm and length is 25.2 mm. The heat flux-sensitive area, however, is smaller than this; it measures 14 mm by 18 mm, slightly smaller than a small postage stamp. In addition a single thermocouple is located at one end of the sensor to measure the sensor's temperature.

Provided that the sensors are used properly, and corrections are made for the heat transfer disturbances caused by their presence, they should become a powerful tool in heat transfer research.

3.4.6. REFERENCES

Maneffa M.G.: "A Laboratory Study of Surfactants as Foam Diverting Agents," Master's Dissertation, Stanford University, Stanford, California (1987).

Shallcross D.C.: "Melting of an Axisymmetric Body Due to Convective Heat Transfer," Ph.D. Dissertation, University of Melbourne, Parkville, Victoria, (1986).

Wang F.P.: "A Study of Heat transfer of Steam Injection and the Effect of Surfactants on Steam Mobility Reduction," Ph.D. Dissertation, Stanford University, Stanford, California (1986).

3.4.7. ACKNOWLEDGEMENTS

The author wishes to gratefully acknowledge the support of the Commonwealth Scientific and Industrial Research Organizaion of Australia through their Postdoctoral Fellowship Programme.

Task 36 - INTEVEP shall provide DOE with information and results from steam with additives field tests to be performed with MARAVEN in Bolivar Coast oilfields.

EVALUATION OF A CYCLIC STEAM-SURFACTANT INJECTION PILOT TEST IN THE BOLIVAR COAST, VENEZUELA

(Task 36 of Annex IV of the Implementing Agreement)

Prepared by:
José Luis Ziritt
Orlando Rivas
Guido Bresolin

INTEVEP, S.A.
Los Teques, Venezuela

March, 1988

SUMMARY

In this report we present laboratory and field test results of steam soak with surfactant additives. Sixteen wells in the Bolivar Coast of Lake Maracaibo were steam-foamed using two commercial surfactants under different operating conditions.

For the pilot test we selected wells which covered different characteristics and stages of drainage in the Bolivar Coast. Parameters such as injection pressure surfactant concentration, presence of an electrolyte and a non-condensable gas and steam quality were changed during the test. Flowmeters were run with each set of conditions and results were evaluated by a mathematical procedure which gives the "Steam Divertion Factor". Additionally, the actual production performance was compared with the predicted production for a convencional cycle.

Even though the production cycle of the steam-foamed wells has not been completed, results at present show an average incremental oil production of 24%.

CONTENTS

	Page
SUMMARY	36-3
1. INTRODUCTION	36-5
2. FIELD TEST	36-6
3. FLOWMETER EVALUATION	36-7
4. PRODUCTION EVALUATION	36-8
5. STEAM DIVERSION RESULTS	36-9
6. PRODUCTION RESPONSE	36-11
7. CONCLUSIONS	36-13
REFERENCES	36-14
TABLES AND FIGURES	36-16

1. INTRODUCTION

Steam soak has proven to be an effective process to produce heavy oil from Bolivar Coast reservoirs. Nevertheless, the performance of the process has been influenced by poor distribution of steam in the different oil sands.

In fact, the Bolivar Coast reservoirs consist of several sand bodies separated by shale breaks. When steam is injected into these reservoirs it often channels through certain sands, leaving others untouched. The vertical poor distribution of steam has caused uneven depletion of the oil sands.

The injection of foaming agents has been proposed as a method to improve the vertical distribution of steam (1). Accordingly, a research program on the use of foaming agents was conducted and two surfactants were selected for their ability to reduce steam mobility through porous media under Bolivar Coast reservoir conditions (2).

The laboratory work was followed by a field pilot test involving 16 cyclic steam injection wells in the Tia Juana, Lagunillas and Bachaquero fields (3, 4). The fields are operated by MARAVEN, S.A. and the pilot test was carried out as part of a joint research project.

This paper presents the field perfomance of the selected surfactants with respect to their ability to improve the steam-injection profile and to enhance oil recovery.

2. FIELD TEST

The field test program had two main objetives:

First, the evaluation of steam diversion with regard to the influencing parameters which were identified through laboratory work; and second, the feasibility of improving oil production by improving the steam injection profile and by the interfacial effects caused by the presence of the surfactant.

The selected wells covered different characteristics and stages of drainage existing throughout the Bolivar Coast. General reservoir characteristics and oil properties are given in Table 1.

Two surfactants were used. A linear alkyltoluene sodium sulphonate (LTS) was injected in nine wells (Dec. 84 - Aug. 85) while a branched alkylbenzene sodium sulphonate (BBS) was tested in seven other wells (Nov. 85 - Mar. 86). Pertinent test data is given in Table 2 where wells are listed in chronological order.

All wells, with the exception of LSE-1335, were stimulated with steam for 3 to 7 days before any surfactant was injected. This responded to the need of establishing a base steam injection profile to evaluate any change. The steam distribution was determined by flowmeter surveys. Once the base profile was established, surfactant injection was started and the new injection profiles were measured.

Flowmeters were also used any time an operating parameter was changed. In this way, the influence of surfactant concentration, steam quality, presence of an electrolyte (NaCl) and the addition of natural gas was determined.

A detailed description of the test and the injection procedure practiced in each well was made by D'Orazio et al (3) and more recently by Robaina and Ziritt (4).

3. FLOWMETER EVALUATION

Flowmeters are commonly used in steam-surfactant field injection tests to evaluate the effectiveness of additives in improving the injection profile. Nevertheless, up to now, these profiles were only qualitatively interpreted by visual comparison of the steam and steam-additive measurements. Fig. 1, for instance, shows flowmeter readings obtained in well LSE-2705. Curve 1 represents the injection profile when only steam was injected. In this case only 36 feet of oil sand were stimulated. On the other hand, curves 2 through 6 are the injection profiles obtained when injecting steam with additives under different operating conditions. Compared to the first case, all the new steam profiles, which cover up to 130 feet, are better. However, due to the fact that these curves are qualitatively too similar, it is difficult to decide which one is the best, based only on visual interpretation. Therefore, to properly evaluate the field test, a quantitative flowmeter evaluation procedure was developed by Rivas (5).

The evaluation model compares the distribution profiles through a "Steam Diversion Factor" (SDF) which is mathematically calculated for each survey. This factor considers the intervals receiving steam with respect to the total sand thickness, the blocking effect and the maximum blocking which one desires to obtain with the additive.

A positive value of SDF is an indication that steam distribution was improved, while a negative value indicates steam profile deteriorates with the new operating conditions.

In this paper, all flowmeters were compared with the base steam injection profile measured before the surfactant injection started. In the case of well LSE 1335, a flowmeter runned during the injection of the previous steam cycle was used as the base profile.

A computer program which automatically calculates the SDF by reading the flowmeters through a digitazing table was also developed.

4. PRODUCTION EVALUATION

Production response to the steam-surfactant stimulation was evaluated by comparing it to the predicted production if only steam had been injected.

The expected production for each well was determined by MARAVEN, S.A. through a statistical procedure (3, 4). The model used considers the production history of the particular well and the performance of up to 36 representative surrounding wells.

The production prediction as well as the oil production for the steam-surfactant cycle and the previous steam cycle were compared for each well. As an example, the production behavior of well LSE-2705 is presented in Fig. 2. Details of the other wells has been reported in Ref. (3, 4).

5. STEAM DIVERSION RESULTS

The influence of surfactant concentration on the injection profile was studied in wells LSE-2705, LSE-3782 and LSE-1335 where LTS was injected. As it may be seen in Fig. 3, the highest SDF value was obtained with a surfactant concentration of 0.5% W/W active matter in the liquid phase. In the case of BBS the optimum SDF was obtained at 1.0% surfactant concentration.

Well head injection pressure was monitored during the tests. The injection pressure in well LSE-3116 showed a small pressure increase during the initial 5 day steam injection period (Fig. 4). This behavior was attributed to the accumulation of steam. On the other hand, when BBS surfactant injection started at 0.5% A.M. concentration, a substancial injection pressure increase was observed (i.e. aprox. 90 psi). Moreover, when surfactant concentration was increased to the optimun (1% A.M.) a higher pressure increment was monitored (i.e. aprox. 140 psi).

This phenomenon is caused by the blocking effect of the additive which was also noticed through the SDF values calculated from the profile surveys (see Fig. 4).

Our previous laboratory work (2,6) showed that injection of an electrolyte could change the blocking ability of a surfactant depending on the initial condition of the porous media. The convenience of injecting NaCl electrolyte in Bolivar Coast reservoirs was evaluated in wells LSE-2705 and LSE-2282. As shown in Fig. 5, brine seems to have an adverse effect on the efficiency of surfactants when applied to Bolivar Coast reservoirs.

Well LSE-1831 and LSE-3547 were used to study the evolution of SDF with time when surfactant injection was started or stopped. Even though only low values of SDF were achieved in the wells, it was observed that within short periods of time (i.e. 1 to 2 hours) the SDF increased when surfactant injection was alternately stopped and started.

Fig. 6 presents the SDF values at different stages of a steam surfactant and steam cyclic injection. Whenever surfactant injection is started, steam diversion increases, reaches a maximum point and then decreases with time. If surfactant injection is then stopped, a diversion increase is reestablished and a new peak value is reached. Therefore, to maintain a high steam diversion it seems to be necessary to inject the surfactant in a cyclic way. A steam-surfactant and steam alone cyclic injection scheme was used to stimulate the rest of the wells (i.e. LSE-1609, LSE-1693, LSE-1452 and LSE-1549).

Keeping a fixed surfactant injection rate, steam quality was varied in well LSE-1609. A visual evaluation of the flowmeters suggested there was no mayor variation in the steam injection profile for 70% and 95% steam quality (3). However, SDF has shown that there is a difference in the profiles. When steam quality was increased, the SDF value changed from 0.08 to 0.17. This shows that BBS surfactant diverted more steam when the quality was higher.

On the other hand, the use of natural gas was tested in wells LSE-1693 and LSE-1452. The field test confirmed our laboratory findings. The addition of gas increased the blocking ability of the surfactant. However, the blocking was accomplished without diverting steam into new oil sands as it could be seem through the corresponding SDF values. In well LSE-1693 for example, before any gas injection the SDF value for the steam-surfactant profile was 0.27, when gas was added it decreased to 0.20. With these results, the use of gas was considered adverse when injecting BBS in Bolivar Coast reservoirs.

6. PRODUCTION RESPONSE

In all the wells treated with LTS the initial oil produc- tion was associated with very high water-cuts (90%). These cuts progressively decreased to normal 20% - 30% over about 8 months. On the contrary, oil production generally started at low rates but increase with time to levels higher than the expected for a conventional steam soak, specially in those wells where a high SDF was achieved.

Production behavior of the wells differs depending on the additive used. On the contrary of LTS wells, when using BBS water-cuts where similar to those of a conventional steam soak (20% - 30%) and high oil production rates where achieved from the beginning of the cycles.

Through laboratory experiments it has been determined that the high water production observed when using LTS is probably due to a change in the water relative permeability curve (7).

The influence of LTS (0.5% A.M.) on the water/oil relative permeability curves is presented in Fig. 7. It was found that LTS dramatically increases relative permeability to water while, in the case of BBS the relative permeability to water seems to stay unchanged (Fig. 8).

These two figures also show a certain increase in the oil relative permeability curves. This phenomenon will help oil production, specially if the residual oil saturation (end point) is shifted to a lower value, as it seems to be the case for the two surfactants.

The incremental oil production rate was calculated from the production and prediction data and compared to the SDF values obtained during the injection of each well. As it is shown in Fig. 9, there exists a good correlation between these two parameters. If properly handled the correlation can be used to estimate the incremental oil production of a steam diversion operation.

In general, there are more wells with high SDF and significant incremental oil rate in the case where LTS was injected than in the case of BBS. These results show that for Bolivar Coast reservoirs LTS is a better diverting agent than BBS.

In wells LSE-2705, LSE-2282, LSE-1335 and LSE-3670 a separated new sand body was stimulated with the use of the surfactant. From this fact and the above results it can be assured that a good diverting agent can increment oil production, specially, if new oil sands are stimulated.

Additionaly, it must be pointed out that wells LSE-1335 and LSE-1609 have had operational production problems. Therefore, their production potencial should be somewhat higher than what it is shown in Fig. 9.

The production cycle of steam-soaked wells in the Bolivar Coast normally lasts over 36 months. Thus, the production of the steam-foamed wells has not been completed. Nervertheless, the performance of the first nine wells, which have been producing during 23 to 31 months (26 months in average), show an average incremental oil production of 24% as shown in Fig. 10.

A rough economical evaluation of the pilot test at present establishes the cost of the additional oil, due to the surfactant, in 3.7 US$ per barrel. However, this does not takes into account the fact that the production cycles have not been completed, that we are probably producing additional reserves and that we have rised our production potential. At the end of the production cycles we expect to have a final cost for the pilot of around 3 US$ per barrel of extra oil. Moreover, if the process is used at a commercial level in the Bolivar Coast reservoirs, the cost of the additional oil will probably be in the range of 0.6 to 1.6 US$ per barrel, depending on the price of the surfactant.

7. CONCLUSIONS

The Steam Diversion Factor is a valuable parameter that quantifies the effectiveness of a steam diversion operation.

In this work we found that the incremental oil production correlates with the SDF, and among the different mechanisms that influence the steam-foam performance, steam diversion to new oil sands seems to be the most important one.

Flowmeter surveys with different set of parameters showed that the SDF decreases when using brine, non-condensable gas and low steam quality for Bolivar Coast reservoirs. Therefore, care should be exercised when using foaming surfactants under these conditions.

Alternating injection of steam-surfactant and steam alone cycles should be practiced to optimize the SDF.

Finally, even though the production cycle of steam-foamed wells has hot been completed, results at present show an average incremental oil production of 24%.

REFERENCES

(1) DILGREN, R.E., DEERMER, A.R. and OWENS, K.B.:
"The Laboratory Development and Field Testing of Steam/Non-Condensable Gas Foams for Mobility Control in Heavy oil", Paper SPE 10774, presented at the California Regional Meeting of the SPE of AIME, San Francisco, March 1982.

(2) ZIRITT, J. L., PAZ, F. and RANCEL, C.:
"Inyección de Vapor con Agentes Espumantes", paper presented at the I Simposio Internacional sobre Recuperación Mejorada de Crudo, Maracaibo, February 1985.

(3) D'ORAZIO, F., ZIRITT, J. L., RONDON, L., RUBIO, R., PAEZ, E., RIVAS, O. and PAZ, F.:
"Pruebas Piloto de Inyección Alternada de Vapor con Surfactantes" paper presented at the II Simposio Internacional sobre Recuperación Mejorada de Crudo, Maracaibo, February 1987, Proc. Vol. II, pp. 245-273.

(4) ROBAINA, R.and ZIRITT, J.L.:
"Evaluation of a Surfactant-Steam Soak Pilot Test in the Bolivar Coast, Venezuela", Paper SPE/DOE 17386, presented at the SPE/DOE Sixth Symposium on EOR, Tulsa, April 1988.

(5) RIVAS, O.:
"Interpretación Cuantitativa de Registros de Flujo en Pruebas Piloto de Inyección de Vapor con Espuma"., paper presented at the II Simposio Internacional sobre Recuperación Mejorada de Crudo, Maracaibo, February 1987, Proc. Vol. I, pp 585-604.

(6) ZIRITT, J.L., PAZ, F., and RANCEL, C.:
"Steam-Surfactant Process - A Laboratory Research and a Field Application", paper presented at the 3rd European Meeting on Improved Oil Recovery, Rome, April 1985, Proc. Vol. I, pp. 341 - 348.

(7) ZIRITT, J.L.:
"Efecto de un Tensoactivo Sobre los Parámetros Característicos del Proceso de Inyección Cíclica de Vapor", paper presented at the II Simposio Internacional sobre Recuperación Mejorada de Crudo, Maracaibo, February 1987, Proc. Vol. II, pp 817 - 835.

TABLE 1

Reservoir characteristics and properties of the selected well

OIL PRODUCTION RATE, BPD	10	-	50
WATER CUT, %	10	-	20
INJECTION PRESSURE, psi	400	-	800
STEAM INJECTION RATE, ton/D	280	-	340
STEAM SLUG SIZE, Ton	5000	-	6000
INJECTIVITY, ton/D/psi	0.4	-	1.0
PROGRAMMED STEAM CYCLE	II	-	IV
DEPTH AT TOP OF PUY ZONE, ft	1000	-	2000
NET OIL SAND, ft	70	-	400
ESTIMULATED SAND, ft	50	-	150
STATIC PRESSURE AT TOP OF PAY ZONE, psi	50	-	350
POROSITY, %	30	-	40
OIL VISCOSITY, (100°F), cP	500	-	10000
OIL GRAVITY, °API	10	-	15
RESERVOIR TEMPERATURE, °F	100	-	140

TABLE 2

Test data information of the injected wells

FIELD	PROJECT	WELL	CYCLE	INJECTION PRESSURE (psi)	STEAM QUALITY (%)	STEAM INJECTED (ton)	SURFACTANT INJECTED (ton)	OTHER FLUIDS INJECTED
			LINEAR ALKYLTOLUENE SULPHONATE (14.3% A.M.)					BRINE (ton)
Tia Juana Este	F-7	LSE-2705	IV	450	85	5650	40.8	1.65
Tia Juana Este	F-7	LSE-2282	III	320	92	6017	21.5	3.52
Tia Juana Este	F-7	LSE-3782	II	480	83	6104	45.0	---
Tia Juana Este	F-7	LSE-1335	IV	400	90	6322	36.1	---
Tia Juana Este	F-7	LSE-1317	IV	430	75	7125	40.6	---
Lagunillas	V-7	LS-3670	II	780	70	6323	54.2	---
Lagunillas	V-7	LS-2687	IV	560	50	6104	61.4	---
Lagunillas	T-6	LS-2093	IV	800	50	6105	63.4	---
Bachaquero	HH-8	LB-1908	II	760	50	5755	47.8	---
			BRANCHED ALKYLBENZENE SULPHONATE (14.7% A.M.)					NATURAL GAS (MSCF)
Tia Juana Este	D-6	LSE-3116	IV	533	85	5245	29.1	---
TiA Juana Este	F-7	LSE-1831	IV	383	75	5960	39.4	---
Tia Juana Este	J-7	LSE-3547	III	344	75	5179	20.5	---
Tia Juana Este	J-7	LSE-1609	IV	550	70-95	5468	40.8	---
Tia Juana Este	M-6 ALT.	LSE-1693	III	440	90	5297	18.3	1200
Tia Juana Este	M-6 ALT.	LSE-1452	IV	420	90	5598	46.8	274
Tia Juana Este	J-7	LSE-1549	IV	410	98	6426	49.9	---

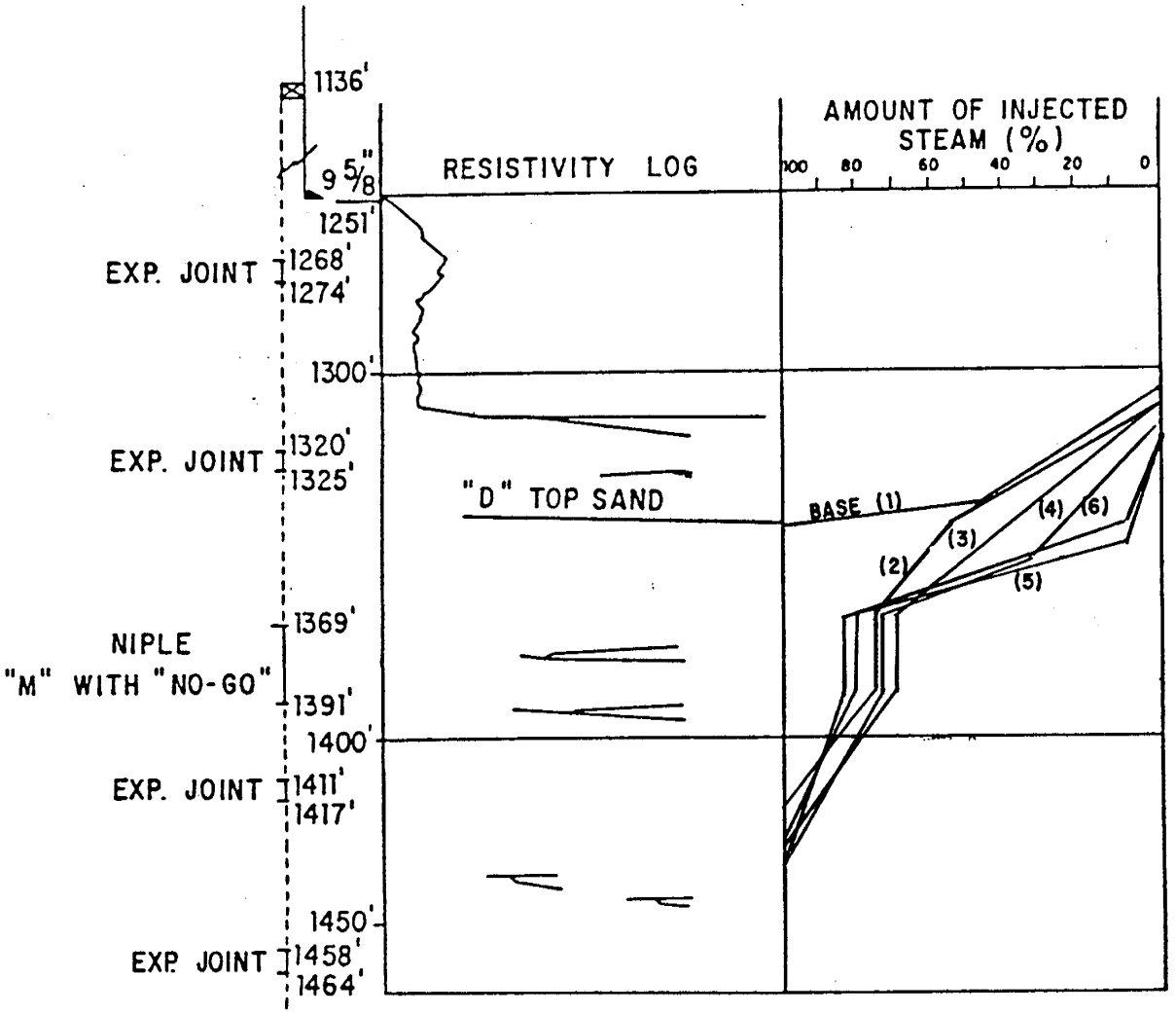

FIG. 1: STEAM INJECTION PROFILES IN WELL LSE-2705

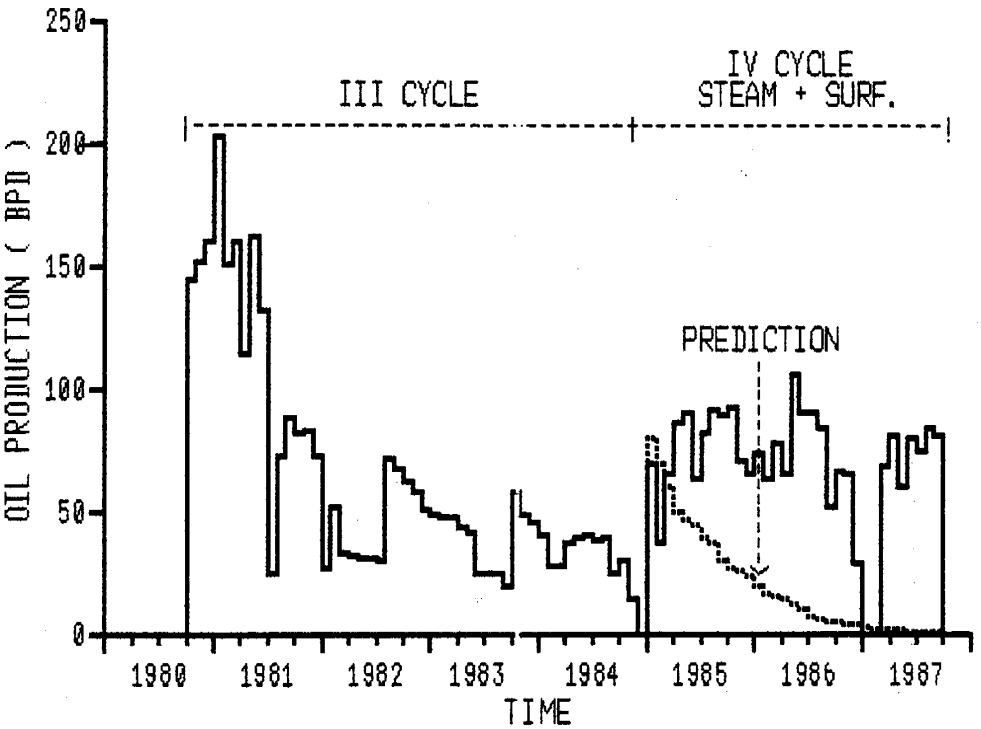

FIG. 2: OIL PRODUCTION PERFORMANCE IN WELL LSE-2705

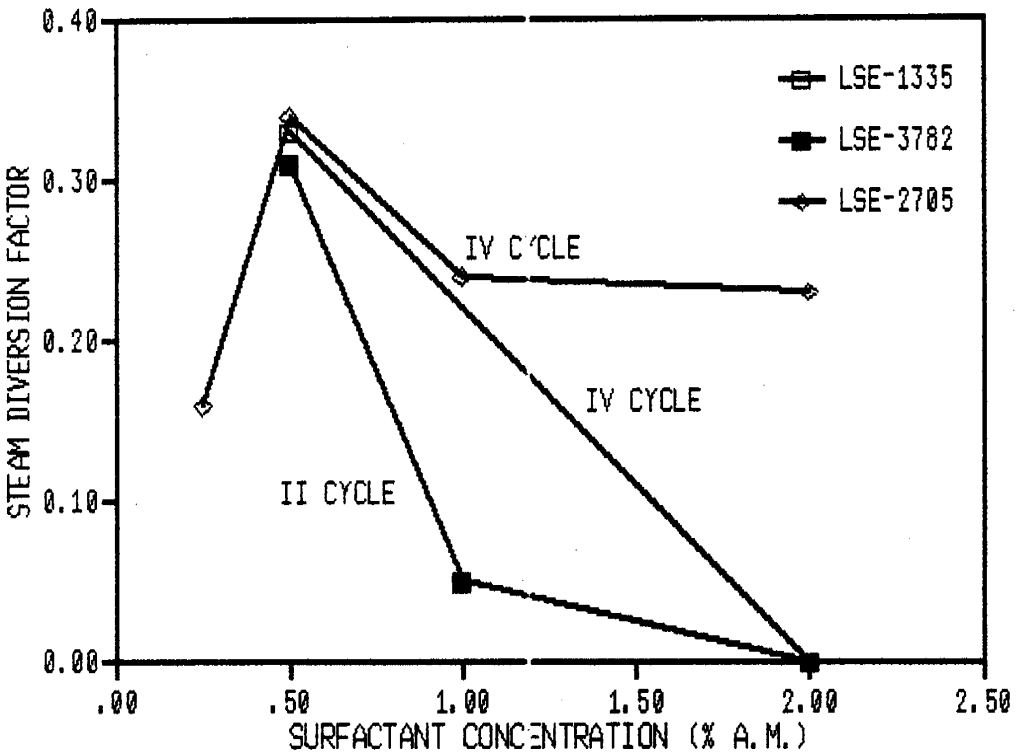

FIG. 3: LINEAR ALKYLTOLUENE SODIUM SULPHONATE

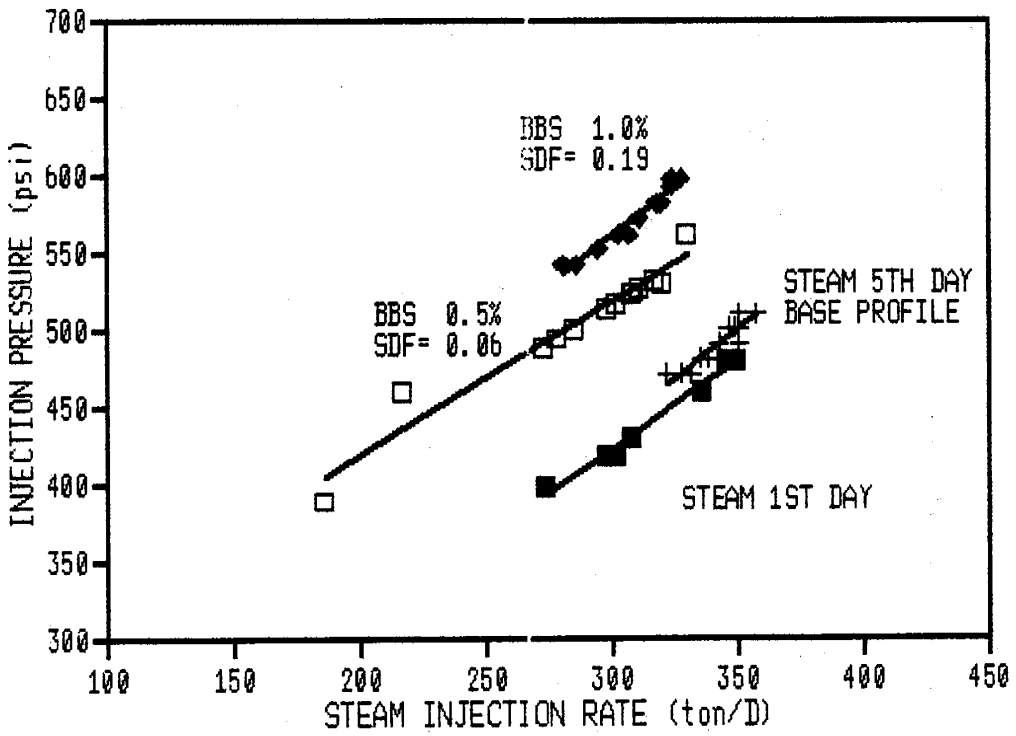

FIG 4: INFLUENCE OF SURFACTANT CONCENTRATION ON THE WELL HEAD INJECTION PRESSURE OF WELL LSE-3116

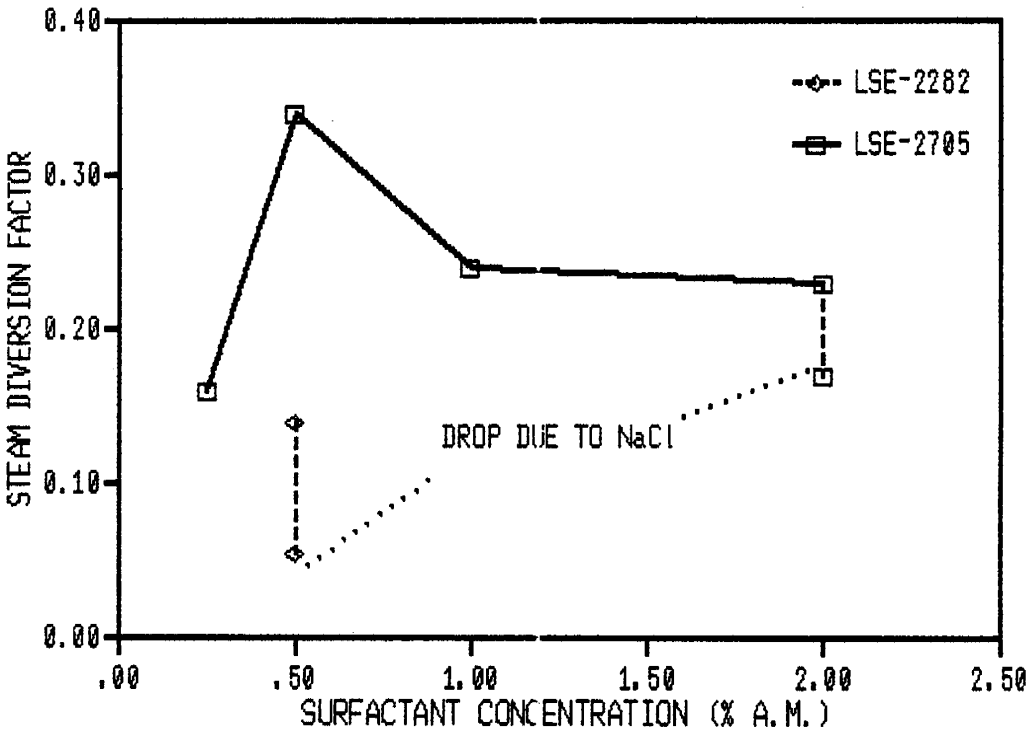

FIG. 5: INFLUENCE OF NaCl ELECTROLYTE ON THE STEAM DIVERSION FACTOR

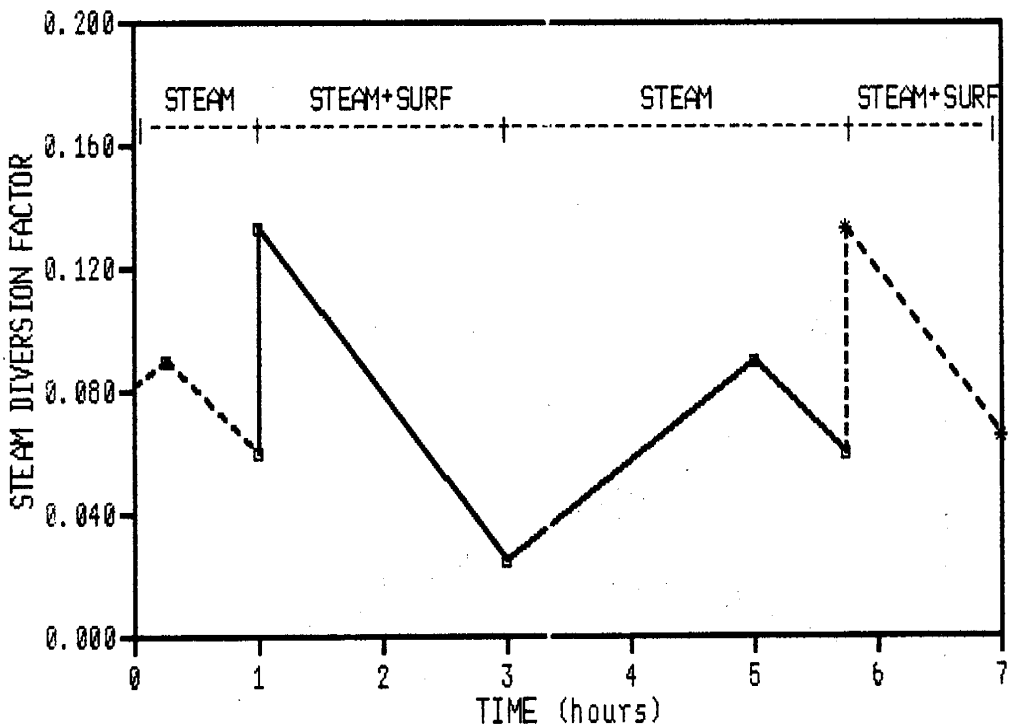

FIG. 6: INFLUENCE OF SURFACTANT CYCLIC INJECTION ON THE "SDF" VALUES IN WELL LSE-3547

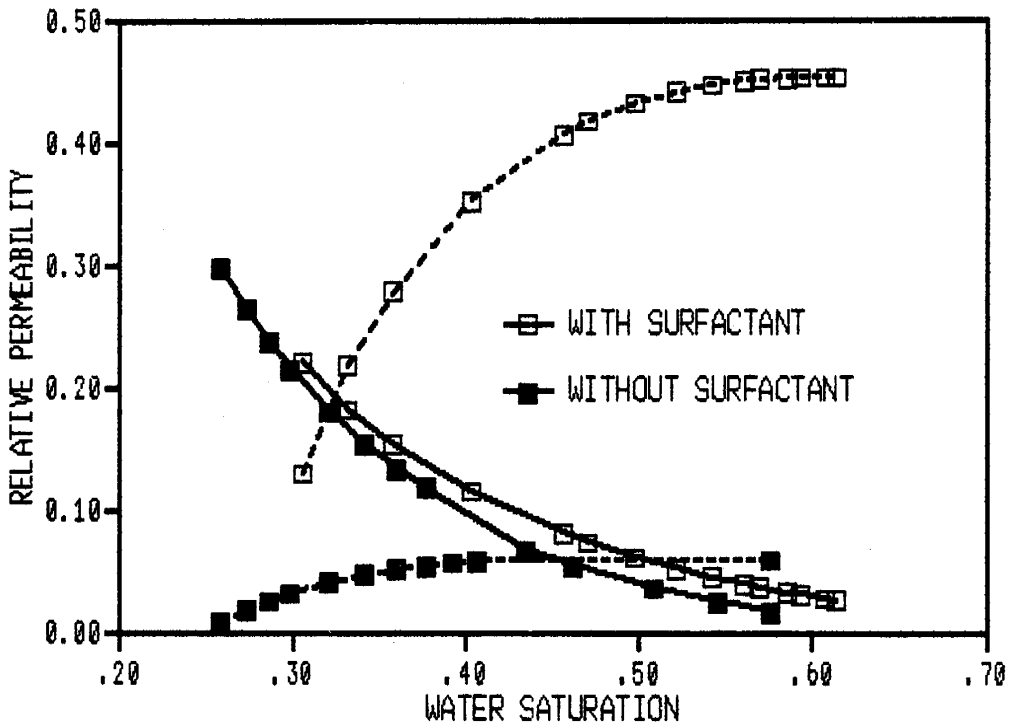

FIG. 7: INFLUENCE OF LTS SURFACTANT ON THE OIL/WATER RELATIVE PERMEABILITY CURVES

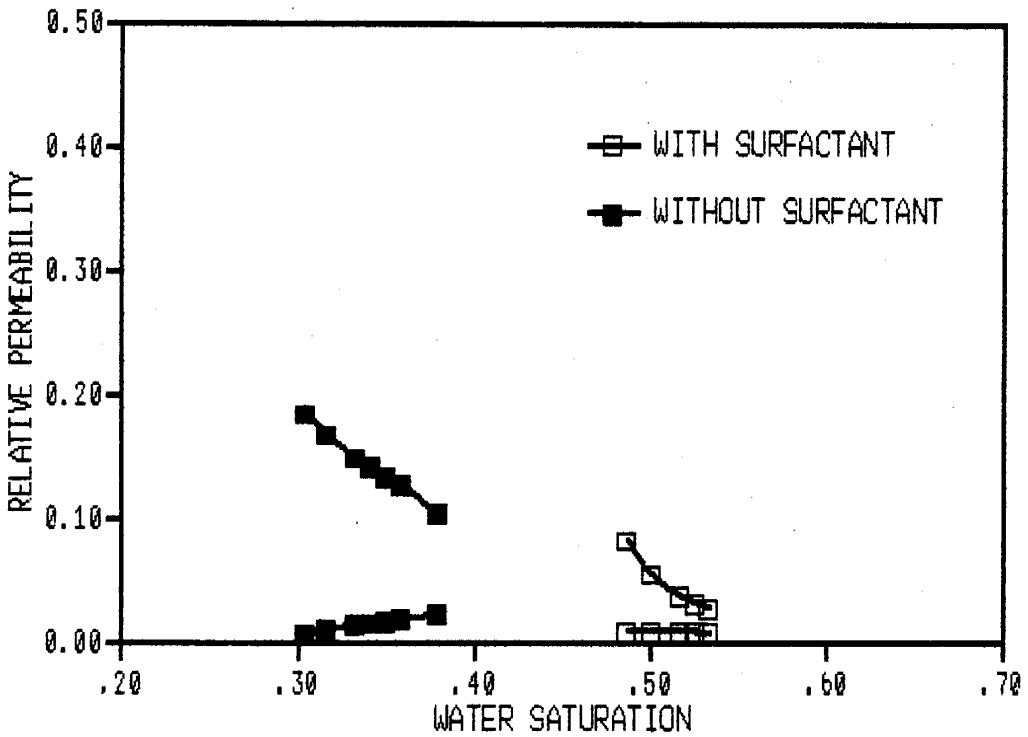

FIG. 8: INFLUENCE OF BBS SURFACTANT ON THE OIL/WATER RELATIVE PERMEABILITY

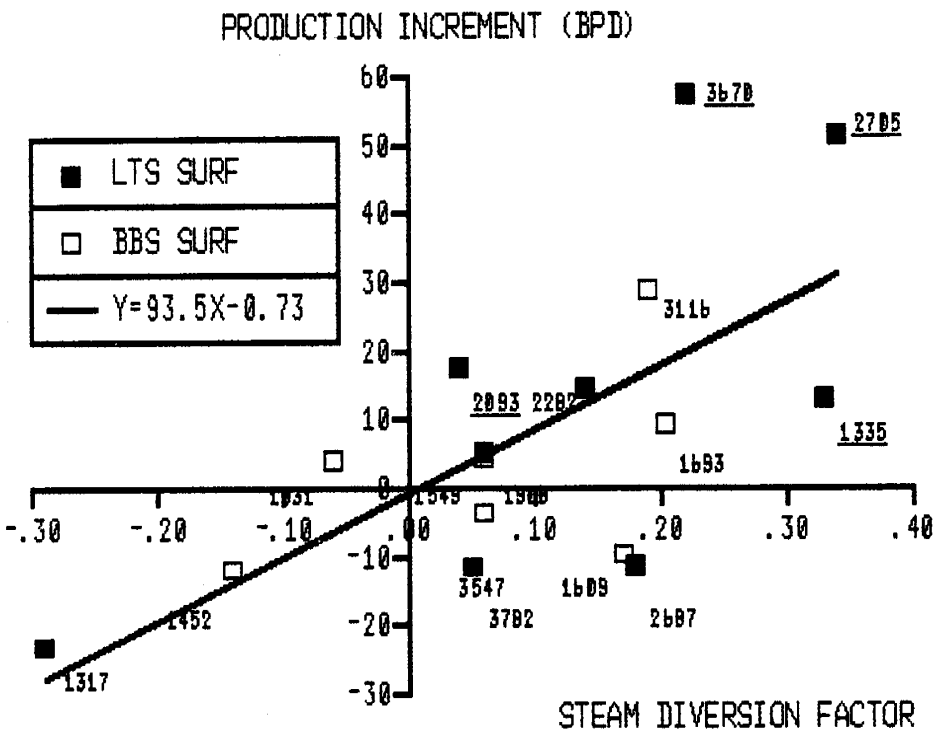

FIG. 9: INFLUENCE OF THE STEAM DIVERSION FACTOR ON OIL PRODUCTION

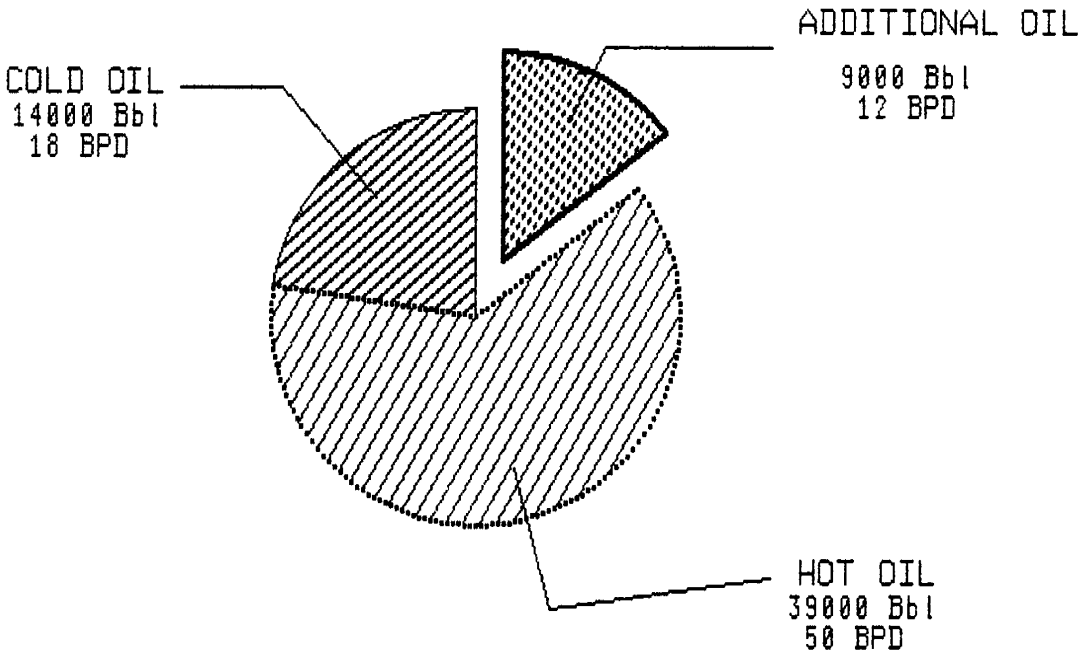

FIG. 10: AVERAGE PRODUCTION PERFORMANCE PER WELL FOR THE STEAM-SURFACTANT FIELD TEST

Task 37--DOE shall provide INTEVEP with information and results from the DOE funded research at NIPER on steamflooding light oil.

NIPER-347

Thermal Recovery of Light Crude Oils Using Steam--A Laboratory Study Using a Two-Dimensional Physical Model

(Task 37 of Annex IV of the Implementing Agreement)

Project BE11A, Milestone 5, FY88

By Arden Strycker

Prepared for
U.S. Department of Energy
Under Cooperative Agreement
DE-FC22-83FE60149

Thomas Reid
Project Manager
Bartlesville Project Office
U.S. Department of Energy

DISCLAIMER

This report was prepared as an account of work sponsored by an agency of the United States Government. Neither the United States Government nor any agency thereof, nor any of their employees, makes any warranty, express or implied, or assumes any legal liability or responsibility for the accuracy, completeness, or usefulness of any information, apparatus, product, or process disclosed, or represents that its use would not infringe privately owned rights. Reference herein to any specific commercial product, process, or service by trade name, trademark, manufacturer, or otherwise, does not necessarily constitute or imply its endorsement, recommendation, or favoring by the United States Government or any agency thereof. The views and opinions of authors expressed herein do not necessarily state or reflect those of the United States Government or any agency thereof.

IIT Research Institute
National Institute for Petroleum and Energy Research
P.O. Box 2128
Bartlesville, Oklahoma 74005

TABLE OF CONTENTS

	Page
Task 37	37-1
Cover Page	37-2
Table of Contents	37-3
Abstract	37-4
Introduction	37-5
Acknowledgment	37-7
Experimental Conditions	37-7
Oil Production Characteristics	37-9
Residual Saturation Patterns	37-11
Conclusions	37-12
References	37-12

TABLES

1. Properties of crude oils studied 37-15
2. Gas-chromatography simulated distillation (°F) of crude used 37-15
3. Sieve analysis of sand 37-15
4. Summary of experimental runs 37-16
5. Residual oil saturations, in % PV (and total steam contact time, hr) distribution in the 2-D model-Wade lease crude (run 1A) 37-17
6. Residual oil saturations, in % PV (and total steam contact time, hr) distribution in the 2-D model-Delaware-Childers crude (run 2B) 37-17
7. Residual oil saturations, in % PV (and total steam contact time, hr) distribution in the 2-D model-New London crude (run 3B) 37-18
8. Residual oil saturations, in % PV (and total steam contact time, hr) distribution in the 2-D model-Mt. Pleasant crude (run 4A) 37-18

ILLUSTRATIONS

1. Schematic diagram of 2-D steamflood experimental assembly 37-19
2. Cumulative oil production as function of time 37-20
3. Composition of produced oil during steamflood (Wade Lease crude) .. 37-20
4. Composition of produced oil during steamflood (Delaware-Childers crude) 37-21
5. Composition of produced oil during steamflood (New London crude) .. 37-21
6. Effect of light ends on light oil recovery by steamflood 37-22
7. Temperature profile after 8 hours of steam injection (run 1B) 37-23
8. Effect of light ends on steam breakthrough time 37-24
9. Comparison of residual oil saturation with steam contact time for Wade Lease crude oil 37-24
10. Comparison of residual oil saturation with steam contact time for Delaware-Childers crude oil 37-25
11. Comparison of residual oil saturation with steam contact time time for New London crude oil 37-25
12. Comparison of residual oil saturation with steam contact time for Mt. Pleasant crude oil 37-26
13. Comparison of residual oil saturation with steam contact time for Huntington Beach crude oil 37-26

THERMAL RECOVERY OF LIGHT CRUDE OILS USING STEAM--A LABORATORY STUDY USING A TWO-DIMENSIONAL PHYSICAL MODEL

By Arden Strycker

ABSTRACT

Although steamflooding is traditionally used to recover heavy oils, some pilot projects have demonstrated steamflooding to be an effective technique for recovering higher gravity oils. In contrast to steamflooding of heavy crude oil reservoirs, steam distillation is predicted to be more important and gravity override less important for light crude oils. In this investigation, we compared results from the steamflooding of four light crude oils (30° to 48° API and about 4 to 7 cP at 78° F) with that of a heavy oil (14° API and 2,700 cP at 78° F). Most of the experiments were conducted using a two-dimensional physical model. In addition to the usual measurement of oil recoveries, compositional analyses of the crude oils, produced oils (as a function of time), and residual oils in the sandpack were made to determine what compositional changes occurred during the steamfloods.

The study showed that recovery efficiencies of light oil steamfloods are strongly influenced by the chemical nature of the crude and that substantial gravity override of steam remains a potential problem for light oil steamflooding. The reported numerical simulation findings of a piston-like steam movement in light oil reservoirs were not validated by the data resulting from this study. The residual oil saturation at the bottom of the model was substantially higher than that from the top of the model. An analysis of the residual oil at various levels in the model also indicated that the oil remaining near the bottom of the model contained greater concentrations of the lighter components than the residual oil near the top of the model.

The study also showed that light oil steamfloods are typified by an early production response to steam injection. Assuming that steamfloods become uneconomical when the instantaneous steam-oil ratio exceeds 10, the investigation showed that as much as 65% of the OOIP can be recovered economically. The amount of oil that can be recovered economically is, however, dependent upon a number of factors, including the chemical composition of the crude oil.

INTRODUCTION

Steamdrive is the most common enhanced oil recovery (EOR) process currently in use. Steamflooding has been used commercially for over two decades to recover heavy oil from shallow reservoirs. In recent years, much attention has been given to extending this technology to light oil reservoirs, as made evident by the reports of several pilot projects,[1-3] and laboratory[4-11] and computer simulation studies.[12-20] Results of these studies indicate that light oil steamflooding is a viable process and that steam distillation during steamflooding is the principal recovery mechanism. Results of numerical simulation studies indicate that gravity override of steam is expected to be minimal for light oil reservoirs and that good sweep efficiencies are possible in homogeneous production zones.

Most of the previous experimental studies were focused to generate crude oil steam distillation data and to correlate steam distillation yields with crude oil API gravity. Other studies were focused on the overall recovery and the temperature distribution in linear models. Effects of such important variables as rock properties, nature of the crude, steam injection rate, and degree of gravity override on the process have not been addressed. Reported simulation studies made allowances for only a few components, and the assumptions built into these reservoir models have limited their predictive ability for light crude oils.

Many laboratory studies and computer simulations of light oil steamflooding have been reported previously. Wu and Brown[4] concluded from their steam distillation studies on six crudes (9° to 36° API gravity) that changes in saturated steam temperature and pressure have insignificant effects on yields and that oil composition controls steam distillation yields. They also concluded that superheated steam gives much higher yields than saturated steam. Wu and Elder[5] found that steam distillation yields could be correlated with crude oil API gravity and oil viscosity. Duerksen and Hsueh[6] concluded from their investigations that steam distillation yields can be correlated with API gravity and wax content of crude oils. Ozen and Farouq-Ali[7] investigated the recovery of a 45° API gravity crude from a previously waterflooded sandpack by steam injection. They concluded that oil recovery is a function of injection rate--the higher the injection rate the greater the recovery. Flock and Lee[8] investigated temperature distribution during the steam

injection process in a previously waterflooded linear sandpack containing a 19° API gravity oil and concluded that the steam displacement process was relatively independent of the initial starting conditions. Crichlow, et al.[9] concluded from their linear coreflood experiments that steam can recover a substantial amount of oil even after waterflooding to an infinite water-oil ratio and that higher recovery can be expected from an unconsolidated pack than from a consolidated pack. They also concluded that steamdrive as a primary oil recovery process recovers more oil than when used as a tertiary process. Cheung, et al.[10] investigated the effect of steam injection on the recovery of a 43° API crude oil from a linear sandpack and concluded that steam can be very effective in recovering light oil and that steam-water floods are more energy efficient than steam injection alone. Madden and Sarathi[11] conducted light oil steamflood experiments in linear Berea sandstone cores and found that residual oil saturation was independent of initial oil or water saturations, steam quality, steam injection rate, and core permeability. They also found that oil recovery was affected by the chemical nature of the crude. The presence of large amounts of polar compounds in the crude lowered the ultimate recovery.

Many simulation studies on light oil steamflooding have appeared in the literature. These studies were performed to generate information useful for designing steamdrives for light oil reservoirs. Some of the findings of these studies were as follows:

(a) Light oil steamflooding is characterized by a reduced gravity override and a piston-like propagation of steam.[16,19]

(b) Recovery efficiency is a function of oil distillation characteristics.[16-17,19-20]

(c) An early production response is expected.[19]

(d) Oil recovery is independent of initial water and gas saturations.[16]

(e) Increased reservoir thickness reduces the ultimate steam-oil ratio.[16]

(f) Sweep efficiency is a function of API gravity.[16,19-20]

(g) Recovery rate is a function of permeability.[20]

(h) Noncondensable gas injection with steam accelerates production during early injection periods.[18]

(i) Steamflood performance improves with an increase in steam injection rate.[20]

(j) Cumulative steam-oil ratio (SOR) decreases with an increase in steam quality.[20]

To make light oil steamflooding a fully proven method, the key economic and technical risks associated with the process must be identified and addressed. Assessment of these risks requires an understanding of the process variables. The goal of this project was to identify those factors that could have a direct bearing on the success of the process. Some of these factors are rock properties, crude oil composition, degree of steam override, sweep efficiency, steam quality, and steam injection rate. The specific objective of this study was to determine experimentally the extent of steam override in the light oil steamflood process and to determine if certain numerical simulation findings are validated. Previous studies[11] conducted by NIPER investigated the effects of oil and rock properties on the performance of light oil steamfloods. Findings of our earlier studies are summarized elsewhere in this report. Our previous investigations were carried out using linear Berea sandstone cores, but most of the present work was conducted using a two-dimensional physical model.

ACKNOWLEDGMENT

The Author would like to acknowledge Partha Sarathi of NIPER for much of the development of this work, Doug Roark and Anita Stepp of NIPER for doing much of the laboratory work, Thomas Reid of the DOE Bartlesville Project Office for his suggestions, and the U.S. Department of Energy for the financial support of this project through cooperative agreement DE-FC22-83FE60149.

EXPERIMENTAL CONDITIONS

Although previous laboratory tests have yielded useful information on the effect of several parameters on light oil steamflood performance, those tests were performed under idealized conditions. The porous media used in those investigations were linear, small, and homogeneous compared to an actual reservoir. Hence, to obtain more realistic test results that can be related to field situations, NIPER conducted experiments in a two-dimensional sandpack which is more representative of a small reservoir element.

The crude oils used in this study are listed with their properties in table 1. The gas chromatographic (GC) simulated distillation results for the

crude oils are presented in table 2. Sandpacks were prepared from 140-230 mesh quartz-silica sand giving absolute permeabilities in the range of 2 to 3 darcies. The sieve analysis of the sand used in the study is given in table 3.

Major components of the experimental setup are the two-dimensional physical model, the injection system, the production system, and the data-monitoring system. A schematic diagram of the steamflood system is shown in figure 1. Specially designed distribution plugs with provisions for selective introduction of a fluid to the upper half, lower half, or to the entire cross section of the model were used at the inlet. Similar plugs were used at the outlet to permit the production of fluids from either the top or bottom half of the cell. In these experiments, the steam was specifically injected into the lower half of the sandpack and produced from both halves of the sandpack at the other end of the model. The interior walls of the model were lined with 3/8-in.-thick, zircon-based refractory cement. The outside of the model was covered with two layers of 'Temp-Mat' fiberglass blankets of 1-in. thickness. These insulations (inside and outside of the model) were provided to minimize heat losses. The inside insulation also minimized the conduction of heat through the stainless steel wall. One side of the model was a removable cover plate designed to expose the porous medium. A 1/4-in.-thick, high-temperature ethylene propylene terpolymer (EPDM) rubber pad was glued to the inside of the cover plate with a high-temperature epoxy cement to prevent the shifting and migration of sand during a run.

Each steamflood run was made using a new sandpack. The model was dry packed with sand using a vibrational technique designed to obtain reproducible packs with porosities less than 36% and absolute permeabilities between 2 and 3 darcies. After packing, carbon dioxide was allowed to flow through the pack for several hours to displace the air. The pack then was evacuated and saturated with 2% brine, and about 3 PV of crude was pumped through the sandpack to achieve residual water saturation. Initial oil and water saturations then were calculated by mass balance. Next, the sandpack was connected to the steamflood system, heated to initial reservoir temperature (125° F), and then flooded with steam. The backpressure was maintained at 190 to 200 psig, which corresponds to an average saturation temperature of about 388° F. Steam of 0.95 quality was injected at a rate of 0.35 lb/hr (250 cm/hr of cold water equivalent) in all tests.

Temperatures across the model were recorded in accordance with a predetermined schedule. The produced fluids were collected in graduated cylinders, and sample effluents were collected periodically for analysis. Steam injection was discontinued when the produced water-oil ratio exceeded 100 or after 3 hours of steam breakthrough. Following this, cold water was pumped into the model, and the injection was continued until the model was well below the steam temperature. The sandpack was next allowed to cool, and the cover plate was removed. The sandpack was photographed and divided into 18 sections, and the residual oil saturations in each section were determined by Dean-Stark analysis (oil saturation was determined by difference knowing the sandpack porosity). Additional oil samples from selected sandpack sections were extracted with methylene chloride. The compositions of the effluent samples and residual oils were determined by GC analysis. The API gravities of the effluents and residual oils were determined using a densitometer. The results of the experimental runs conducted in this investigation are summarized in table 4. Runs 1 through 5 were conducted in the two-dimensional sandpack and 6 through 8, in a linear sandpack using the same experimental conditions as for the two-dimensional sandpack experiment. In table 4, the letters A and B in runs 1 through 3 indicate duplicate runs.

OIL PRODUCTION CHARACTERISTICS

The cumulative oil production versus time plot of figure 2 shows that the light crude oils responded to steam injection much more quickly than the heavy crude oils. This observation is consistent with that of Hong.[19] While all of the light crudes responded to steam injection within 50 minutes after the start of the steam injection, no such early response was observed for the heavy crude. A production response for the heavy crude was noted only after 2 hours of steam injection. The initial response characteristics were probably due to the differences in mobility between light oils and heavy oils at reservoir temperatures. Later in the steamflood, the distillate bank ahead of the steam zone could mix with the unheated oil at the condensation front and increase the crude mobility.

Figures 3 through 5 summarize the changes in composition of produced crude oils with time for selected light crudes and clearly show that during steamflooding the composition of the produced oil changes. For these crudes, the

composition of the oil produced during early stages differed only slightly from the original composition. After 3 hours of steam injection, the light ends content of the produced oil began to rise, reaching a maximum after about 10 hours of steam injection. The oil gravity followed the trend of produced lighter components. Near the end of the run, the produced fluids became richer in heavier components. These data can be explained by the selective steam distillation of lighter components in the oil and the recondensing of these components to form a solvent bank ahead of the steamfront.

A comparison of results among different oils indicated that the chemical makeup of each oil determined which molecular weight fraction of chemical compounds predominate at the termination of the run. For example, after about 17 hours of steam injection, the produced sample of the Delaware-Childers crude was richer in C_{15}-C_{22} compounds, whereas the New London and Wade lease samples were richer in C_{21}+ compounds. Because of similar composition distributions, New London and Wade lease crudes had more similar production histories than Delaware-Childers crude. This observation suggests that the chemical makeup of the crude greatly influences steamflood performance.

The steamflood oil recovery is plotted against the percent of light ends (C_5 to C_{10}) in the crude in figure 6. This figure shows that as the amount of light ends in the crude increased, the ultimate oil recovery also increased. Although other investigations[4-6,20] correlated yields with API gravities of crudes, this study indicated that the major factor affecting ultimate oil recovery was the amount of light ends in the crude. For example, even though the New London crude and Delaware-Childers crude are of similar API gravities (34° API), the ultimate recovery was lower for the Delaware-Childers crude, presumably because it contained a higher percentage of heavy ends ($\geq C_{21}$). The ultimate recovery for the Wade lease crude also was higher than that for the Delaware-Childers crude and comparable to that of the New London crude, even though the API gravity of the Wade lease crude was lower (30.3° API). Figure 6 shows that for very volatile crude oils (crudes with less than 12% heavy ends) the expected oil recovery is about 68% OOIP, whereas the expected recovery drops to less than 45% OOIP for heavy crude oils (crudes containing more than 50% heavy ends).

The temperature distribution in the model after 8 hours of steam injection for run 1B is shown in figure 7. The steamfront advanced only to about 3 in.

from the injection port at the bottom and to about 9 in. at the top, indicating preferential movement of steam at the top. As the run progressed, the steam zone grew, but because of increased heat losses, the rate of growth of the steam zone declined. Thus, at the termination of the run, the bottom one-eighth of the model was never contacted by steam. Thus, Hong's[19] conclusion of a piston-like steamfront advancement in light oil reservoirs was not validated by the data from this experimental study.

A plot of steam breakthrough time versus the percent of light ends (C_5-C_{10}) in the crude shows that steam-breakthrough times decrease with increases in oil volatility. (See Fig. 8.) Steam-breakthrough time obviously is dependent on other factors, such as heat loss rate, reservoir heterogeneity, and injection rate. However, this study indicates that while other variables remain the same, a relationship may exist between oil volatility and steam-breakthrough time.

RESIDUAL SATURATION PATTERNS

At the termination of each run, representative sandpack samples were analyzed for residual oil content. The residual oil saturations at selected locations for some of the runs are presented in tables 5 through 8. These tables show that the oil saturation at the sampling point nearest the injection port in the bottom was very low compared to that of other sites. This site was exposed to steam for the entire duration of the experiment resulting in very low residual oil saturation. We also noted that the values of residual oil saturations depended on the nature of the crude, and in no case were the residual oil saturations less than 5%. The data on residual oil saturation clearly indicate that gravity override of steam remains a potential problem for light oil steamflooding. This conclusion also was supported by observation of temperature gradient patterns and sandpack photographs.

A comparison of residual oil saturations with steam contact times also indicates a general trend. The linear least square plots for the crude oils tested (Figures 9 through 13) show that longer steam contact times correspond with lower residual oil saturations for any given crude oil. Although the correlation coefficients are somewhat low (average = 0.92), such a relationship could be explained if the oil was recovered from the sandpack by a steam

distillation mechanism, where the less volatile components of the crude oil would steam distill at slower rates.

CONCLUSIONS

Conclusions from this study are as follows:

1. The recovery efficiency of a light oil steamflood is strongly influenced by the chemical nature of the crude oil.

2. Gravity override of steam remains a potential problem in light oil steamflooding.

3. Fifty-five to 65% of original oil in place (OOIP) can be recovered efficiently by steamflooding light oils.

4. The data obtained do not support the validity of numerical simulation findings that suggested piston-like steamfront advancement for light crude oils.

5. Steam distillation of lighter components in the crude oils plays a major role in the recovery of the oil. Steam distillation causes light ends of a crude oil to be produced preferentially to heavy ends. As a result the light ends of any particular crude oil are preferentially produced in the early stages of the steamflood, and crude oils with more light ends are produced more quickly leaving lower residual oil saturations.

REFERENCES

1. Volek, C. W. and J. A. Pryor. Steam Distillation Drive--Berea Field, California. J. Pet. Tech., Aug. 1972, pp. 899-906.

2. Konopnicki, D. T. et al. Design and Evaluation of the Shields Canyon Field Steam-Distillation Drive Pilot Project. J. Pet. Tech., May 1979 pp. 546-552.

3. Chappelle, H. H., G. P. Emsurak Jr., and S. L. Obernyer. Screening and Evaluation of Enhanced Oil Recovery at Teapot Dome in the Shannon Sandstone, A Shallow Heterogeneous Light Oil Reservoir. Pres. at the SPE/DOE Fifth Symposium on Enhanced Oil Recovery, Tulsa, OK, Apr. 20-23, 1986. SPE/DOE paper 14918.

4. Wu, C. H. and A. Brown. A Laboratory Study on Steam Distillation in Porous Media. Pres. at the 1975 SPE Annual Fall Tech. Conf. and Exhib., Dallas, Sept. 28-Oct. 1. SPE paper 5569.

5. Wu, C. H. and R. B. Elder. Correlation of Crude Oil Steam Distillation Yields With Basic Crude Oil Properties. Soc. of Pet. Eng. J., Dec. 1983, pp. 937-945.

6. Duerksen, J. H. and L. Hsueh. Steam Distillation of Crude Oils. Soc. Pet Eng. J., April 1983, pp. 265-271.

7. Ozen, A. S. and S. M. Farouq-Ali. An Investigation of the Recovery of the Bradford Crude by Steam Injection. Pres. at the SPE 4th Annual Eastern Regional Meeting, Pittsburgh, PA, Nov. 2-3, 1967. SPE paper 1972.

8. Flock, D. L. and J. Lee. An Experimental Investigation of Steam Displacement of a Medium Gravity Crude Oil in The Oil Sands of Canada-Venezuela-1977. CIM Special Vol. No. 17, Eds. D. A. Redford and A. G. Winestock. Canadian Institute of Mining and Metallurgy, Montreal, Quebec H3A 2M8 Canada, pp. 386-394.

9. Crichlow, H. B. et al. Maximizing Steam Drive Recovery in Light Oil Reservoirs. Final Report, Department of Energy Report No. BC/10316-26, 1983.

10. Cheung, Y. L., A. Brown and W. S. Huang. A Laboratory Study of the Tapered-Quality Steam-Water Process on Light Oil. Pres. at the 58th SPE Annual Fall Tech. Conf. and Exhib., San Francisco, CA, Oct. 5-8, 1983. SPE paper 12005.

11. Madden, M. P. and P. Sarathi. Light Oil Steamflooding-Core Flood Experiments. National Institute for Petroleum and Energy Research, Department of Energy Report No. NIPER-44, 1985.

12. Hsueh, L., K. C. Hong, and J. H. Duerksen. Simulation of High Pressure and High Temperature Steam Distillation of Crude Oils. Pres. at the Second Int'l. Conf. on Heavy Crude and Tar Sands, Caracas, Venezuela, Feb. 7-17, 1982. Paper No. UNITAR/CF10/VIII/2.

13. Coats, K. H. Simulation of Steamflooding With Distillation and Solution Gas. Soc. Pet. Eng. J, Oct. 1976, pp. 235-247.

14. Ferrer, J. and S. M. Farouq-Ali. A Three Phase, Two Dimensional Compositional Thermal Simulator for Steam Injection Processes. J. Can. Pet. Tech., Jan.-Mar. 1977, pp. 78-90.

15. Rhee, S. W. and T. M. Doscher. A Method for Predicting Oil Recovery by Steamflooding Including the Effects of Distillation and Gravity Override. Soc. Pet. Eng. J, Aug. 1980, pp. 249-266.

16. Aydelotte, S. R. and A. B. Ramesh. Economic Feasibility of Steam Drive in Light Oil Reservoirs. Final Report, Department of Energy Report No. BC/00044-1, Sept. 1979.

17. Hanzlik, E. J. Steamflooding as an Alternative EOR Process for Light Oil Reservoirs. Pres. at the 56th Annual Fall Tech. Conf. and Exhib. San Antonio, TX, Oct. 5-7, 1981. SPE paper 10319.

18. Hong, K. C. and J. W. Ault. Effects of Noncondensable Gas Injection on Oil Recovery by Steamflooding. J. Pet. Tech., Dec. 1984, pp. 2160-2170.

19. Hong, K. C. Numerical Simulation of Light Oil Steamflooding in the Buena Vista Hills Field, California. Pres. at the SPE Int'l. Meeting on Petroleum Engineering, Beijing, China, March 17-20, 1986. SPE paper 14104.

20. Chu, C. A Comprehensive Simulation Study of Steamflooding Light Oil Reservoirs After Waterflood. Pres. at the 62nd Annual Fall Tech. Conf. and Exhib., Dallas, TX, Sept. 27-30, 1987. SPE paper 16738.

TABLE 1. - Properties of crude oils studied

Oil No.	Supplier	Field	API gravity, degrees	Viscosity, cP @ 78° F
1	Cities Service Oil & Gas Corp.	Wade Lease Ponotoc Co., OK	30.3	7.2
2	B&N Oil Co.	Delaware-Childers Nowata Co., OK	34.5	6.1
3	Murphy Oil Co.	New London Union Co., AR	34.2	6.9
4	Sun Oil Co.	Mount Pleasant Midland, MI	48	4.1
5	Phillips	Huntington Beach, CA	14	2,700

TABLE 2. - Gas-chromatography simulated distillation (°F) of crude used

Crude oil	10%	20%	30%	40%	50%	60%	70%	80%
Wade Lease	305	444	542	626	711	798	890	1,000
Delaware-Childers	283	378	457	540	624	710	804	907
New London	272	385	478	562	648	741	847	976
Mt. Pleasant	209	325	407	490	591	675	788	891
Huntington Beach	560	670	780	870	952	1,080	---	---

TABLE 3. - Sieve analysis of sand

Sieve mesh size	Percent by weight retained	
100	0.45	
140	22.05)	
170	36.76)	84.01
200	25.2)	
230	6.70	
270	3.65	
325	2.09	
Pan	3.10	
	100.00	

TABLE 4. - Summary of experimental runs

Run No.	Oil	Initial oil sat'n, % PV	Sandpack		Total steam inj., PV[1]	Time of steam breakthrough, hours	Oil recovery, % OOIP
			Permeability, darcies	Porosity, %			
1A	Wade Lease	83.1	2.7	34.6	3.62	17.1	62.7
1B[2]	Wade Lease	82.8	2.4	35.2	3.51	16.7	63.1
2A	Delaware-Childers	83.9	2.5	33.8	4.39	21.3	55.8
2B[2]		84.6	2.1	34.7	4.51	21.8	57.1
3A	New London	84.3	2.4	35.4	4.01	19.1	65.1
3B[2]	New London	82.9	2.7	34.7	3.98	18.8	64.2
4	Mt. Pleasant	84.8	2.8	34.9	3.31	15.1	68.3
5	Huntington Beach	76.8	2.9	34.9	5.8	27.2	44.2
6[3]	Wade Lease	87.8	2.1	33.9	3.2	11.8	76.8
7[3]	Delaware	88.1	2.1	34.8	3.5	12.3	74.2
8[3]	New London	88.3	2.2	34.3	2.9	10.9	69.7

[1] Cold water equivalent.
[2] Duplicate run.
[3] Linear steamfloods.

TABLE 5. - Residual oil saturations, in % PV (and total steam contact time, hr) distribution in the 2-D model-Wade lease crude (run 1A)

Level	Distance from top, inches	Distance from steam injection port, inches					
		2	6	10	14	18	22
Top	1	9.0 (17)	9.0 (14)	13.7 (11)	13.9 (8)	18.9 (5)	19.1 (2.5)
Middle	3	9.0 (18)	11.3 (13)	15.7 (9)	16.1 (6)	22.7 (3)	25.3 (1)
Bottom	5	6.7 (19)	12.0 (10)	20.8 (7)	21.1 (3)	27.4 (2)	43.8 (-)

TABLE 6. - Residual oil saturations, in % PV (and total steam contact time, hr) distribution in the 2-D model-Delaware-Childers crude (run 2B)

Level	Distance from top, inches	Distance from steam injection port, inches					
		2	6	10	14	18	22
Top	1	9.3 (20)	8.9 (19)	11.8 (14)	16.5 (11)	18.7 (7)	19.3 (2)
Middle	3	8.0 (21)	10.5 (18)	11.5 (12)	16.1 (8)	20.0 (4)	22.7 (1)
Bottom	5	6.3 (22)	12.6 (15)	12.1 (10)	16.6 (5)	28.6 (3)	42.4 (-)

TABLE 7. - Residual oil saturations, in % PV (and total steam contact time, hr) distribution in the 2-D model-New London Crude (run 3B)

Level	Distance from top, inches	Distance from steam injection port, inches					
		2	6	10	14	18	22
Top	1	10.0 (18)	8.4 (17)	14.9 (14)	13.6 (11)	16.8 (6)	16.9 (3)
Middle	3	10.0 (18)	12.1 (15)	16.0 (11)	13.7 (8)	20.9 (3)	21.8 (2)
Bottom	5	5.2 (20)	12.9 (12)	23.7 (9)	19.8 (4)	26.3 (1)	38.9 (-)

TABLE 8. - Residual oil saturations, in % PV (and total steam contact time, hr) distribution in the 2-D model-Mt. Pleasant crude (run 4A)

Level	Distance from top, inches	Distance from steam injection port, inches					
		2	6	10	14	18	22
Top	1	8.3 (15)	9.1 (14)	13.6 (11)	14.4 (8)	16.2 (5)	17.5 (2)
Middle	3	8.8 (15)	9.5 (13)	14.5 (8)	15.6 (5)	17.4 (2)	20.1 (1)
Bottom	5	6.8 (17)	16.0 (11)	16.8 (5)	21.1 (3)	25.6 (1)	41.7 (-)

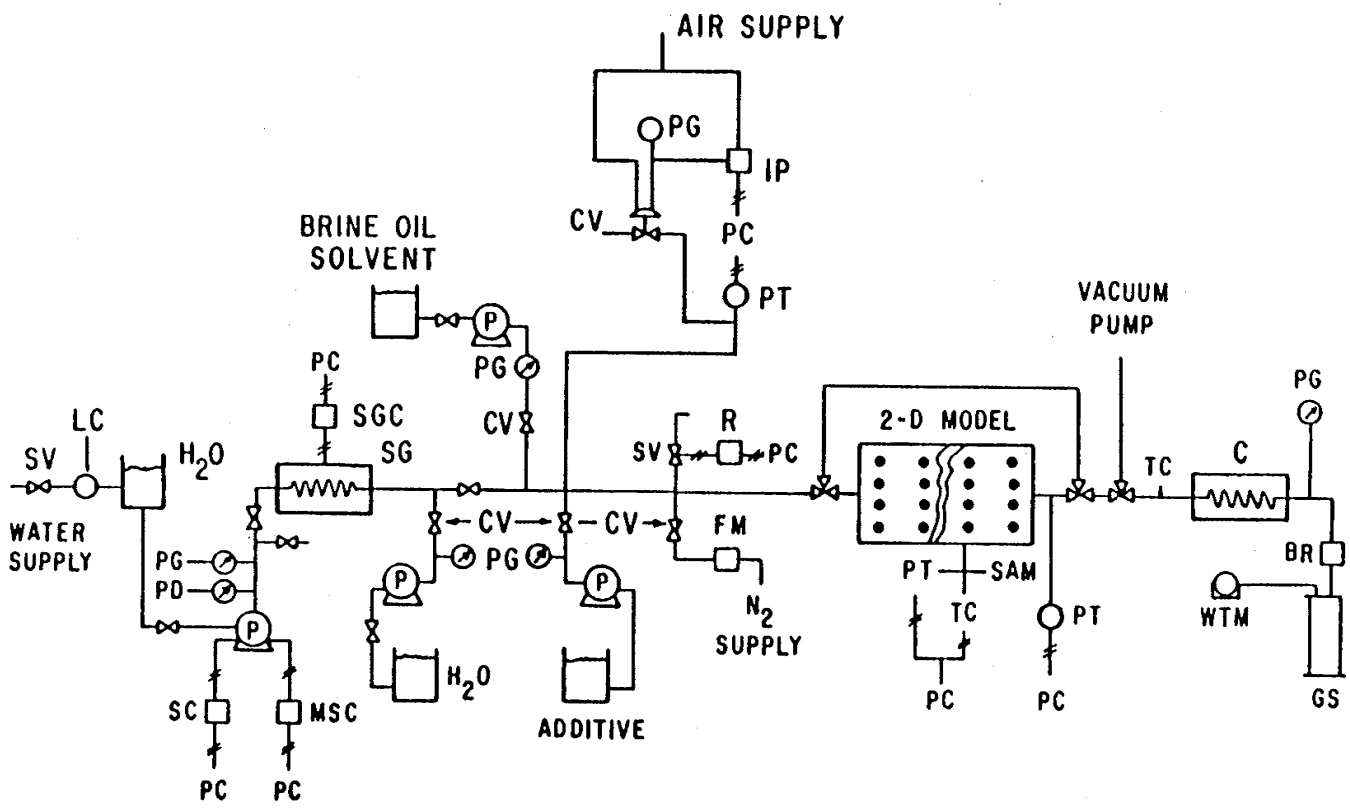

BR-Back Pressure Regulator
C -Condenser
CV-Control/Check Valve
FM-Flow Meter (GAS)
GS-Graduated Cylinder
IP-Current/Pressure Converter
LC-Level Control

MSC-Motor Speed Control
P -Pump
PC -Personal Computer
PD -Pulsation Dampener
PG -Pressure Gauge
PT -Pressure Transmitter/
Pressure Transducer
R -Relay

SA -Stroke Length Control
SAM-Sampling Port
SG -Steam Generator
SGC-Steam Generator Console
SV -Solonoid Valve
TC -Thermocouple
WTM-Wet Test Meter

FIGURE 1. - Schematic diagram of 2-D steamflood experimental assembly.

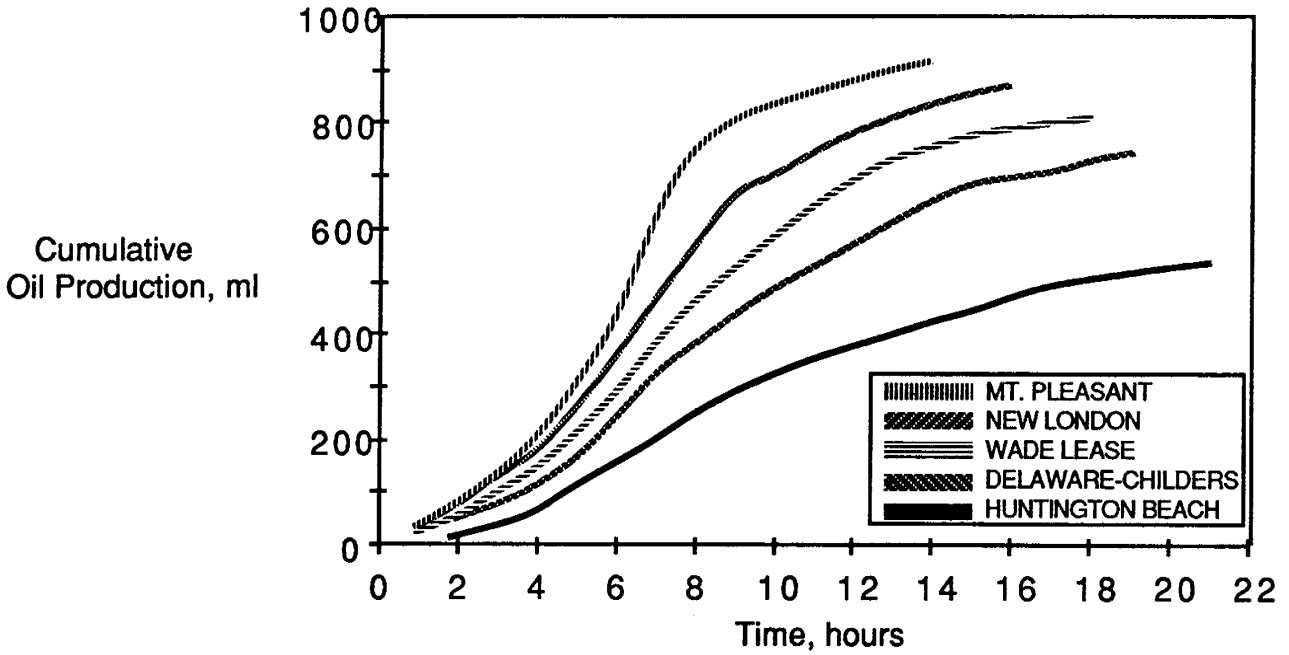

FIGURE 2. - Cumulative oil production as function of time.

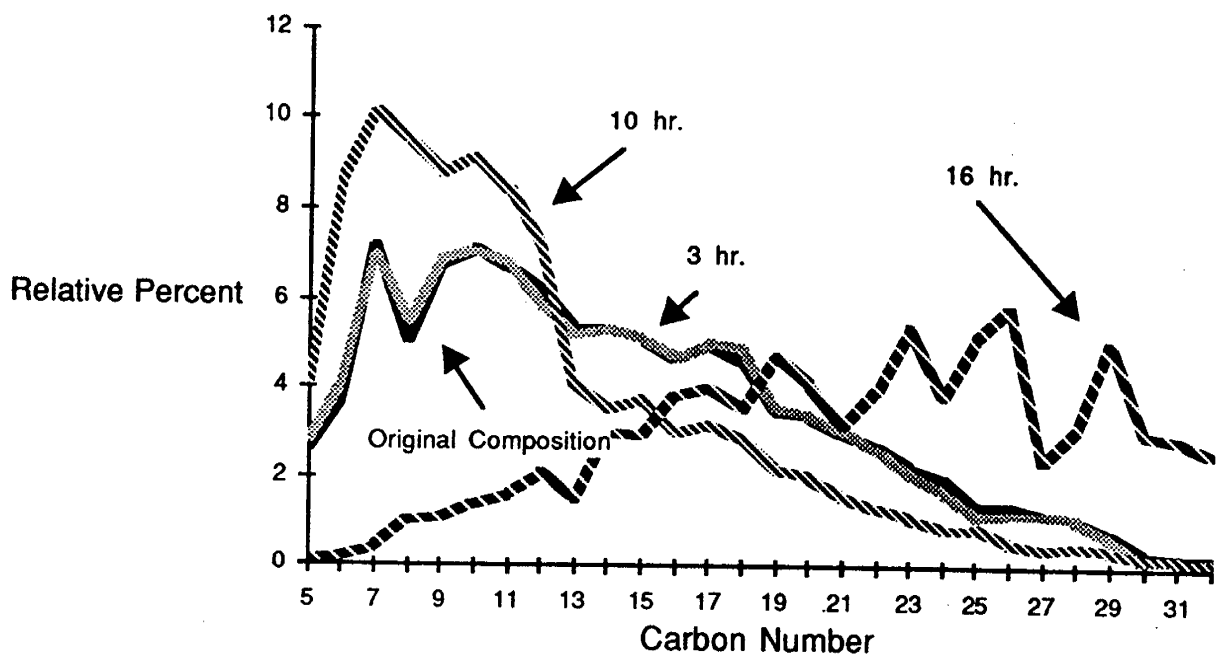

FIGURE 3. - Composition of produced oil during steamflood (Wade Lease crude).

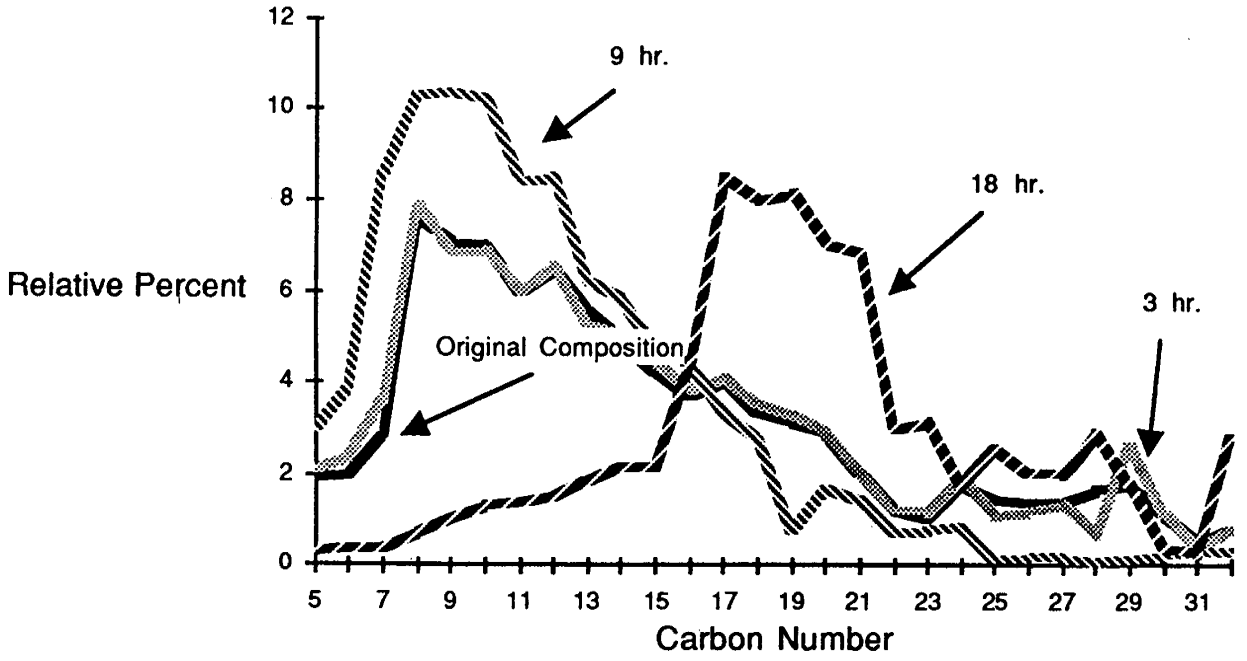

FIGURE 4. - Composition of produced oil during steamflood (Delaware-Childers crude).

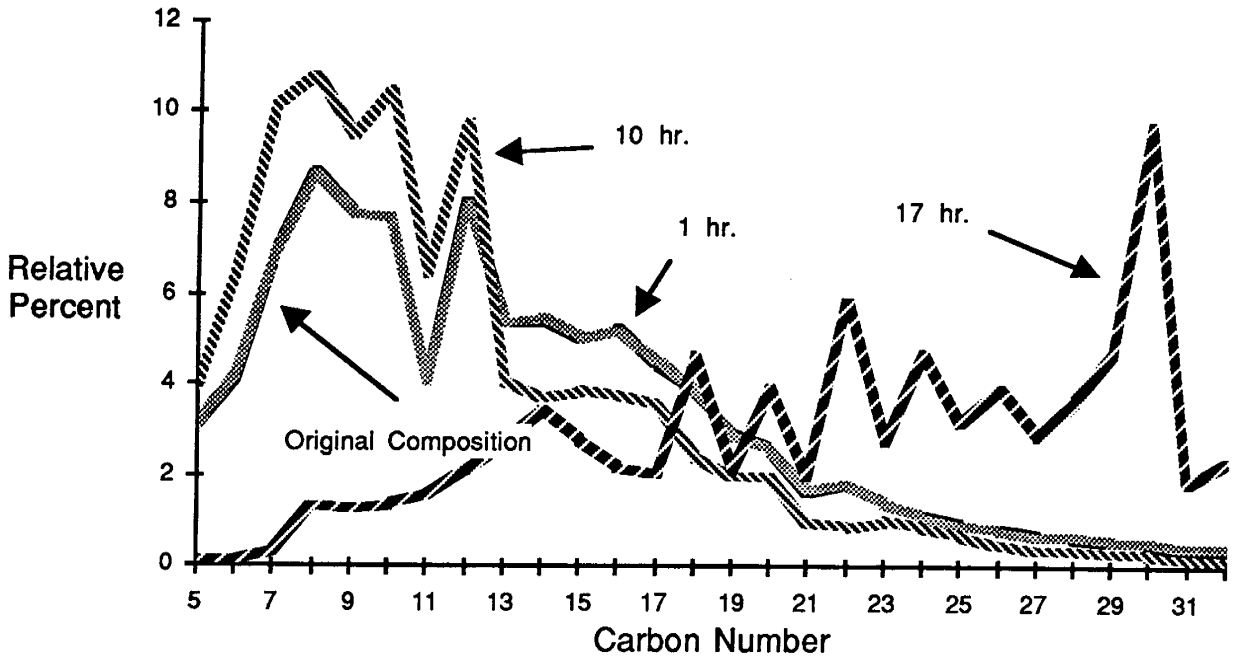

FIGURE 5. - Composition of produced oil during steamflood (New London crude).

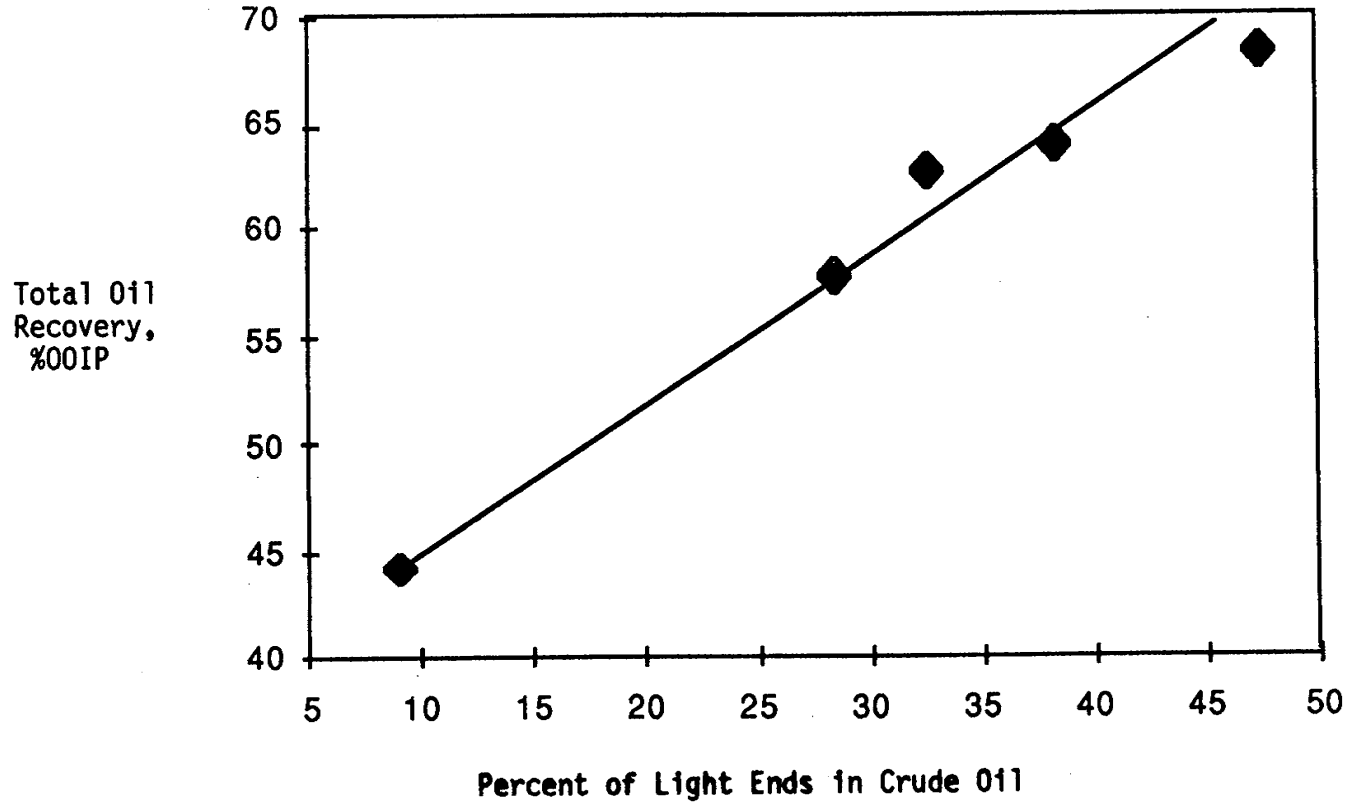

FIGURE 6. - Effect of light ends on light oil recovery by steamflood.

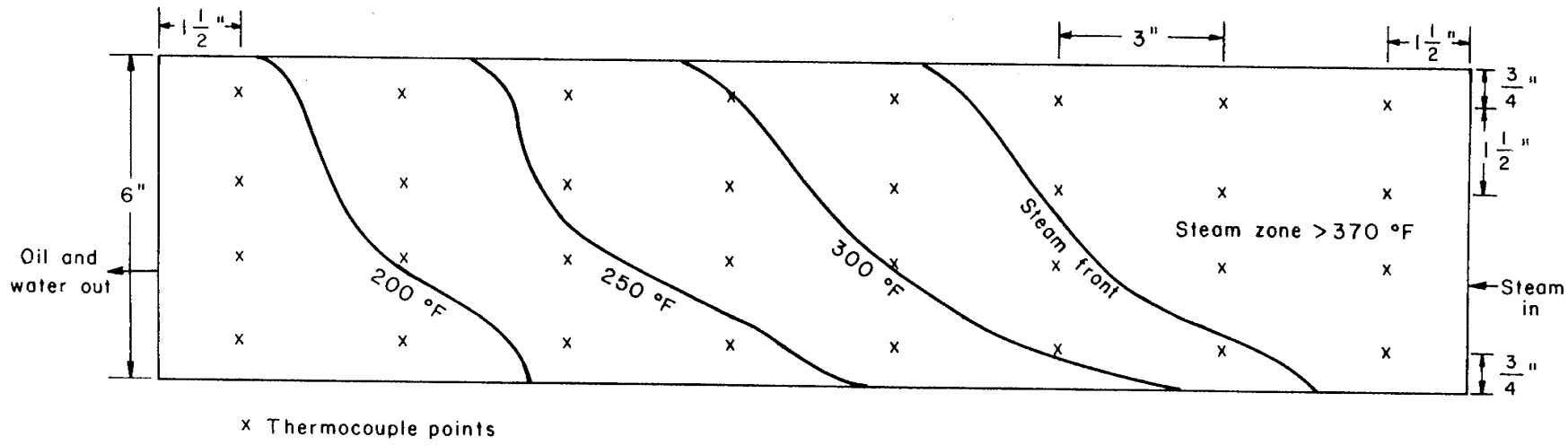

FIGURE 7. - Temperature profile after 8 hours of steam injection (Run 1B).

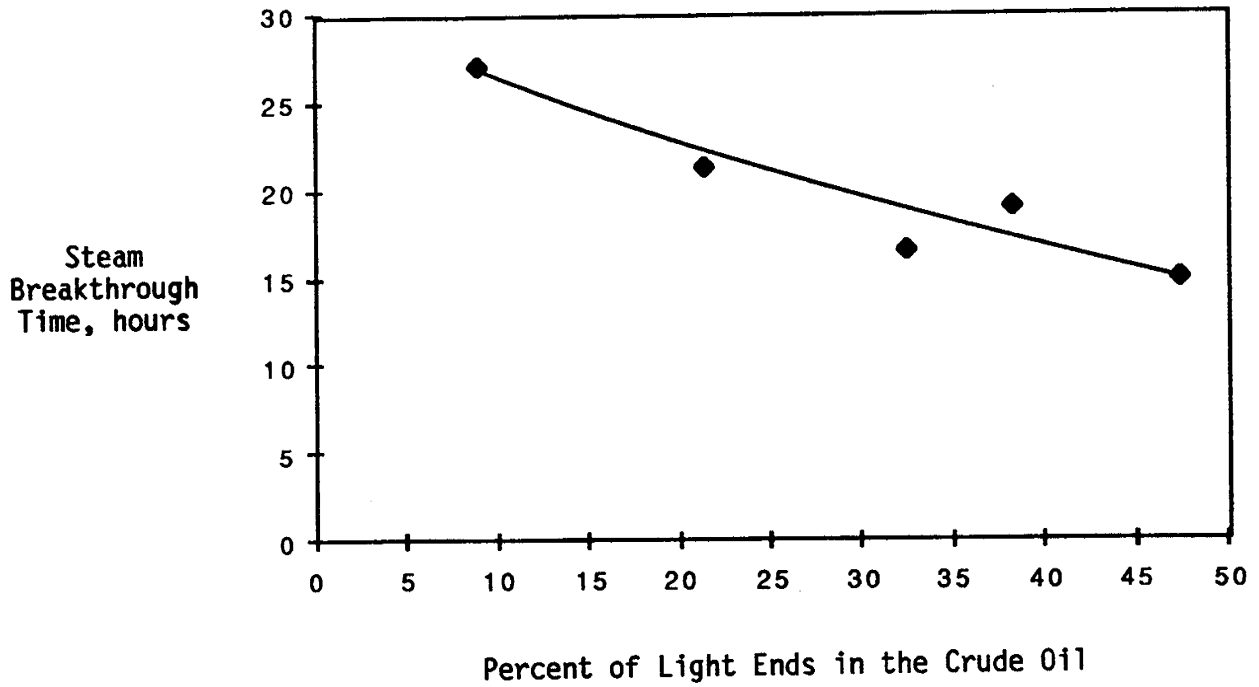

FIGURE 8. - Effect of light ends on steam breakthrough time.

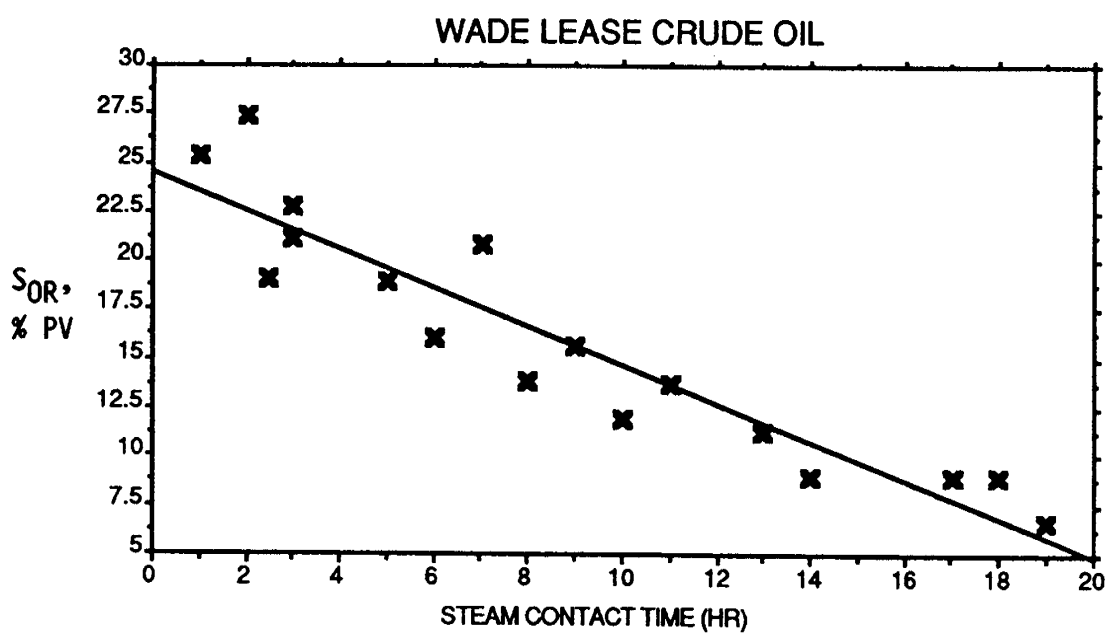

FIGURE 9. - Comparison of residual oil saturation with steam contact time for Wade lease crude oil.

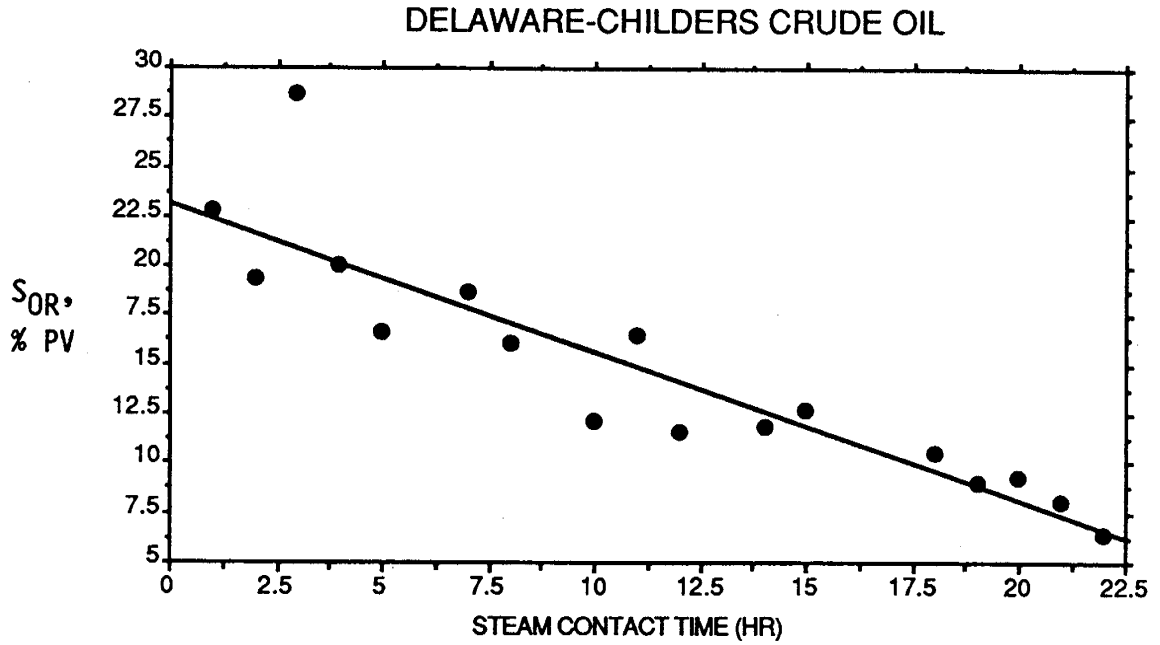

FIGURE 10. - Comparison of residual oil saturation with steam contact time for Delaware-Childers crude oil.

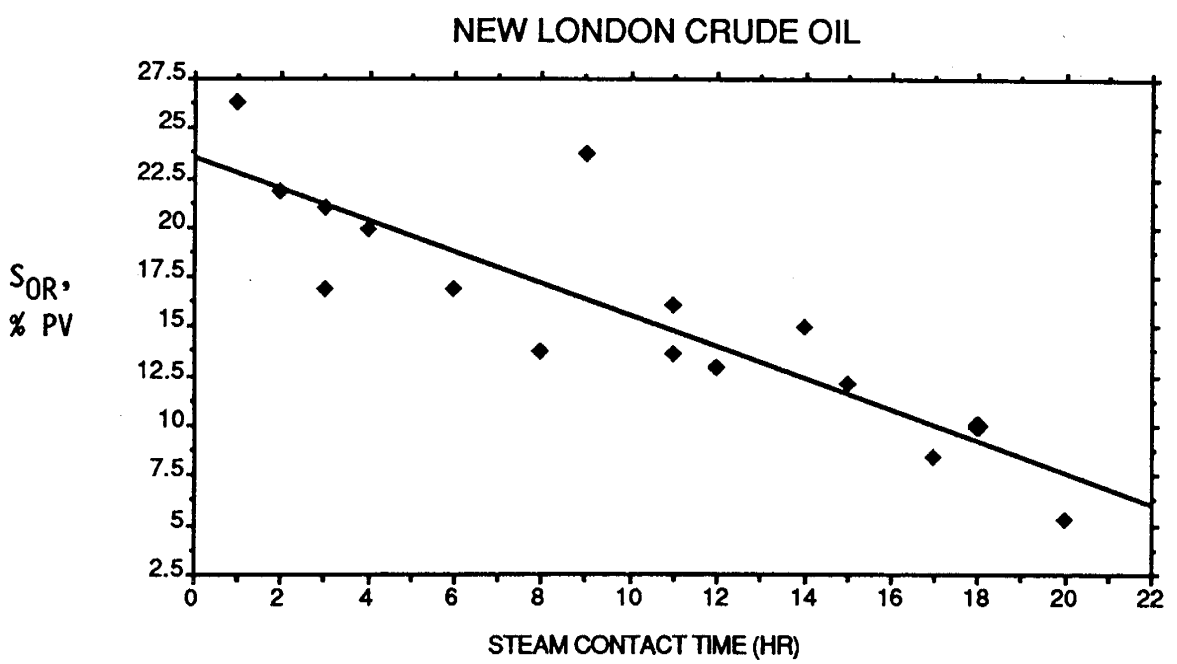

FIGURE 11. - Comparison of residual oil saturation with steam contact time for New London crude oil.

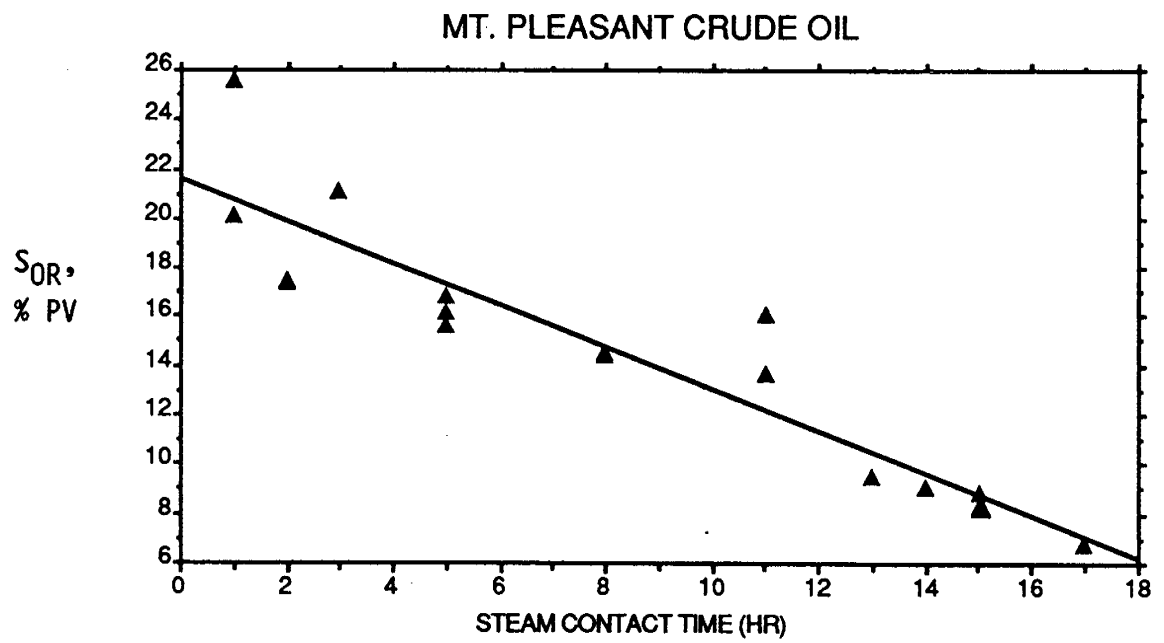

FIGURE 12. - Comparison of residual oil saturation with steam contact time for Mt. Pleasant crude oil.

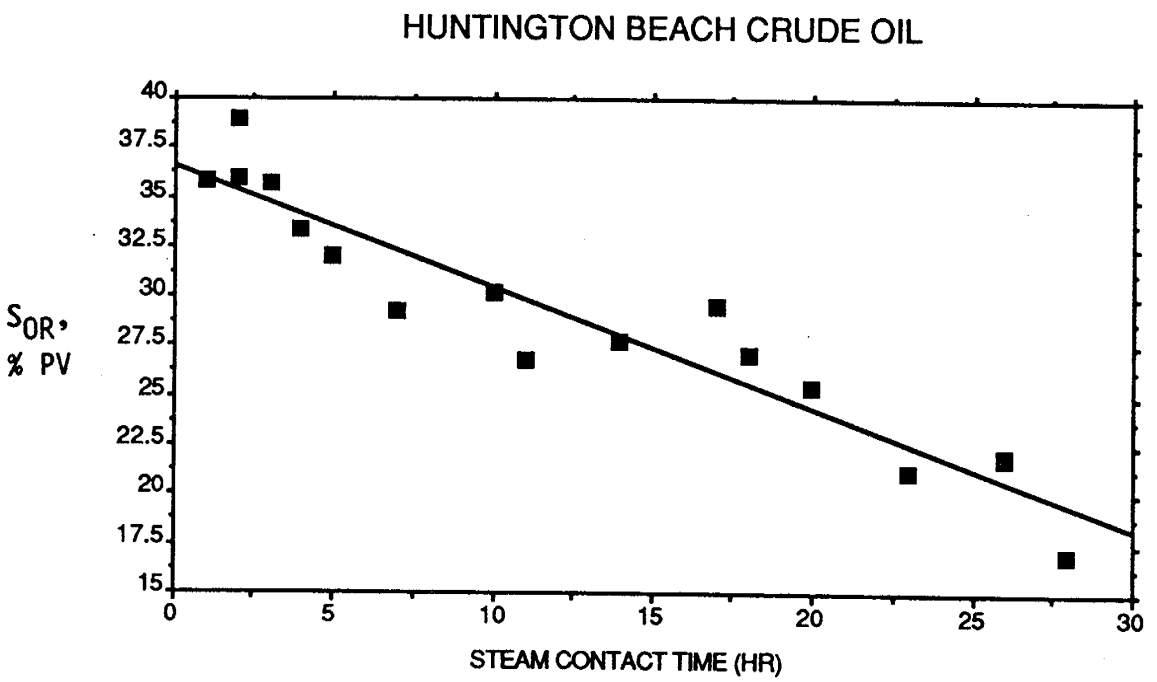

FIGURE 13. - Comparison of residual oil saturation with steam contact time for Huntington Beach crude oil.

APPENDIX A

Full text of the "Fourth Amendment and Extension of Implementing Agreement IV Between the Department of Energy of the United States of America and the Ministry of Energy and Mines of the Republic of Venezuela in the Area of Enhanced Oil Recovery Thermal Processes."

FOURTH AMENDMENT AND EXTENSION

OF THE

IMPLEMENTING AGREEMENT

BETWEEN

THE DEPARTMENT OF ENERGY OF THE UNITED STATES OF AMERICA

AND

THE MINISTRY OF ENERGY AND MINES OF THE REPUBLIC OF VENEZUELA

IN THE AREA OF

ENHANCED OIL RECOVERY THERMAL PROCESSES

WHEREAS, the United States Department of Energy (DOE) and the Ministry of Energy and Mines of Venezuela (MEMV) did on the 29th of September 1980, enter into an Implementing Agreement for cooperation in the area of Enhanced Oil Recovery Thermal Processes (hereinafter referred to as the Implementing Agreement);

WHEREAS, DOE and MEMV have previously agreed to the First, Second and Third Amendments and Extensions to the Implementing Agreement;

WHEREAS, DOE and MEMV have discharged their principal obligations and duties under the Implementing Agreement and the First, Second and Third Amendments and Extensions to their mutual satisfaction and benefit;

WHEREAS, DOE and MEMV now desire to further extend ongoing cooperative efforts and further desire to initiate and pursue new and additional cooperative activities;

WHEREAS, the need exists to increase the recovery efficiency of steam injection methods for the recovery of heavy crude oil, and the use of additives is an attractive method of potentially increasing recovery efficiency;

WHEREAS, DOE and MEMV desire to cooperate in the application of additives to injection steam for the recovery of heavy oil;

WHEREAS, DOE and MEMV desire to further pursue cooperative efforts on the development of thermal front tracking and steam quality measurement methods;

IT IS AGREED AS FOLLOWS;

ARTICLE 1

In accordance with Article 7 of Implementing Agreement, and in accordance with Article V of the Energy Research and Development Agreement of March 6, 1980, DOE and MEMV hereby further amend and extend the Implementing Agreement as hereinafter provided.

ARTICLE 2

Article 1 of the Implementing Agreement and all other articles and provisions not herein amended are extended as written. The identification of Parties in Article 1 of the Implementing Agreement shall be used throughout this Amendment and Extension Agreement.

ARTICLE 3

Article 2 of the Implementing Agreement is amended by adding the following Tasks 32 through 37.

A. <u>Thermal Front Tracking</u>

Task 32 - DOE shall provide INTEVEP with information from the project and field tests conducted by the Lawrence Livermore Laboratory on the use of seismic and electromagnetic methods for cross borehole probing to determine the location of steam zones and fronts within a reservoir.

Task 33 - INTEVEP shall provide DOE with information and results pertaining to electromagnetic properties of stratified media. Modeling of close hole arrays shall be performed to define optimum parameters for the design of surveys requiring well to well geometry.

B. Steam Additives

Task 34 - INTEVEP shall provide DOE with information from research and screening tests performed by INTEVEP related to steam-foam displacement and cyclic stimulation. The Project Managers shall consult with one another concering screening tests and exchange information obtained to avoid unnecessary duplication of research efforts.

Task 35 - DOE shall provide INTEVEP with information from the foam diversion research and steam additive modeling conducted by DOE contractors. The Project Managers will consult with one another on the foam diversion research and modeling conducted by DOE and INTEVEP laboratories with a view to avoid duplication of effort and enhancing the respective research efforts.

Task 36 - INTEVEP shall provide DOE with information and results from steam with additives field tests to be performed with Maraven in Boliver Coast oilfields.

C. Steam Quality Measurement

Task 37 - DOE shall provide INTEVEP with information and results from the DOE funded research at Sandia Laboratories on steam quality measurement. The research includes the development of a tool to measure steam quality downhole during normal steam injection and transmit the data to the surface.

ARTICLE 4

The Implementing Agreement between DOE and INTEVEP shall hereafter consist of the Implementing Agreement as amended by the First, Second, Third and Fourth Amendments and Extensions.

ARTICLE 5

This Fourth Amendment and Extension shall become effective when signed by the members of the Joint Steering Committee or their designated representatives. The Implementing Agreement, as amended, shall remain in effect until March 31, 1988, or until terminated by written notice as provided in Article 8.

Done at Pittsburgh PA, USA.

THE JOINT STEERING COMMITTEE

On behalf of DOE

Member Keith Frye

Member George stosur

for Member Robert Folstein

Aug. 12, 1986
Date

On behalf of MEMV

Member Enrique Vasquez

Member Manuel Alayeto

Member Aldo Boccardo

Aug. 12th, 1986.
Date

★ U.S. GPO: 1988 661-023/80053